Summer 2020

Combustion and emission characteristics of IC engines fueled by hydrogen and hydrogen/diesel mixtures and multi-objective optimization of operating parameters

Abdulhakim Issa Jabbr

Department: Mechanical and Aerospace Engineering

COMBUSTION AND EMISSION CHARACTERISTICS OF IC ENGINES FUELED BY HYDROGEN AND HYDROGEN/DIESEL MIXTURES AND MULTI-OBJECTIVE OPTIMIZATION OF OPERATING PARAMETERS

by

ABDULHAKIM ISSA JABBR

A DISSERTATION

Presented to the Faculty of the Graduate School of the

MISSOURI UNIVERSITY OF SCIENCE AND TECHNOLOGY

In Partial Fulfillment of the Requirements for the Degree

DOCTOR OF PHILOSOPHY

in

MECHANICAL ENGINEERING

2020

Approved by:

Umit O. Koylu, Advisor
John W. Sheffield
James A. Drallmeier
K. Chandrashekhara
V.A. Samaranayake

PUBLICATION DISSERTATION OPTION

This dissertation has been prepared in the form of three papers for publication, formatted in the style used by the Missouri University of Science and Technology:

Paper I, found on Pages 5-34 have been published in International Journal of Hydrogen Energy.

Paper II, found on Pages 35- 62 have been published in International Journal of Hydrogen Energy.

Paper III, found on Pages 63-92 have been published to International Journal of Hydrogen Energy.

ABSTRACT

The present study considers combustion of hydrogen in IC engines. In general, the work focuses on simulating the engine performance and emissions at different operation parameters, and using optimization techniques. Task I work deals with the engine performance and emissions of a single cylinder spark-ignition (SI) engine fueled by hydrogen. The engine was simulated at different equivalence ratios, exhaust gas recirculation (EGR) and ignition timing. The results indicate that NO_X emissions, engine power, and efficiency are reduced by increasing EGR level, and increased with increasing equivalence ratio and advanced ignition timing. The best operating conditions for hydrogen engines were obtained by solving the multi-objective problem of maximizing engine power and efficiency while minimizing the NO_X. Task II deals with the engine performance and emissions of dual-fuel CI engines fueled by a hydrogen/diesel mixture. The engine was simulated under conditions of various hydrogen levels (%) by energy, diesel injection timing, and EGR levels (%). More hydrogen present inside the engine cylinder led to lower soot emissions, higher thermal efficiency, and higher NO_X emissions. Ignition timing delayed as the hydrogen rate increased, due to a delay in OH radical formation. Exhaust gas recirculation (EGR) method and diesel injection timing were considered as well, due to their potential effects on the engine outputs. To obtain the best possible maximum efficiency along with lower NO_X and soot emissions, optimization methods in (Task III) for the operating parameters were considered. Multi-objective problem with conflicting objectives was solved by using regression analysis, artificial neural networks, and genetic algorithms.

ACKNOWLEDGMENTS

First of all, I would like to express my sincere thanks to the Libyan government for financial support during my research work. I am also very thankful to Missouri University of Science and Technology and the Department of Mechanical and Aerospace Engineering for providing the necessary facilities.

I hereby take the opportunity to thank my advisor, Professor Umit Koylu, for his extensive help and suggestions, as well as for providing valuable information regarding my research work. I am also deeply indebted to my committee members for their time and effort in reviewing this work.

I would like to extend my sincerest thanks and appreciation to all of the faculty and staff in the Department of Mechanical and Aerospace Engineering at Missouri University of Science and Technology for their help and input.

I would like to thank my colleagues, Dr. Hassan Khairallah of Tobruk University, Dr. Warren Vaz of University of Wisconsin Oshkosh, and Dr. Haythem Gaja of Tripoli University for their co-operation and support for my research work. I thank my close friend Dr. Abdulaziz Abutunis for his support.

I must express my special thanks to my wife, Salwa, for her moral support and precious love while always standing by me in the hard times during my study.

Finally, I feel especially indebted to my parents Issa Jabbr and Zaynab Jabbr for their love and support. They are my first teachers, and without their encouragement throughout my entire life, I would never have been successful.

TABLE OF CONTENTS

LIST OF ILLUSTRATIONS

LIST OF TABLES

NOMENCLATURE

Abbreviations		Description
ATDC	=	After Top Dead Center
BTDC	=	Before Top Dead Center
BP	=	Brake Power
CA	=	Crank Angle
CI	=	Compression Ignition
CNG	=	Compressed Natural Gas
EGR	=	Exhaust Gas Recirculation
ER	=	Equivalence Ratio
EGR	=	Exhaust Gas Recirculation
HC	=	Hydrocarbon
HRR	=	Heat Release Rate
IMEP	=	Indicated Mean Effective Pressure
LHV	=	Lower Heating Value
NOx	=	Nitrogen Oxides
RPM	=	Revolution per Minute
SI	=	Spark Ignition
SOC	=	Start of Combustion
SOI	=	Start of Injection

1. INTRODUCTION

The demand for energy remains persistent due to the continuing rise in world population and the increasing demand by developed/developing countries. At the present time, more and more fossil fuels are consumed, contributing to the emergence of two significant crises: the exhaustibility of fossil fuels and their combustion products, each a cause of global environmental problems. In 2008, about 65% of the world's energy production needs were met by fossil fuels due to their availability and convenient use. Availability was expected to peak soon, and then began to decrease [1]. The contribution at the current time is not so deference, even though countries around the world pay attention to renewable energy sources.

The effect of burning fossil fuels on the environment will likely garner considerable attention after the world's war against the Coronavirus Disease 2019 (COVID-19). Despite the darkness sweeping across the world due to this outbreak, there is an unexpected environmental consequence: a dramatic reduction in air pollution over wide areas around the world. According to China's Ministry of Ecology and Environment, air quality, as of February 2020, has increased by 21%, compared to any time in the last year [2]. Figure 1.1 shows satellite images released by NASA and the European Space Agency. The figure depicts a reduction in nitrogen dioxide emissions in China's larger cities between January and February, 2020 [3]. As people stay in their homes to minimize the spread of the virus, reduction in vehicle traffic and shutdowns of industrial facilities have resulted in this significant decrease of emissions. [4].

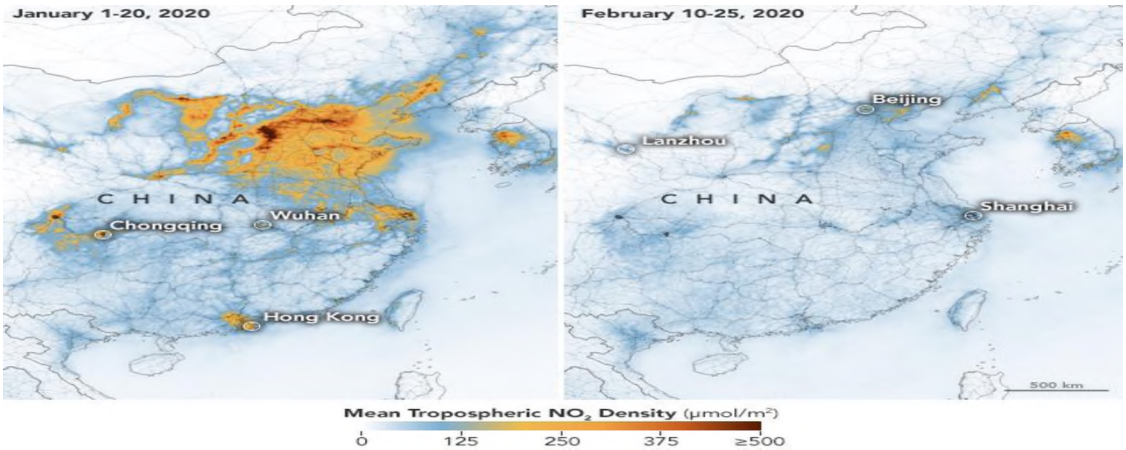

Figure 1.1. Satellite images of air pollution in China.

The predicaments of environmental degradation associated with fossil fuel depletion have forced researchers to think about alternate methods of producing energy without polluting the environment. Hydrogen, as a clean fuel, is an obvious alternative that can mitigate utilization of hydrocarbon fuels such as gasoline, diesel, and natural gas. Hydrogen can be produced from different sources such as methane, biomass, and water. Hydrogen has excellent combustion characteristics, including a wide flammability limit (4-75% by volume), high auto ignition temperature (858 K), a high octane number (130), and high flame velocity (2.6 to 3.2 m/s). As a carbon-free fuel, hydrogen will not emit carbon-based emissions such as hydrocarbons (HC), carbon monoxide (CO), and carbon dioxide (CO_2); instead, its main products are water (H_2O) and nitrogen oxide (NO_x). These desirable qualities encourage hydrogen utilization in internal combustion (IC) engines. Generally, fuel economy is greater when an IC engine is run with a lean mixture. Hydrogen has a very low ignition energy compared to conventional fuels, permitting hydrogen engines to ignite lean mixtures and ensuring prompt ignition.

However, due to the higher combustion temperatures, NO_x formation is an inherent problem in hydrogen engines. There are common methods to reduce NO_x, such as exhaust gas recirculation (EGR) and modifying ignition timing, which are promising technologies for IC engines. Both EGR and IT methods are effective in reducing the NO_x formation by reducing the in-cylinder temperature, but, as a side effect, the power is also significantly reduced. Even though EGR techniques in diesel engines may not be attractive due to increasing soot emissions, it can still be considered for hydrogen/diesel dual-fuel engines, since modifying diesel injection timing can overcome this problem. Engine designers would like maximum power and minimum NO_x and soot emissions, while the commonly adopted measures to reduce emissions also cause the power to decrease. Therefore, this method becomes a classical multi-objective optimization problem with conflicting objectives. It is necessary to adopt a multi-objective approach in order to find multiple suitable points from a Pareto-optimal front to give the designer a wide range of suitable operating points. This would allow the designer to account for real-world conditions where the engine is likely to face different loads and speeds.

The layout of the dissertation is as follows. The first part investigates the relation between three engine outputs power, efficiency, and NO_x emissions and three operating parameters the equivalence ratio (ER), exhaust gas recirculation rate (EGR), and the ignition timing (IT) for a hydrogen-fueled SI engine. The second part investigates the effect of operating parameters, including hydrogen variation, EGR ratios, and Injection timing, on the engine performance and output emissions in dual-fuel compression-ignition engine. The engine model was fueled with a hydrogen/diesel mixture. The third part utilizes the optimization techniques in dual fuel compression ignition engine fueled

by hydrogen/diesel mixtures. The goal of this part is to obtain the best operating parameters among hydrogen variations, exhaust gas recirculation levels, and diesel injection timing that result in lower NO_X and soot emissions and increased engine performance.

PAPER

I. MULTI-OBJECTIVE OPTIMIZATION OF OPERATING PARAMETERS FOR HYDROGEN FUELED SPARK-IGNITION ENGINES

ABSTRACT

This work deals with the engine performance and emissions of a single cylinder spark-ignition (SI) engine fueled by hydrogen. Advanced simulations of the combustion process were performed using a commercial software package. The extended Zeldovich mechanism with coefficients for carbon-free fuel was utilized to investigate the most accurate formation rate of nitrogen oxide (NOx) emissions within the engine. The first part of this work focuses on simulating the engine performance and emissions at different equivalence ratios. Different techniques that have significant effects on engine performance and emissions, such as exhaust gas recirculation (EGR) and ignition timing, were also were studied. A thorough explanation of the relationship between the performance, emissions, and the operating parameters considered is presented. The second part of this work focuses on optimization of the operating parameters. The best operating conditions for hydrogen engines were obtained by solving the multi-objective problem of maximizing engine power and efficiency while minimizing the NO_X.

Keywords: Hydrogen; IC engine; NO_X formation; ignition timing; multi-objective optimization; genetic algorithms; neural networks.

1. INTRODUCTION

In recent years, a lot of attention has been given to alternative sources of energy due to the pollution associated with fossil fuels as well as rising concerns about shortages. One of the main strategies to improve the combustion processes of internal combustion engines (ICEs) is to discover useful ways to decrease exhaust emissions without major modifications to the design. With the growing needs to conserve fossil fuels and minimize emissions, various alternative fuels have been studied. Compared to other fuels such as natural gas, biodiesel, and ethanol, hydrogen (H_2) has unique combustion properties. Hydrogen can be directly used in spark-ignition (SI) engines as a single fuel because it has a spark plug for ignition. In addition, hydrogen has the widest flammability range, so an engine fueled by hydrogen can run on a very lean mixture with high efficiency. Consequently, nitrogen oxide (NO_x) emissions can be reduced at lower equivalence ratios [1, 2]. Hydrogen also has very low ignition energy, which ensures that timely ignition occurs even with a fairly weak spark and permits a hydrogen engine to ignite lean mixtures. The combustion duration of hydrogen-air blends is appreciably shorter than other fuel-air mixtures due to hydrogen having the highest flame speed. Because hydrogen has no carbon in its structure, no carbon-based pollutants are formed and emitted from hydrogen-powered engines. Oxides of nitrogen (NO_x) are the only unwanted emissions of hydrogen combustion. Many studies of IC engines using hydrogen have been carried out in the past [3-6]. Experimental [3] and computational investigations [6] have studied the performance of SI engines fueled by hydrogen and

have estimated the combustion and pollutant characteristics under different engine operating conditions.

Due to the higher combustion temperatures, NO_X formation is an inherent problem in hydrogen engines. One way to reduce NO_X is through exhaust gas recirculation (EGR), which is a promising technology for IC engines. The EGR mechanism recirculates a significant amount of the engine's exhaust gas back to the cylinders. Several studies have been conducted in the area of hydrogen combustion using the EGR technique [6-9]. EGR is used to regulate the engine load and reduce NO_X. In CI and homogenous charge compression-ignition (HCCI) engines, high levels of EGR are common practice [9-13]. However, in gasoline engines, less EGR levels are used due to severe decrease in the flame speed. Recently, higher EGR rates have been conducted in SI engines using other fuels such as natural gas and hydrogen [14-17]. More specifically, the use of EGR in SI engines fueled by hydrogen aims at decreasing the NO_X and regulating the engine load with no throttling necessary. The primary goal is achieved by higher specific heat capacity of the mixture diluted with exhaust gases, thereby decreasing the maximum combustion temperature. The secondary goal (engine load regulation) is accomplished due to the wide flammability limits of hydrogen by appropriately adjusting the EGR rate up to a certain point. Beyond this limit, significant cycle-to-cycle variations, as well as some amount of unburned fuel, appears in the exhaust, causing a decrease in combustion efficiency [18, 19].

Another common method to reduce NO_X is modifying the ignition timing (IT) or spark timing. Ignition timing is a factor that has a significant effect on engine performance and emissions. Advancing the spark timing up to a certain point causes the

combustion to occur earlier and, as a result, the in-cylinder pressure and temperature increase. This causes engine power and NO_X to increase as well [20, 21]. Both EGR and IT methods are effective in reducing the NO_X formation by reducing the in-cylinder temperature, but as a side effect, the power is also significantly reduced. The designer would like maximum power and minimum NO_X while the commonly adopted measures to reduce NO_X also cause the power to decrease. Therefore, this method becomes a classical multi-objective optimization problem with conflicting objectives.

The study in [22] focuses on the effect of the compression ratio, equivalence ratio, and engine speed on the engine performance and emissions of an SI engine fueled by hydrogen. An analytical model was developed and validated against the experimental data of the engine. The equivalence ratio was varied between 0.5 and 1.3. As a result, the engine operating at lean mixture (ER<0.8) tends to decrease the engine power and NO_X emissions for all compression ratios due to a reduction in the volumetric lower heating value of the intake mixture and decreasing combustion temperature, respectively. At richer mixture, the engine power and the concentration of NO emission also decrease due to decreasing combustion efficiency and amount of oxygen, respectively. An experimental study [23] on the performance and emission characteristics of an SI engine fueled by a natural gas-hydrogen mixture found that the break thermal efficiency and NO_X emissions increase with hydrogen added to natural gas; however, at lean and rich mixtures, the break thermal efficiency and NO_X emission are found to reduce. The effect of spark timing on performance and emissions was considered in the study [24]. Advance ignition timings can be considered as a solution of an engine knock at equivalence ratio of 0.55 by reducing the combustion rate; however, highly retarded spark timing rises the

residual gas temperature at the higher equivalence ratio and, as a result, backfiring could take place in the engine. Also, advanced ignition timing causes a lowering of the rate of pressure rise, so the power and the break thermal efficiency decrease.

Several studies researched the optimization of IC engines. Optimization studies can broadly be categorized as geometry optimization or optimization of operating conditions. Geometry optimization typically involves using an optimization algorithm to find the best cylinder geometry that minimizes certain fitness functions. The study in [25] parameterized the cylinder geometry for a direct-injection diesel engine. Eight different parameters were used to optimize three fitness functions (HC, NO_x, and soot) for different operating conditions, as well (load and speed). This was similar to a previous study [26] that included nine parameters, three of which related to the geometry. Genetic algorithms (GA) were used to minimize the same emissions and the fuel consumption, as well. The more recent study in [27] focuses on stoichiometric diesel combustion targeted towards lowering the gross indicated specific fuel consumption. The emissions were not considered as optimization objectives due to the claim that they are manageable with after-treatments. The study in [28] was conducted for a CI engine fueled with dimethyl ether. Eleven decision variables were used, including some related to operating conditions, with the objectives being the same as [26]. The study in [29] introduces neural networks (NN) to reduce the computational time needed by GAs. NNs were used to estimate the efficiency and NO_x for a spark-ignition engine. Several engine parameters were used as inputs, but the geometry was fixed. The study in [30] is a more comprehensive version that uses GA-NN methods to optimize the NO_x, soot, and gross

indicated mean effective pressure. Three different piston bowl geometries were considered.

The problem with geometry optimization is that implementation of the results could be very difficult given that new geometries are usually proposed. In the short term, it is more practical to consider finding the optimum (in the context of multiple conflicting objectives) operating conditions for existing engine geometries. It is necessary to adopt a multi-objective approach in order to find multiple suitable points from a Pareto-optimal front in order to give the designer a wide range of suitable operating points. This would allow the designer to account for real-world conditions where the engine is likely to face different loads and speeds.

The study in [31] focused on the trade-off between NO_x, soot, and specific fuel consumption using a phenomenological model of a diesel engine. The only decision variable used was the shape of the injection rate. The same group later considered more operating conditions as decision variables (boost pressure, EGR rate, etc.) and obtained Pareto fronts for the three objectives [32]. The study in [33] used a similar approach as [30] to estimate the objective functions, which were NO_x, opacity, and brake-specific fuel consumption of diesel fuel for a CI engine enriched with hydrogen. Nine decision variables were used. However, there was no multi-objective optimization to obtain Pareto fronts. Instead, the trade-offs of the considered cases were presented. An experimental approach to study the effects of the compression ratio and the equivalence ratio on the emissions (CO, HO, and NO_x) of an 80% hydrogen-ethanol SI engine was presented in [34]. Once again, no multi-objective optimization was performed. A study on a hybrid hydrogen-gasoline engine [35] was conducted. This engine was fueled by hydrogen at

start-up conditions, a blend of idle and low loading conditions, and pure gasoline at high loading conditions. Various operating conditions were tested, all at lean conditions. The researchers did not consider any optimization of trade-offs between the efficiency, emissions, and other performance measures studied. The same group presented results for a spark-ignition pure hydrogen engine for a range of lean operating conditions [36]. The power output was not considered. Instead, the emphasis was on emissions reduction. Another similar example for a diesel engine run using biofuels is [37]. The aim was to find the best fuel blend and EGR rate. However, only a limited number of blends were tested. The study in [38] was performed for an SI engine. The goal was to optimize the spark timing (IT) and the air-fuel ratio. The objectives, which were considered separately, were brake specific fuel consumption and torque. No emissions were considered as objectives. The study in [39] followed a classical multi-objective approach for hydrogen/diesel mixtures. However, no emissions were considered in any of the objective functions and the authors failed to note the precise operating conditions corresponding to the optimal solution. The study in [40] was performed for a hydrogen SI engine. The excess air ratio and the IT were used to optimize the brake thermal efficiency and the power output. No emissions were considered, and the two objectives were not considered in a multi-objective sense. A similar study was conducted in [41]. Several operational parameters were used to optimize an abnormal combustion objective and a power objective. The decision variables were the excess air coefficient and the IT. The study in [42] examined the effect of hydrogen enrichment in a diesel engine. It was noted that the CO and smoke decreased, but the NO_X increased. However, no optimization was done as only a few cases were considered.

The present study systematically investigates the relation between three engine outputs (power, efficiency, and NO_X emissions) and three operating parameters (equivalence ratio [ER], EGR rate, and IT) for a hydrogen-fueled SI engine. Each parameter was varied over an extensive search domain, while the other two were held constant in order to properly characterize the input-output relationship and guarantee that the best operating points lay within the search domain considered. Studies that deal with the size of the search domain considered here for hydrogen are limited, and the operating conditions have not been considered before for hydrogen. Furthermore, there are few studies that solve a multi-objective optimization problem (MOOP) and present a range of alternate solutions. The advantage of the present approach is that multiple conflicting objectives can be considered simultaneously in an equitable manner and the solution produces multiple alternate solutions. Using a GA approach is more likely to find a global optimum, as well. The main contribution of this study is the presentation of detailed explanations of the computational results obtained using a 3D commercial-grade combustion code, and solving a MOOP for the goal to minimize the NO_X and maximize the power and efficiency.

2. COMPUTATIONAL METHODS

Computational Fluid Dynamics (CFD) is a tool that is used, especially in the last few years, to design and develop engineering devices. Multi-dimension CFD software has become widely utilized to fully understand the combustion processes in IC engines, especially inside the engine cylinder. In this study, the simulation of the combustion

process was performed using AVL FIRE® 3D CFD code, coupled with detailed chemical reaction kinetics of hydrogen using the CHEMKIN software package. The engine model used in this study was created and validated by [43] in a previous work to predict the engine power, thermal efficiency, and NO_X emissions. This model was validated with experimental data presented [3]. The detailed mechanism for the chemical reaction kinetics of hydrogen, which includes 29 elementary reactions and 10 species, excludes the oxidation reactions of nitrogen. Thus, eight NO_X reactions of formation, as shown in Table 1, were added to the hydrogen mechanism, and the final chemical kinetic model includes 37 elementary reactions and 13 species. With the mentioned additions, a spark-ignition module was added to successfully implement an SI engine in AVL.

2.1. NOX FORMATION

In general, prompt NO_X, fuel NO_X, and thermal NO_X are the three known mechanisms for NO_X formation. One of the most complicated processes to form NO_X is the prompt NO_X mechanism. It includes hundreds of reactions and species. Prompt NO_X is generated under faster reaction conditions between N_2, O_2, and hydrocarbons as follows:

$$\mathrm{CH} + \mathrm{O_2} + \mathrm{N_2} \rightarrow \mathrm{NO}, \mathrm{NO_2}, \mathrm{CO_2}. \tag{1}$$

At low-temperature combustion and in the presence of hydrocarbon fuel at rich conditions, prompt NO_X is considered to be an important mechanism. However, at higher temperatures it is trivial compared to the thermal NO_X mechanism. The second NO_X formation mechanism is fuel NO_X. It is generated by the direct oxidation of organic nitrogen compounds found in the fuel:

$$\mathrm{RxN} + \mathrm{O_2} \rightarrow \mathrm{NO}, \mathrm{NO_2}, \mathrm{CO_2}, \mathrm{HO_2O}. \tag{2}$$

Even though fuel NO_x is a trivial mechanism for a high-quality fuel such as natural gas that has no organic nitrogen compounds, it could be an important mechanism when fuels such as coal and oil (e.g. residual fuel oil) are used. Those kinds of fuel might have significant amounts of organically bound nitrogen. Thermal NO_x is produced by the high temperature reaction of N_2 with O_2, and it is known as the Zeldovich mechanism:

$$N_2 + O_2 \rightarrow NO, NO_2 \tag{3}$$

In this study, the adopted NO_x formation mechanism was derived from the Zeldovich model [44]. In order to predict NO formation accurately, carbon-free fuel constants [45] were used.

Table 1. List of reactions in the NO formation mechanism.

$N_2 + O = N + NO$	(R1)
$N + O_2 = NO + O$	(R2)
$N + OH = NO + H$	(R3)
$N_2O + O = N_2 + O_2$	(R4)
$N_2O + O = NO + NO$	(R5)
$N_2O + H = N_2 + OH$	(R6)
$N_2O + OH = N_2 + HO_2$	(R7)
$N_2O + M = N_2 + O + M$	(R8)

The reactions R1, R2, and R3 in Table 1 describe NO formation and are known as the extended Zeldovich mechanism. The extended Zeldovich mechanism is only important at high temperatures because the species O and OH are only generated at high temperatures.

2.2. MODEL PARAMETERS

The specifications of the engine model is listed in Table 2 below.

Table 2. Engine specifications.

Fuel	Hydrogen
Number of cylinders	1
Bore × Stroke	85 × 95 mm
Displacement volume	530 cm^3
Compression ratio	9:1
Engine speed	2500 rpm
Initial operating conditions	
Start angle (BTDC)	540 degree
End angle (ATDC)	850 degree
Piston surface temperature	423 K
Turbulence model	k-ζ-f model
Turbulence kinetic energy	2 m^2/s^2
Turbulence length scale	4.5 mm
Initial temperature	330 K
Initial pressure	1 bar

CFD results have shown high agreement with the experimental results for peak pressure, brake thermal efficiency, and NO_x emissions at different equivalence ratios with constant engine speed [43].

3. PROBLEM DESCRIPTION

In the present study, a hydrogen-fueled SI engine was simulated using 3D AVL Fire® software at different operating parameters. The EGR ratio was considered at 0%, 5%, 10%, and 15%. The ignition timing was considered at 5, 10, 15, and 20 degrees

crank angle (CA) before top-dead-center (BTDC). The equivalence ratio was considered at 0.7, 0.8, 0.9, 1.0, 1.1, and 1.2. Consequently, the total number of runs was 4x4x6, or 96. Table 3 summarizes the simulation operating parameters and objectives. The objectives were the maximization of power and efficiency and the minimization of NO_X.

Table 3. Operating conditions and objectives for MOOP.

Parameters		Objectives
Ignition Timing (CA BTDC)	5, 10, 15, and 20	max[Indicated power (kW)]
EGR Level (%)	0%, 5%, 10%, 15%, and 20%	max[Indicated thermal efficiency (%)]
Equivalence Ratio	0.7, 0.8, 0.9, 1.0, 1.1, and 1.2	min[NOx emission (ppm)]

4. COMPUTATIONAL RESULTS AND DISCUSSION

4.1. EFFECT OF EQUIVALENCE RATIO ON POWER, NO_X, AND EFFICIENCY

Lean conditions at equivalence ratios 0.3, 0.5, and 0.84 were considered previously by [43]. The results show a reduction in NO_X emissions, as well as power and efficiency. Since the aim of this work is finding the optimal operating conditions that lead to a reduction in NO_X emissions and an increase power and efficiency, equivalence ratios close to stoichiometric conditions (0.7-1.3) were considered in this study, as shown in Figure 1. The EGR level was 0% and the IT was 5 CA BTDC. It was found that power and efficiency increase as the equivalence ratio increases from a lean mixture (0.7) to a stoichiometric-rich mixture (almost 1.1). This is because as the equivalence ratio increases, the in-cylinder peak pressure increases; thus, the power and efficiency increase

at stoichiometric conditions, no energy is wasted because the ideal amounts of fuel and air are present. However, at rich conditions, the curve slightly declines due to lack of enough air to combust the fuel (incomplete combustion). Therefore, the peak pressure decreases, resulting in a decline in the power and efficiency of the engine. Figure 1 also shows the effect of the equivalence ratio on the NO_x emissions. In the lean mixture region (less than 0.8), NO_x emissions increase with an increase in equivalence ratio (0.8-0.9) because high in-cylinder temperature and high oxygen concentration are the essential routes of NO formation: therefore NO_x emissions increase. However, with the equivalence ratio greater than 0.9, the NO_x starts to reduce until it approaches zero at 1.2. The main reason is the reduction in oxygen concentration and in-cylinder temperature.

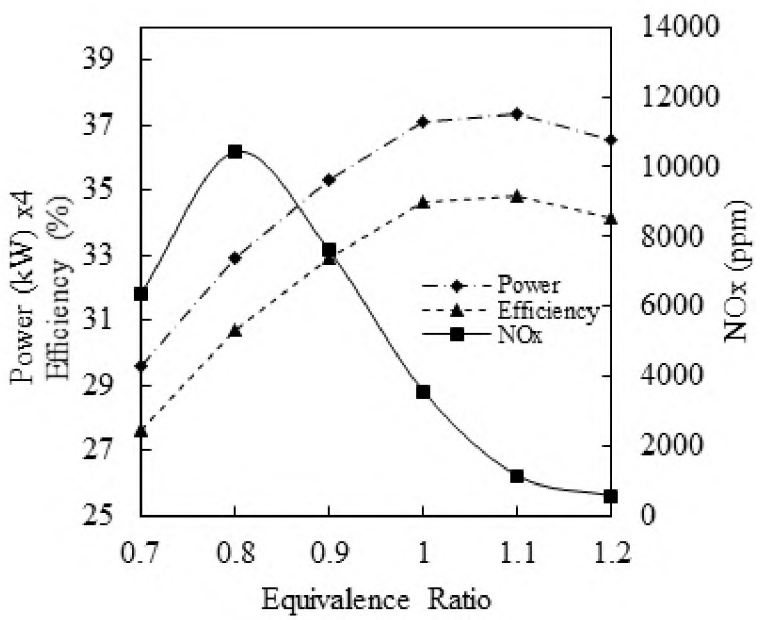

Figure 1. Effect of equivalence ratio on power, NOx, and efficiency.

4.2. EFFECT OF EXHAUST GAS RECIRCULATION ON POWER, NO_X, AND EFFICIENCY

Figure 2 illustrates the effect of EGR levels on the objectives. The equivalence ratio was 1.0 and the IT was 5 CA BTDC. The figure clearly shows that the EGR technique is very useful in reducing the NO_X emissions: the NO_X is reduced by approximately 87 ppm at 5% EGR and 883 ppm at 15% EGR. NO_X is reduced because EGR reduces the in-cylinder temperature, which is one of the main routes of NO_X formation. On the other hand, power and efficiency also decrease. This is because increasing the EGR level leads to a reduction in the volume of air and fuel inside the cylinder, as well as a reduction in the hydrogen flame speed, so engine power and efficiency decrease as well.

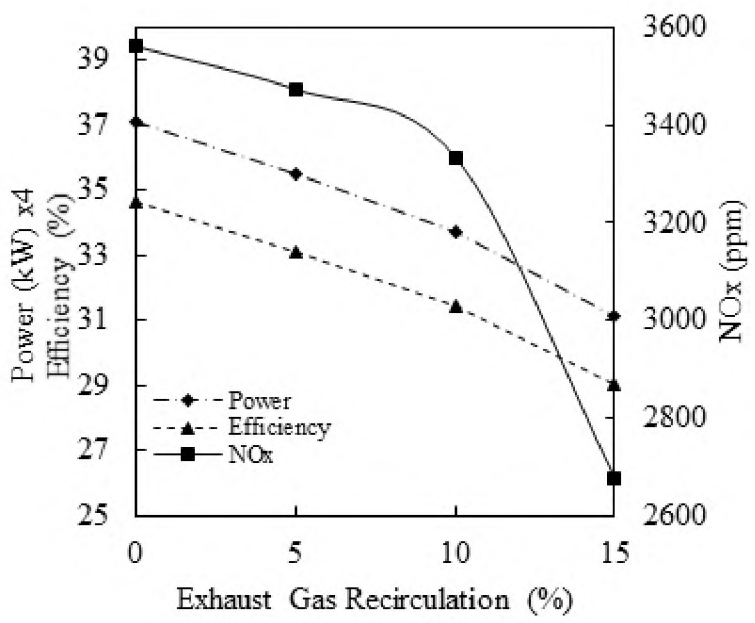

Figure 2. Effect of Exhaust Gas Recirculation on power, NOx, and efficiency.

4.3. EFFECT OF IGNITION TIMING ON POWER, NOX, AND EFFICIENCY

Ignition timing has a direct effect on the engine performance and NO_x emissions in hydrogen engines, as shown in Figure 3. The equivalence ratio was 1.0 and the EGR level was 0%. As shown,, engine power output and efficiency significantly increase as IT is increased. However, NO_x emissions also increase because as the IT advances relative to the top-dead-center (TDC), combustion occurs earlier. With enough time to complete combustion, the in-cylinder peak pressure and temperature increase, which improves power and efficiency but also increases the NO_x.

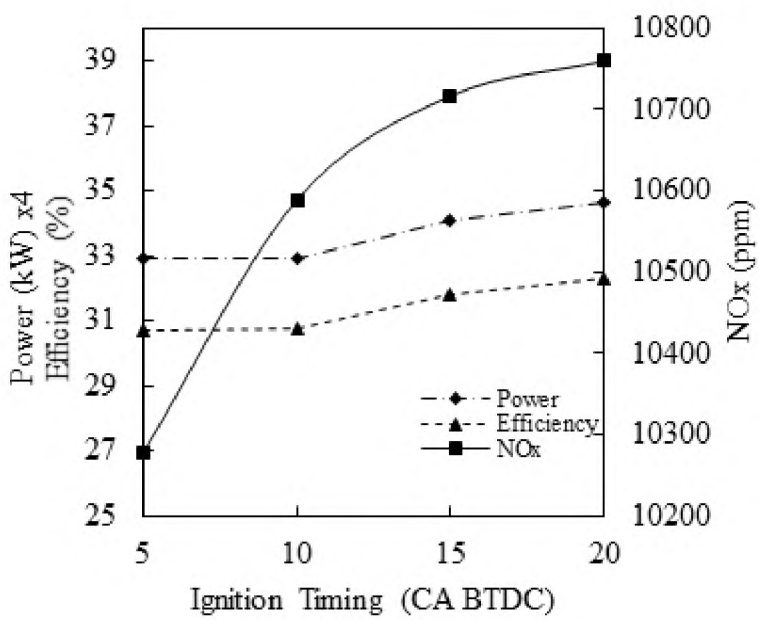

Figure 3. Effect of ignition timing on power, NO_x, and efficiency.

Efficiency is an important objective. However, Figures 1-3 show that the power and efficiency strongly correlate, meaning improving one also improves the other.

Therefore, it is sufficient to consider only one of them and reduce the problem from 3D to 2D, thereby reducing the computing costs. Figure 4 shows a parametric plot of the computational results: the power and NO_x for each run are plotted on the same plot. Non-dominated points or solutions, where an improvement in one objective comes at the expense of the other, are specially demarcated.

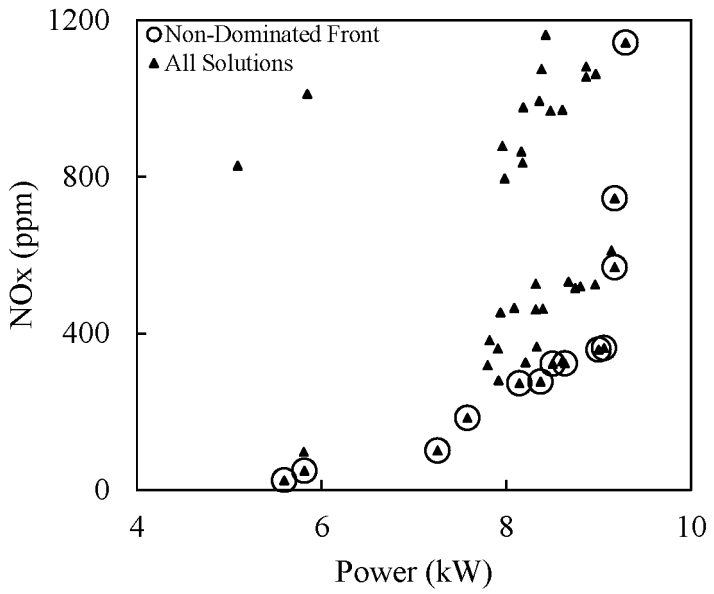

Figure 4. Computational results: parametric objective space plot of power and NO_x.

The set of non-dominated solutions is called the Pareto front. The shape of the front in Figure 4 is not developed. The operating parameters corresponding to these non-dominated solutions were inspected, and more runs were conducted by making small variations in the parameters corresponding to these non-dominated solutions in order to develop the front further. However, considering the AVL run time, searching for a

Pareto-optimal front (or fully-developed front) in this manner is very inefficient, with no guarantee of ever finding the front.

5.INTRODUCTION TO THE GENETIC ALGORITHM (GA) AND NEURAL NETWORK (NN) APPROACH (GA-NN)

5.1. MULTI-OBJECTIVE GENETIC ALGORITHM

Multi-objective genetic algorithms (MOGA) are a class of tools based on genetic algorithms (GAs) to solve multi-objective optimization problems (MOOP) with conflicting objectives. A GA is an optimization technique that mimics the principle of natural selection and natural genetics to find the best solution, with respect to an objective function for an engineering problem. Genetic algorithms operate on a population of feasible solutions (defined as a set of three operating parameter values in the present problem) by applying the principle of "survival of the fittest" to successively produce better approximations in each generation (i.e., iteration of the algorithm). During each generation, a new set of solutions is created by the process of selecting individuals according to their level of fitness (i.e., value of their objective functions) and breeding them using operators, such as crossover and mutation, borrowed from natural genetics. This process leads to the evolution of populations of individuals that are better suited to their environment (i.e., they have better objective functions) than the individuals that they were created from, just as in natural adaptation. The working principle of a binary-coded GA is lucidly described by Nandi [46]. GAs have been used to solve engineering problems in several areas such as electric vehicles [47] and diesel engine combustion [28].

Unlike a single-objective optimization problem where the objective is to find a single solution, the task of an optimizer in a MOOP is to obtain a set of solutions based on the concept of domination by comparing two solutions on the basis of whether one dominates the other solution, meaning both objectives' values are better. The plot of the objective function values corresponding to non-dominated solutions is called a non-dominated front. If the non-dominated solutions are optimal in terms of the objectives, then the non-dominated front is called the Pareto-optimal front; the solutions lying on the Pareto-optimal front are called Pareto-optimal solutions. Thus, the primary goal in a multi-objective optimization problem is to obtain a set of solutions as close as possible to the true Pareto-optimal front, in addition to being spread out as diversely as possible. Optimization techniques based on GAs were found to be most suitable to solve such kinds of multi-objective optimization problems because a GA is itself a population-based algorithm. In the present work, NSGA-II [48], one of the most popular non-dominated sorting GA, was adopted.

5.2. NEURAL NETWORK APPROACH

Neural networks (NN) have been successfully used in classification, function approximation, identification, and pattern recognition in various engineering applications [49]. Feed-forward neural networks with a sufficient number of hidden neurons can approximate any finite function arbitrarily well. In this study, a neural network was used to map the complex relation between the operating parameters (equivalence ratio, EGR level, and ignition timing) and the objectives (NO_X emissions and power). The network was implemented in MATLAB and trained using 110 data points obtained from AVL

simulations. The R-value was 0.99997. The optimized results were tested and validated using the numerical model seen in Figures 5 (a) and (b).

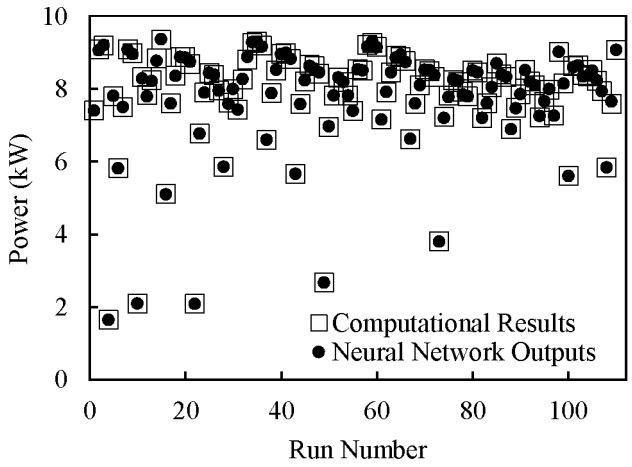

(a)

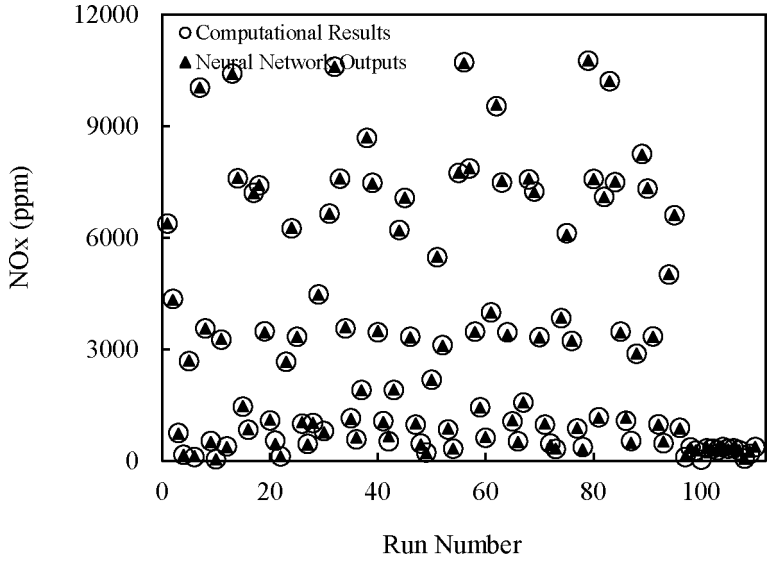

(b)

Figure 5. Neural network training results for (a) the power objective, and (b) NO_X objective.

The figures show a plot of the NN outputs compared with the AVL computational results. Since every NN point coincides with the associated AVL point, it may be concluded that the NN training was successful in learning the input-output relationship. The trained NN was used to approximate the objective values for different solutions (combinations of input parameters) chosen by GA, similar to Banerjee and Bose [33]. The GA-NN process is depicted in Figure 6.

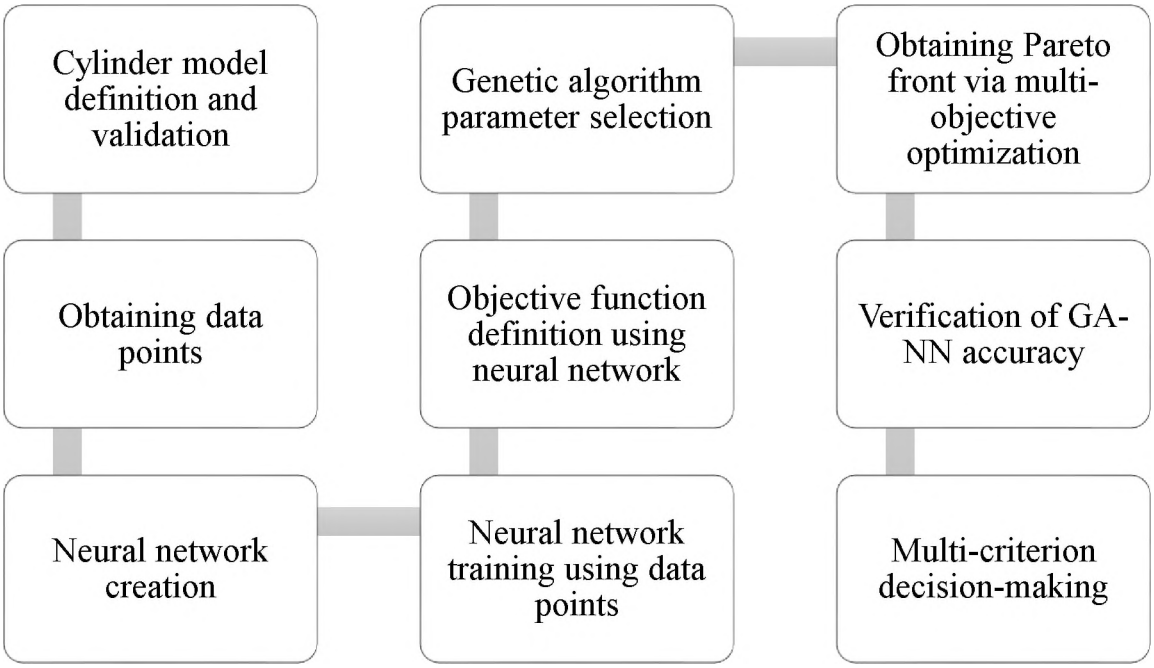

Figure 6. Flowchart of the GA-NN process.

6.GA-NN RESULTS

The EGR ratios of 0%, 5%, 10%, and 15%., Equivalence ratios 0.7 to 1.2, and ignition timings from 5 to 20 CA BTDC were the operating condition boundaries to be

used for optimization. Tables 4 and 5 show the GA parameters and NN parameters, respectively.

Table 4. GA parameters.

Algorithm	NSGA-II
Population size	20
Number of generations	100
Crossover probability	0.9
Mutation probability	0.33

Table 5. Neural network parameters.

Type	Feed-forward
Number of inputs	3
Number of outputs	2
Number of hidden layers	2
Number of neurons per hidden layer	10
Hidden layer activation function	Log sigmoid
Output layer activation function	Linear
Training function	'train'
Stopping criterion	1000 epochs
R-value	0.99997

Figure 7 shows the Pareto front obtained using the GA-NN approach superimposed on the original computational non-dominated front from Figure 4. A Pareto front that contains GA-NN estimated points as well as computational points has not been presented until now. As shown, there are several new non-dominated solutions. It is important to keep in mind that the GA-NN approach estimates the solutions. Therefore, a few randomly chosen NN estimated points from this new Pareto front were run using AVL to get an estimate of the error involved. Figure 8 shows that the NN estimated points are in close agreement with the computational points. The average error was found to be 9.6%, with the lowest error being 1.4%. Finally, Figure 9 shows the combined front derived from both the computational and the NN fronts. Its shape is typical of a max-min Pareto-optimal front that is fully developed.

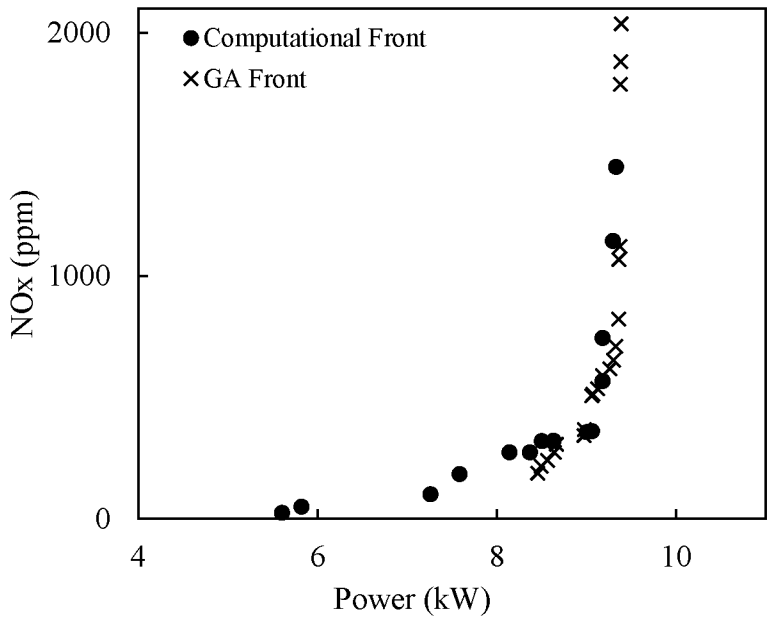

Figure 7. Comparison of original computational non-dominated front with GA front.

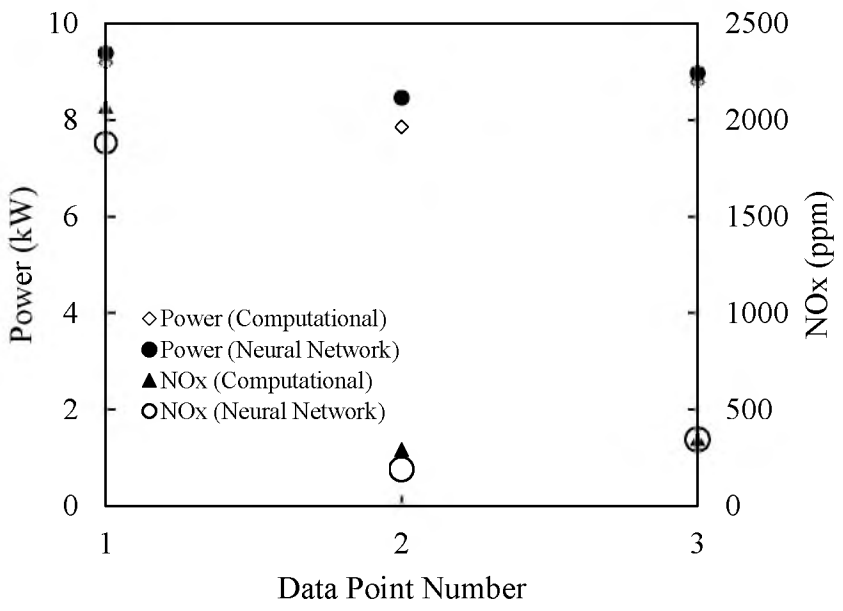

Figure 8. Comparison of AVL computational results with NN estimated results

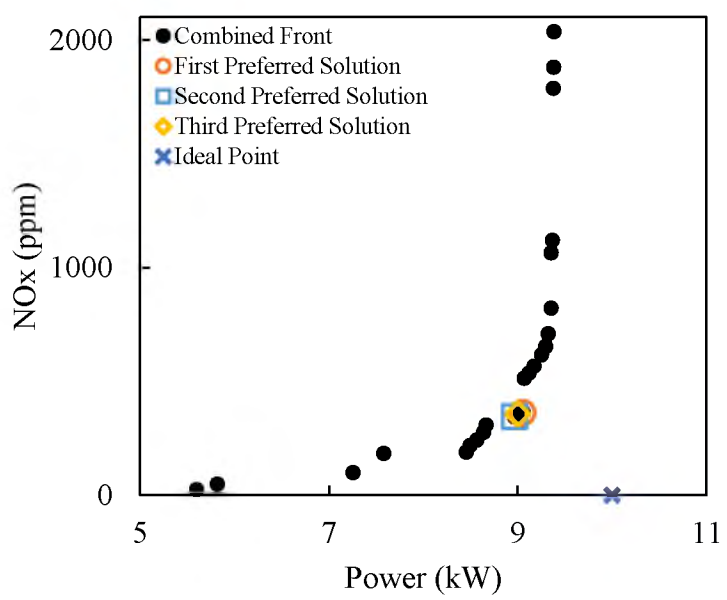

Figure 9. Combined Pareto front with top three preferred solutions.

7.MULTI-CRITERIA DECISION-MAKING (MCDM)

While the Pareto front presented in Figure 9 provides the user with several alternate solutions at medium to high power, it is sometimes necessary to select one solution for implementation. Typically, such a solution is chosen with the application of some higher-level criterion or multiple criteria. This is called multi-criteria decision-making (MCDM). The reference point method is one such MCDM technique [50]. The ideal reference point was taken to be (10 kW, 0 ppm). Practically, no set of operating parameters considered in this study can produce such an output. However, points on the Pareto front whose Euclidean distance from this ideal point at least could be considered as preferred solutions for implementation. Figure 9 shows the top three preferred solutions. They are expectedly close to one another on the front and it can be seen that, while they are not extreme in either objective, they represent a good trade-off.

Table 6 shows the operating parameters associated with the top three preferred solutions. A common theme can be seen: the conditions are fuel-rich (high ER) with low EGR and moderately high IT advancement. These conditions can be explained by considering the relation between the operating parameters and the performance objectives. The equivalence ratio (around 1.0) gives maximum power, but also high NO_X. Therefore, some value on either side of 1.0 is expected. Fuel-rich conditions support higher power levels than fuel-lean conditions. Fuel-rich conditions are typically avoided in engine operation due to backfire issues, except possibly during hill climbing. For hydrogen, this is not expected to be an issue due to the fast combustion. These same conditions tend to result in lower NO_X emissions, so the EGR ratio of the preferred

solutions is close to zero. Finally, the IT being advanced by 5-10 CA BTDC is consistent with observations. Either extreme (0 CA BTDC or 20 CA BTDC) can result in lower power or higher NO_x, respectively, as seen in Figure 3.

Table 6. Operating parameters for top three preferred solutions.

Solution	Equivalence Ratio	EGR Ratio (%)	Ignition Timing (CA BTDC)
1	1.3	0	5
2	1.3	0.47	10.5
3	1.3	0	10

8. SUMMARY AND CONCLUSIONS

The present study considers combustion of hydrogen in an SI single cylinder engine. The relationships among the power, efficiency, and NO_x emissions, as well as three operating parameters of equivalence ratio, exhaust gas recirculation ratio, and ignition timing advancement, were investigated in a systematic manner. The power, efficiency, and NO_x emissions were all highly dependent on in-cylinder temperature and pressure. Therefore, the trend was found that for low (0.7) and high equivalence ratios (>1.1), all three parameters were lower than for medium equivalence ratios (0.8-1.0), where the values reached a maximum. Increasing levels of EGR were found to reduce NO_x emissions as well as the power and efficiency. On the other hand, increasing the ignition timing advancement was found to increase all three parameters. In addition, a

GA-NN approach was applied to find the best operating points that maximize power while minimizing NO_x. The power and efficiency were found to correlate well, so only the power and NO_x were considered. A Pareto front of non-dominated solutions quantified that fuel-rich conditions with low EGR levels (0-0.47%) and moderately advanced timing (5-10 CA BTDC) gave the best trade-offs between power and NO_x (8.99-9.06 kW and 343-362 ppm) for the considered engine conditions.

ACKNOWLEDGMENTS

The authors are thankful to the Libyan government for financial support and Missouri University of Science and Technology for providing the necessary facilities. Also, the authors would like to give their sincere thanks to Jun Li from AVL Advanced Simulation Technology for his support.

REFERENCES

[1] Saravanan N, Nagarajan G. An experimental investigation of hydrogen-enriched air induction in a diesel engine system. International Journal of Hydrogen Energy. 2008;33:1769-75.

[2] Ghazal OH. Performance and combustion characteristic of CI engine fueled with hydrogen enriched diesel. International Journal of Hydrogen Energy. 2013;38:15469-76.

[3] Subramanian V, Mallikarjuna J, Ramesh A. Performance, emission and combustion characteristics of a hydrogen fueled SI engine-an experimental study. SAE Technical Paper; 2005.

[4] Farhad S, Shamecki A, Ali M. Effects of spark advance, A/F ratio and valve timing on emissions and performance characteristics of hydrogen internal combustion engine. SAE Paper. 2009:01-1424.

[5] Karim GA. Hydrogen as a spark ignition engine fuel. International Journal of Hydrogen Energy. 2003;28:569-77.

[6] Khairallah HA, Koylu UO. Combustion Simulation of a Direct Injection Diesel Engine with Hydrogen Fuel Using a 3D Model with Multi-Fuel Chemical Kinetics. SAE Technical Paper; 2014.

[7] Verhelst S, Vancoillie J, Naganuma K, De Paepe M, Dierickx J, Huyghebaert Y, et al. Setting a best practice for determining the EGR rate in hydrogen internal combustion engines. International Journal of Hydrogen Energy. 2013;38:2490-503.

[8] Hu E, Huang Z. Optimization on Ignition Timing and EGR Ratio of a Spark-Ignition Engine Fuelled with Natural Gas-Hydrogen Blends. SAE Technical Paper; 2011.

[9] Shin B, Cho Y, Han D, Song S, Chun KM. Hydrogen effects on NOx emissions and brake thermal efficiency in a diesel engine under low-temperature and heavy-EGR conditions. International Journal of Hydrogen Energy. 2011;36:6281-91.

[10] Hountalas D, Mavropoulos G, Binder K. Effect of exhaust gas recirculation (EGR) temperature for various EGR rates on heavy duty DI diesel engine performance and emissions. Energy. 2008;33:272-83.

[11] Pariotis EG, Hountalas DT, Rakopoulos C. Modeling the effects of EGR on a heavy duty DI diesel engine using a new quasi-dimensional combustion model. SAE Technical Paper; 2005.

[12] Komninos N, Rakopoulos C. Modeling HCCI combustion of biofuels: A review. Renewable and Sustainable Energy Reviews. 2012;16:1588-610.

[13] Shi L, Cui Y, Deng K, Peng H, Chen Y. Study of low emission homogeneous charge compression ignition (HCCI) engine using combined internal and external exhaust gas recirculation (EGR). Energy. 2006;31:2665-76.

[14] Hu E, Huang Z, Liu B, Zheng J, Gu X, Huang B. Experimental investigation on performance and emissions of a spark-ignition engine fuelled with natural gas–hydrogen blends combined with EGR. International Journal of Hydrogen Energy. 2009;34:528-39.

[15] Verhelst S, Maesschalck P, Rombaut N, Sierens R. Increasing the power output of hydrogen internal combustion engines by means of supercharging and exhaust gas recirculation. International Journal of Hydrogen Energy. 2009;34:4406-12.

[16] Fontana G, Galloni E. Experimental analysis of a spark-ignition engine using exhaust gas recycle at WOT operation. Applied Energy. 2010;87:2187-93.

[17] Abd-Alla G. Using exhaust gas recirculation in internal combustion engines: a review. Energy Conversion and Management. 2002;43:1027-42.

[18] Swain M, Swain M, Leisz A, Adt R. Hydrogen peroxide emissions from a hydrogen fueled engine. International Journal of Hydrogen Energy. 1990;15:263-6.

[19] Sinclair L, Wallace J. Lean limit emissions of hydrogen-fueled engines. International Journal of Hydrogen Energy. 1984;9:123-8.

[20] Zareei J, Kakaee A. Study and the effects of ignition timing on gasoline engine performance and emissions. European Transport Research Review. 2013;5:109-16.

[21] Lawankar S, Dhamande DL, Khandare DS. Experimental study of effect of ignition timing and compression ratio on NOx emission of LPG fuelled engine. International Journal of Scientific & Engineering Research. 2012;3.

[22] Al-Baghdadi MAS. Effect of compression ratio, equivalence ratio and engine speed on the performance and emission characteristics of a spark ignition engine using hydrogen as a fuel. Renewable Energy. 2004;29:2245-60.

[23] Sandhu SS. Improvement in Performance and Emission Characteristics of a Single Cylinder SI Engine Operated on Blends of CNG and Hydrogen. Proceedings of World Academy of Science, Engineering and Technology: World Academy of Science, Engineering and Technology (WASET); 2013. p. 698.

[24] Subramanian V, Mallikarjuna J, Ramesh A. Effect of water injection and spark timing on the nitric oxide emission and combustion parameters of a hydrogen fuelled spark ignition engine. International Journal of Hydrogen Energy. 2007;32:1159-73.

[25] De Risi A, Donateo T, Laforgia D. Optimization of the combustion chamber of direct injection diesel engines. SAE Technical Paper; 2003.

[26] Wickman DD, Senecal PK, Reitz RD. Diesel engine combustion chamber geometry optimization using genetic algorithms and multi-dimensional spray and combustion modeling. SAE Technical Paper; 2001.

[27] Park SW. Optimization of combustion chamber geometry for stoichiometric diesel combustion using a micro genetic algorithm. Fuel Processing Technology. 2010;91:1742-52.

[28] Park S. Optimization of combustion chamber geometry and engine operating conditions for compression ignition engines fueled with dimethyl ether. Fuel. 2012;97:61-71.

[29] Kesgin U. Genetic algorithm and artificial neural network for engine optimisation of efficiency and NOx emission. Fuel. 2004;83:885-95.

[30] Costa M, Bianchi GM, Forte C, Cazzoli G. A numerical methodology for the multi-objective optimization of the DI diesel engine combustion. Energy Procedia. 2014;45:711-20.

[31] Hiroyasu T, Miki M, Kamiura J, Watanabe S, Hiroyasu H. Multi-objective optimization of diesel engine emissions and fuel economy using genetic algorithms and phenomenological model. SAE Technical Paper; 2002.

[32] Hiroyasu T, Miki M, Kim M, Watanabe S, Hiroyasu H, Miao H. Reduction of heavy duty diesel engine emission and fuel economy with multi-objective genetic algorithm and phenomenological model. SAE Technical Paper; 2004.

[33] Banerjee R, Bose P. Development of a Neuro Genetic Algorithm Based Virtual Sensing Platform for the Simultaneous Prediction of NOx, Opacity and BSFC in a Diesel Engine Operated in Dual Fuel Mode with Hydrogen under Varying EGR Conditions. SAE Technical Paper; 2012.

[34] Yousufuddin S, Venkateswarlu K. Effect of Compression Ratio and Equivalence Ratio on the Emission Characteristics of a Hydrogen-Ethanol Fuelled Spark Ignition Engine. International Journal of Advanced Science and Technology. 2012;40:91-100.

[35] Ji C, Wang S, Zhang B. Performance of a hybrid hydrogen–gasoline engine under various operating conditions. Applied Energy. 2012;97:584-9.

[36] Ji C, Wang S. Combustion and emissions performance of a hydrogen engine at idle and lean conditions. International Journal of Energy Research. 2013;37:468-74.

[37] Jagadish D, Kumar PR, Murhty KM. Performance and emission characteristics of diesel engine run on biofuels based on experimental and semi analytical methods. International Journal of Energy and Environment. 2011;2:899-908.

[38] Kakee A-H, Sharifipour S, Mashadi B, Keshavarz M, Paykani A. Optimization of spark timing and air-fuel ratio of an SI engine with variable valve timing using genetic algorithm and steepest descend method. UPB Sci Bull. 2015;77:61-76.

[39] Deb M, Banerjee R, Majumder A, Sastry G. Multi objective optimization of performance parameters of a single cylinder diesel engine with hydrogen as a dual fuel using pareto-based genetic algorithm. International Journal of Hydrogen Energy. 2014;39:8063-77.

[40] Yang Z, Wang L, Li S. Investigation into the optimization control technique of hydrogen-fueled engines based on genetic algorithms. International Journal of Hydrogen Energy. 2008;33:6780-91.

[41] Zhenzhong Y, Lijun W, Manlou H, Yongdi C. Research on optimal control to resolve the contradictions between restricting abnormal combustion and improving power output in hydrogen fueled engines. International Journal of Hydrogen Energy. 2012;37:774-82.

[42] Sandalcı T, Karagöz Y. Experimental investigation of the combustion characteristics, emissions and performance of hydrogen port fuel injection in a diesel engine. International Journal of Hydrogen Energy. 2014;39:18480-9.

[43] Khairallah HA, Vaz WS, Koylu UO. Influence of ignition timing and EGR on the NOx emission and the performance of an SI engine fueled with hydrogen. ASME 2015 International Mechanical Engineering Congress and Exposition: American Society of Mechanical Engineers; 2015. p. V06AT7A060-V06AT07A.

[44] GitHub. chem.inp_15. 2015.

[45] Baukal C. Everything You Need to Know About Nitric Oxides. 2006.

[46] Nandi AK. GA-fuzzy approaches: application to modeling of manufacturing process. Statistical and Computational Techniques in Manufacturing: Springer; 2012. p. 145-85.

[47] Vaz W, Nandi AK, Landers RG, Koylu UO. Electric vehicle range prediction for constant speed trip using multi-objective optimization. Journal of Power Sources. 2015;275:435-46.

[48] Deb K, Agrawal S, Pratap A. A fast Elitist Non-dominated Sorting Genetic Algorithm for multi-objective Optimization (NSGA II). 2002.

[49] Demuth H, Beale M. Neural network and signal processing toolboxes for use with MATLAB, user guide version 6.1. The MathWorks Inc. 2002.

[50] Miettinen K. Nonlinear multiobjective optimization Kluwer. Boston, MA, USA. 1999.

II. INFLUENCE OF OPERATING PARAMETERS ON PERFORMANCE AND EMISSIONS FOR A COMPRESSION-IGNITION ENGINE FUELED BY HYDROGEN/DIESEL MIXTURES

ABSTRACT

Hydrocarbon exhaust emissions are mainly recognized as a consequent of carbon-based fuel combustion in compression-ignition (CI) engines. Alternative fuels can be coupled with hydrocarbon fuels to control the pollutant emissions and improve the engine performance. In this study, different parameters that influence the engine performance and emissions are illustrated with more details. This numerical work was carried out on a dual-fuel CI engine to study its performance and emission characteristics at different hydrogen energy ratios. The simulation model was run with diesel as injected fuel and hydrogen, along with air, as inducted fuel. Three-dimensional CFD software for numerical simulations was implemented to simulate the direct-injection CI engine. A reduced-reaction mechanism for n-heptane was considered in this work instead of diesel. The Hiroyasu-Nagel model was presented to examine the rate of soot formation inside the cylinder. This work investigates the effect of hydrogen variation on output efficiency, ignition delay, and emissions. More hydrogen present inside the engine cylinder led to lower soot emissions, higher thermal efficiency, and higher NO_x emissions. Ignition timing delayed as the hydrogen rate increased, due to a delay in OH radical formation. Strategies such as an exhaust gas recirculation (EGR) method and diesel injection timing were considered as well, due to their potential effects on the engine outputs. The relationship among the engine outputs and the operation conditions were also considered.

Keywords: Hydrogen levels; diesel; dual-fuel engine; NO_X formation; soot formation; ignition delay.

1. INTRODUCTION

Internal combustion engines (ICEs), run by burning hydrocarbon (HC) fossil fuels, are essentially used in wide range of applications such as transportation, civil construction, and electrical power generation. Unfortunately, fossil fuels are not renewable and challenging to use as they emit high levels of pollutants. The emitted emissions, such as carbon dioxide (CO_2), carbon monoxide (CO), combinations of nitric oxide and nitrogen dioxide (NO_X), unburned hydrocarbons, and soot, continue to cause multiple problems associated with the environment and human health. The clean, sustainable, and alternative fuels can supplement hydrocarbon fuels to reduce the harmful impacts of emissions while using the existing conventional internal combustion engines.

Use of hydrogen in ICEs is regarded as an option that can meet further energy demands and reduce hydrocarbon emissions while maintaining high thermal efficiency. Hydrogen is known as one of the most trustful, renewable, and sustainable fuels. Utilization of hydrogen as a fuel in ICEs can improve the thermal efficiency associated with a reduction of carbon-based emissions compared to hydrocarbon fuels such as natural gas, gasoline, and diesel. A major benefit of hydrogen usage for power generation or the transportation sector is increasing our dependence on renewable sources and minimizing the usage of non-renewable fossil fuels [1]. Moreover, hydrogen, as a carbon-free fuel, has unique properties. For example, hydrogen is a very flammable gas

compared to all other fuels, and as a result, it can be combusted at different equivalence ratios. Low ignition energy of hydrogen also has a significant advantage because hydrogen can run on a lean mixture and guarantees quick ignition with lower NO_X and high combustion efficiency [2-4]. The high burning velocity of hydrogen (237 cm/s) produces a reduction in exhaust losses and increases engine thermal efficiency. Hydrogen also has a high diffusivity that leads to improved homogeneity in the combustion chamber mixture, which helps the fuel burn completely [5]. Hydrogen as a fuel is more suitable in spark-ignition (SI) engines than CI engines because of its higher auto-ignition temperature (858 K) compared to diesel fuel (525 K). Although many studies have successfully modified SI engines to run with hydrogen as a single fuel, these engines have not been employed in applications on a commercial scale [6, 7]. On the other hand, no studies were able to modify the existing CI engines to run with hydrogen as a single fuel [8, 9].

Recently, researchers [10, 11] have assessed the potential of hydrogen used in combination with diesel in CI engines. While these investigations have shown a large reduction in soot, HC, and CO_2 emissions, higher hydrogen values present inside the engine cylinder can increase the harmful emission of NO_X. Several studies [3, 4, 12, 13] reported on hydrogen-diesel dual-fuel engines and concluded that a significant improvement in thermal efficiency could be achieved with hydrogen addition. The issue of higher NO_X emissions associated with hydrogen as compared to pure diesel has been addressed, and can be attributed to high combustion temperature and oxygen levels in the air. Similar conclusions were also drawn by numerical and experimental studies [11, 12]. The most recent numerical work [13] reported that substituting and adding hydrogen to

diesel fuel has a positive impact on pollutant emissions, excluding NO_x emissions. In addition, replacement of hydrogen in diesel engines causes a long ignition delay period, therefore delaying the start of combustion and more fuel entering the engine. Increasing the hydrogen amount to more than 50% of the total energy led to a knocking phenomenon in the engine [13]. Hydrogen in diesel engines has potential effects not only on regulated emissions but also on unregulated emissions (C_nH_m). It was found that unregulated emissions, such as acetaldehyde (CH_3CHO), BTX (C_6H_6, C_7H_8, and C_8H_{10}), and olefins (C_2H_4 and C_3H_6), decreased when hydrogen was added to diesel fuel in CI engines [14]. Not only should the effect of hydrogen on emissions be considered but also should the effect of hydrogen on the ignition delay on the engine performance.

The ignition delay can be defined as the period of time between the start of the diesel injection into the cylinder and the start of combustion, or, the point of the first noticeable rise in cylinder pressure due to the energy release within the mixture [4]. Ignition delay period increases with the addition of hydrogen due to the formation of some chemical species during the compression caused by oxidation of gases, which then leads to the loss of active OH radicals with the hydrogen molecules [15].

The effect of utilizing different fuels—hydrogen, liquefied petroleum gas (LPG), and hydrogen-LPG mixture—on the ignition timing in dual-fuel diesel engines was experimentally investigated in [16]. The experiments were performed at different load conditions and various diesel substitutions. It was observed that the ignition delay of the dual-fuel engine depends on the type of fuels and their concentrations, charge temperature, pressure, and oxygen concentration.

Besides finding alternative, clean, and sustainable energy sources, it is very important to design effective technologies for existing conventional engines fueled by gasoline and diesel as well as hydrogen to increase the engine performance and reduce emissions. Some common strategies, such as exhaust gas recirculation (EGR) and diesel injection timing, have been used to reduce exhaust emissions and improve engine performance. High temperature of hydrogen combustion is the main route for an inherent problem of NO_X formation. Therefore, EGR was considered as a promising technique to accomplish a significant reduction in NO_X emissions in CI engines [17-19]. The EGR mechanism can be defined as a recirculation of some amount of the exhausted gases from the previous cycle back to the cylinders in order to reduce the in-cylinder temperature. Even though an EGR technique in diesel engines may not be attractive due to increasing soot emissions, it can still be considered for hydrogen/diesel dual-fuel engines [20]. To guarantee the combustion stability and decrease NO_X emissions, several investigations have considered hydrogen combustion with an EGR technique [21-24]. The effects of hydrogen on NO_X emissions and brake thermal efficiency under heavy EGR conditions were studied by Shin [24], who reported that the carbon dioxide concentration increased with the EGR ratio. EGR rate has a significant effect on both nitric oxide (NO) and soot in heavy duty DI diesel engines, whereas the increase of EGR percentage results in a reduction of NO and a sharp increase of soot emission. That effect is much stronger at low engine speeds [25]. High EGR levels are commonly utilized in CI and homogeneous charge compression-ignition (HCCI) engines [26-28]. Generally, increasing hydrocarbon emissions is a consequence of raising EGR rate compared to the dual-fuel engine with no EGR; however, these HC products are significantly lower compared to HCs produced by

pure diesel engines. EGR techniques in dual-fuel engines associated with hydrogen induction are necessary for the control of the in-cylinder temperature and NO_X emissions, and improve the engine performance compared to pure diesel operation [17].

The utilization of EGR techniques in the hydrogen engine helps to lower NO_X emissions, compared to hydrogen combustion with no EGR. Higher specific heat capacity is achieved with EGR and, as a result, a reduction of the in-cylinder temperature occurs. Reducing the combustion temperature results in excessively high unburned fuel and CO, coupled with low NO_X, may decrease the thermal efficiency. Hydrogen is a very flammable fuel, so adjusting the EGR level to a specific point can help for regulating the engine load. [29-31].

Another common strategy to lower NO_X and soot emissions in diesel engines is to modify the start of injection timing. Diesel injection timing has an influence on the engine performance and emissions. The advance timing of diesel injection causes an early combustion, and that leads to an increase in the in-cylinder pressure and temperature. As a result, the engine power and NO_X increase [32, 33]. EGR and injection timing techniques are extremely useful in terms of maximizing NO_X reduction by decreasing the temperature inside the engine cylinder; however, the power is also significantly reduced. Engine designers' goals are to maximize the harmful emission reduction and the output power while, in some cases, maximizing the power can also cause NO_X to increase. Thus, this issue becomes a typical multi-objective optimization problem with conflicting objectives.

The present work systematically studies the relationship between the efficiency, soot, and NO_X emissions as an output and the operating conditions—hydrogen levels,

EGR, and injection timing—for a hydrogen/diesel dual-fuel engine. There is limited research dealing with the operation parameters considered here for dual-fuel engines run by hydrogen/diesel mixtures. Furthermore, there are very few studies that consider the influence of hydrogen/diesel ratio on the ignition delay period affecting the engine performance in a CI engine. The goal of this study is to numerically investigate the effect of operating parameters, including hydrogen variation, on the engine performance and output emissions. A multi-dimensional commercial software package was implemented in this work, as it offers a more concrete understanding of the combustion phenomena, including the formation of species inside the engine cylinder that cannot be achieved experimentally. The software also results in accurate predictions (with less margin of error) and a significant reduction in development costs and time.

2. COMPUTATIONAL METHODS

In hydrogen combustion, obvious issues include higher values of pressure rise, combustion knock, higher temperature, and NO_X emissions. These issues should be considered, carefully studied, and controlled. The present computational work investigated the engine performance and emissions characteristics of diesel engines fueled by a hydrogen/diesel mixture. Reduced dual-fuel reaction mechanisms for both hydrogen and diesel were coupled into the AVL FIRE® 3D CFD software for numerical simulation. This study considered an engine model that was created by using AVL Fire and validated with an experimental work [34, 35] to expect the output power, efficiency, and emissions of the hydrogen/diesel dual-fuel engine. The detailed mechanism [36] for

the chemical reaction kinetics of n-heptane consists of 349 elementary reactions and 76 species, including hydrogen chemical reactions, and excluding the oxidation reactions of nitrogen. N-heptane was considered in this work instead of diesel due to its cetane number (56), which is close to cetane number of diesel fuel (50). Thus, NO_x chemical reactions (a group of nitric oxide [NO] and nitrogen dioxide [NO_2] reactions) are added to obtain the NO_x formation rate. The Zeldovich mechanism of NO formation is shown below.

$$N_2 + O \leftrightarrow N + NO \tag{1}$$

$$N + O_2 \leftrightarrow NO + O \tag{2}$$

$$N + OH \leftrightarrow NO + H \tag{3}$$

357 elementary reactions are considered the final chemical kinetic mechanism. Numerical simulation was implemented to better understand the complex combustion phenomena and pollutant formation process inside the cylinder, which are difficult to observe and measure through experimental studies. Hydrogen is injected at the engine intake port, and when the intake valve is closed, hydrogen is assumed to be in the combustion chamber mixed with air. Diesel fuel was considered to be directly injected into the chamber by using an injector located at the top center of the combustion chamber. The species in the chemical mechanism were used to calculate the pollutant emissions such as CO_2, CO, and NO_x at the exhaust.

2.1. SOOT FORMATION

The regulations on soot emissions have become more rigid due to the emissions' negative influence on human health and the environment. Understanding of soot formation is very important in order to apply the best operating conditions that will result in a reduction in soot emissions. Hydrocarbon fuels exhibit a strong tendency to form carbonaceous particles (soot), which form in the early stages of combustion. Some of the soot formed is depleted due to the follow-up oxidation process. The most significant factors during soot formation are the air/fuel ratio (C/H ratio and C/O ratio), temperature, pressure, and residence time. The Hiroyasu-Nagel model [37], which is by default inserted into AVL software to model the soot emissions, was considered in this work.

2.2. MODEL PARAMETERS

The engine geometry was created by using AVL Fire software (Figure 1). The properties of hydrogen compared to diesel are demonstrated in Table 1, and specifications of the simulated single cylinder engine, as well as the operating conditions, are shown in Table 2.

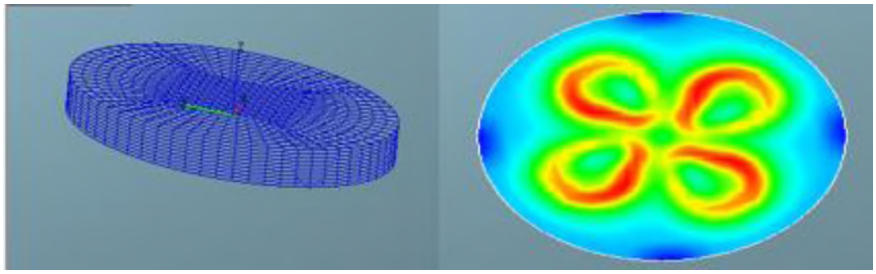

Figure 1. Engine geometry.

Table 1. Properties of fuels.

Properties	Hydrogen	Diesel
Minimum ignition energy (mJ)	0.02	-
Flammability limits in air (vol. %)	4.0-75	-
Lower heating value (MJ/kg)	120	42.2
Stoichiometric fuel/air mass ratio	0.029	0.069
Density at STP (kg/m3)	0.083	824
Auto ignition temperature (K)	858	530
Stoichiometric flame speed (m/s)	2.65-3.25	0.3

Table 2. Engine specifications.

Number of cylinders	1
Bore (mm)	80
Stroke (mm)	110
Engine speed (rpm)	1500
Compression ratio (-)	16.5:1
Connecting rod length (mm)	235
Max. brake power (kW)	3.74
Piston type (-)	Flat
Number of injector nozzle holes (-)	4
Hole diameter (m)	0.000169
Spray angle (-)	160°
Fuel amounts (Vol. %)	7.14
Initial temperature (K)	333
Initial pressure (bar)	1
Injection timing (CA)	23° BTDC
Injection duration (-)	30°

3. MODEL VALIDATION

This numerical work considers an engine model created by using AVL Fire software. The model was run at different operating conditions according to experimental operating conditions. The simulation model was validated with experimental data [34, 35,

38] that considered the same engine geometry to measure the engine output power, efficiency, and emission characteristics of a hydrogen/diesel dual-fuel engine. Both experiments and simulations used the same hydrogen/diesel blends as a fuel. Hydrogen was inducted at flow rate of 7.5 l/min (~12 % by energy at full load) and 20 l/min (~37.5 % by energy at full load) by using two different techniques of carburation and timed port injection (TPI). Diesel was injected inside the cylinder at 23° BTDC with an injection duration of 30° CA. The engine was run at a constant speed of 1500 rpm and brake powers of 1.06, 1.89, 2.9, and 3.74 kW, and engine loads of 25%, 50%, 75%, and 100%, respectively. In the present numerical study, the hydrogen TPI case was considered due to its great improvement in the fuel metering compared to a carburetor. Hydrogen/air mixture was assumed to be inside the cylinder when the diesel fuel was injected. The results were validated against experimental results in terms of the in-cylinder pressure and the output emissions (soot, NO_x, CO, and CO_2). The correlation coefficient (R) and the coefficient of determination (R^2) were used in test validation to evaluate the model performance. The coefficient of determination is the square of coefficient of correlation R. The correlation coefficient is an indicator of the degree of the change between the predicted and the real data. R value of 1 would represent a perfect fit between the simulations and experimental outputs. The pressure curves with crank angle degree show reasonable agreements between the experiments and simulation at 75% and full load for 7.5 l/min hydrogen/diesel mixture, as shown in Figure 2. The correlation coefficient for the pressure data was calculated to evaluate the accuracy of the model. R value for the pressure data is 0.969. This value indicates a perfect fit and best validation performance of the model.

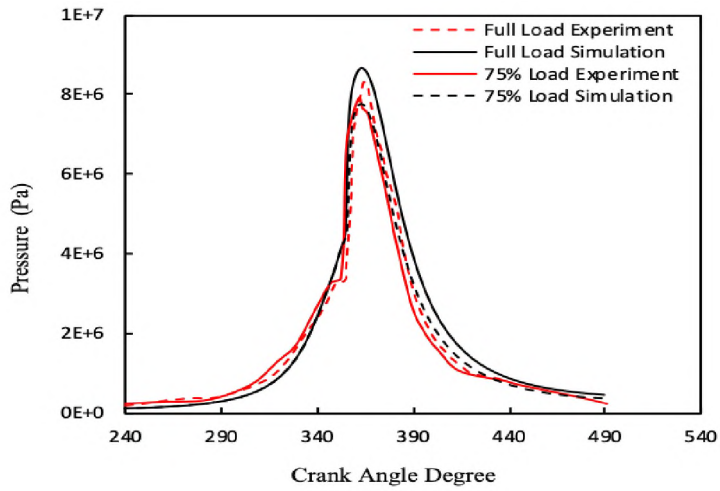

Figure 2. Pressure with crank angle degree for 7.5 l/min H_2 flow rate at 75% and full load [35, 38].

Peak pressure as an important parameter was also considered at different engine loads. The pressure was observed to rise with engine loads due to a higher temperature at higher engine loads. Clearly, predicted and experimental values are in very good agreement, as seen in Figure 3. The correlation coefficient for peak pressure data is 0.992.

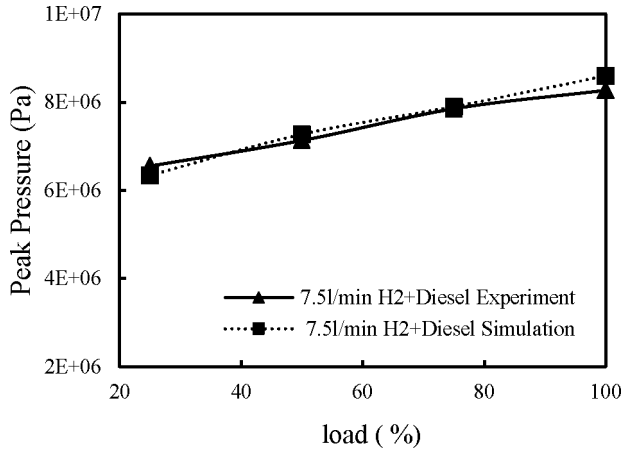

Figure 3. Variation of peak pressure with loads for 7.5 l/min H_2 flow rate [35].

Figures 4 and 5 represent experimental and predicted values of emission parameters at different brake powers. 20 l/min hydrogen/diesel blends were considered for the output emissions validation due to well-documented experimental data. Figure 4 illustrates the variation of soot emission at different engine brake powers. Soot emissions were observed to slightly increase at higher brake power. The reason is that to achieve a higher brake power, more diesel flow inside the cylinder is required; hence, the formation of soot increases with increasing diesel flow. Figure 4 also shows the variation of NO_X emissions with brake power. NO_X emissions, in general, occur at high combustion temperature. NO_X emissions were observed to increase at higher brake power. This is due to an increase in combustion temperature at higher brake powers. Correlation coefficients for individual outputs are 0.9844 for soot, and 0.9859 for NO_X.

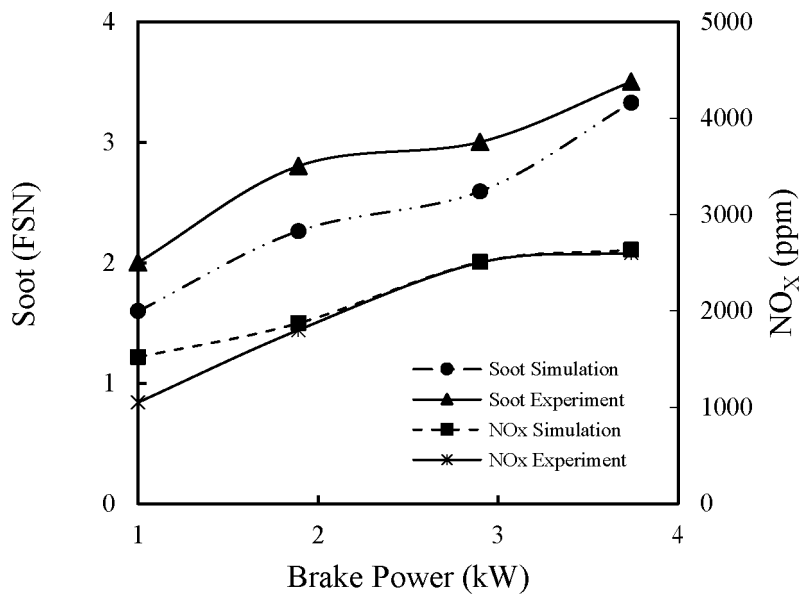

Figure 4. Variation of soot and NO_X emissions with brake power for 20 l/min H_2 flow rate [34].

Variations of CO and CO_2 emissions at different brake powers are shown in Figure 5 for 20 l/min hydrogen/diesel blends. The data clearly displays an increase of CO and CO_2 at high brake powers. This is due to more diesel flows inside the engine producing CO emissions and, with enough oxygen, CO_2 emissions. Correlation coefficients of validation performance for both CO and CO_2 emissions are 0.889 and 0.9958, respectively. The correlation coefficient for CO is slightly lower than CO_2 due to small output values of CO emissions.

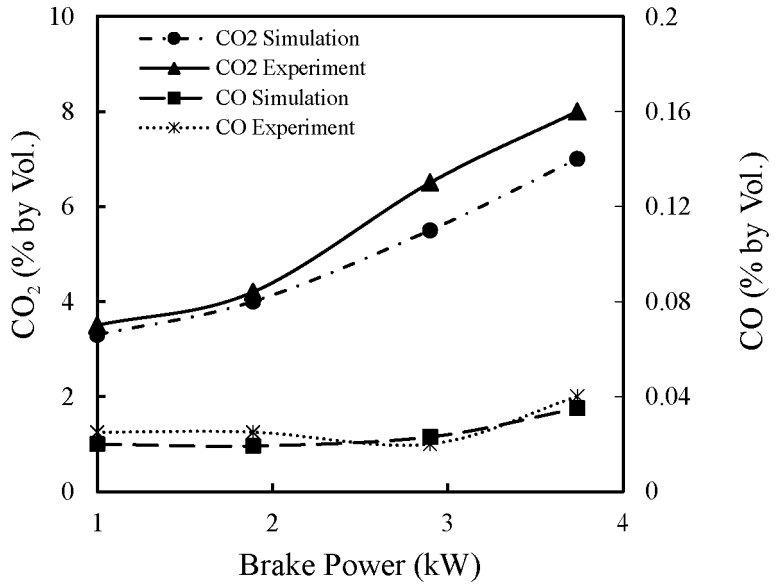

Figure 5. Variation of CO and CO_2 emissions with brake power for 20 l/min H_2 flow rate [34].

The best validation performance was demonstrated by the simulation model. As shown in Table 3, the predicted and measured values are in very good agreement and correlated very well.

Table 3. Comparison between numerical and experimental results.

20 l/min Hydrogen/Diesel								
Brake Power (kW)	Soot (FSN) Sim.	Soot Exp.	NO_x (ppm) Sim.	NO_x Exp.	CO (%) Sim	CO Exp.	CO_2 (%) Sim.	CO_2 Exp.
1	1.597217	2	1518.47	1050	0.02	0.025	3.3	3.5
1.89	2.260728	2.8	1870.52	1800	0.0192	0.025	4	4.2
2.9	2.591341	3	2505.13	2500	0.023	0.02	5.5	6.5
3.74	3.325251	3.5	2632.46	2600	0.035	0.04	7	8
R-Value	0.984415904		0.985931791		0.889265807		0.995820831	
R^2-Value	0.96907		0.97205		0.79078		0.99165	

It is also obvious that the developed model is able to predict emission parameters and engine performance with good accuracy; thus, the model was applied to examine different portions of CI engine to investigate the potential influences of the operation parameters (injection timing, EGR, and hydrogen levels) on the engine outputs (efficiency and emissions).

4. PROBLEM DESCRIPTION

A numerical investigation using AVL Fire software was conducted on a heavy diesel engine under different operating conditions of various hydrogen levels (%), diesel injection timing, and EGR levels (%). The effect in variation of each parameter was analyzed using numerical results and contours extracted from the software. As shown in Table 4, the objective of this work was to investigate the potential effects of considered operating parameters on performance and emission characteristics of a diesel engine

enriched with hydrogen fuel. Minimum soot and NO_X emissions and maximum indicated thermal efficiency are the desired objectives in this study.

Table 4. Operating parameters and objectives.

Parameters	Value	Objective
Injection Time (BTDC)	10, 15, 20, and 30	Min [Soot Emission (FSN)]
H_2 energy ratio (%)	5, 10, 20, 37.5, and 50	Max [Indicated Thermal Efficiency (%)]
EGR Level (%)	0, 5, 10, and 15	Min [NO_x Emission (ppm)]

5. RESULTS AND DISCUSSION

5.1. EFFECT OF HYDROGEN VARIATION ON NO_X, SOOT, AND EFFICIENCY

In this study, different hydrogen energy ratios are considered at engine load of 3.7 kW brake power. The hydrogen energy ratio was calculated according to the measured hydrogen, diesel lower heating values, and mass flow rates of the fuels as seen in the following equation:

$$X_{H2} = \frac{\dot{m}_{H2} * \dot{L}HV_{H2}}{\dot{m}_D * LHV_D + \dot{m}_{H2} * LHV_{H2}} * 100 \quad (4)$$

Where, X_{H2} : is the hydrogen energy ratio [%]

$\dot{m}_{H2}$: is the mass flow rate of hydrogen [kg/s]

LHV_{H2} : is the lower heating value of hydrogen [kJ/kg]

$\dot{m}_D$: is the mass flow rate of diesel [kg/s]

LHV_D : is the lower heating value of diesel [kJ/kg]

The variation of hydrogen with NO_x, soot emissions, and efficiency is shown in Figure 6 and Figure 7, respectively. The EGR level and the injection timing for diesel were kept constant at 0% and 10 CA BTDC, respectively. Figure 6 illustrates the effect of hydrogen rates on NO_x and soot concentrations in the cylinder. NO_x formation was observed to increase by approximately 33% when raising the hydrogen ratio up to 50%, as compared to a 5% hydrogen ratio. This is due to high in-cylinder temperature, which is the essential route of NO formation. On the other hand, with more hydrogen injected into the engine cylinder, soot concentration reduces by ~ 59% at 50% hydrogen, compared to a minimum hydrogen ratio. Because of the increased hydrogen ratio, the volume of hydrocarbon fuel (diesel) is reduced and replaced with clean and free carbon fuel (hydrogen) in the cylinder.

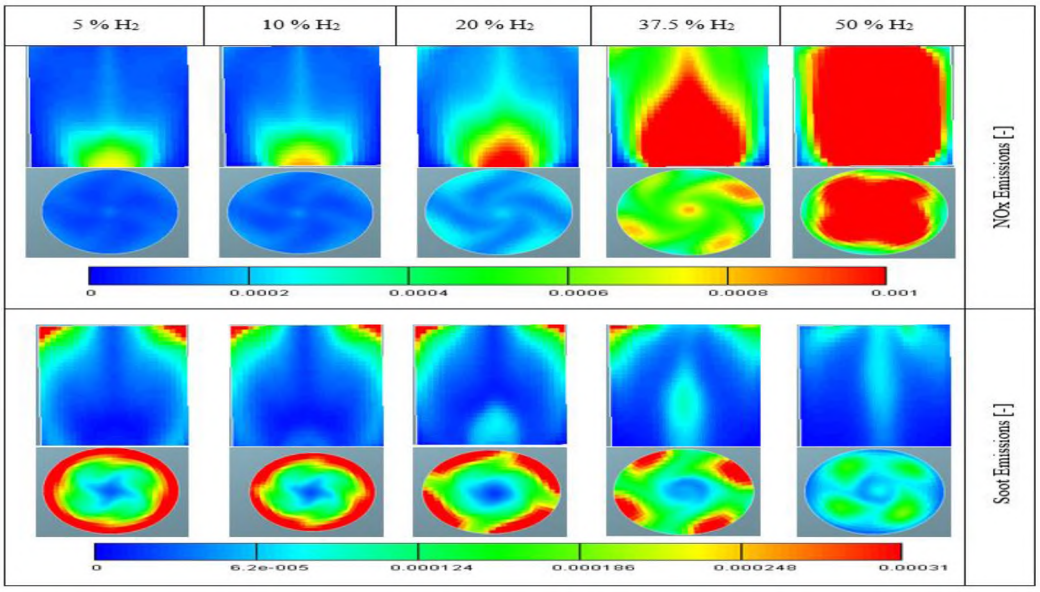

Figure 6. Effect of hydrogen level on soot and NOx emissions within the engine cylinder at 0% EGR and 10 CA BTDC injection timing.

Figure 7 shows the effect of hydrogen levels on the power and efficiency of a CI engine. As the hydrogen amount increased, the pressure inside the cylinder increased; thus, the engine power and efficiency increased.

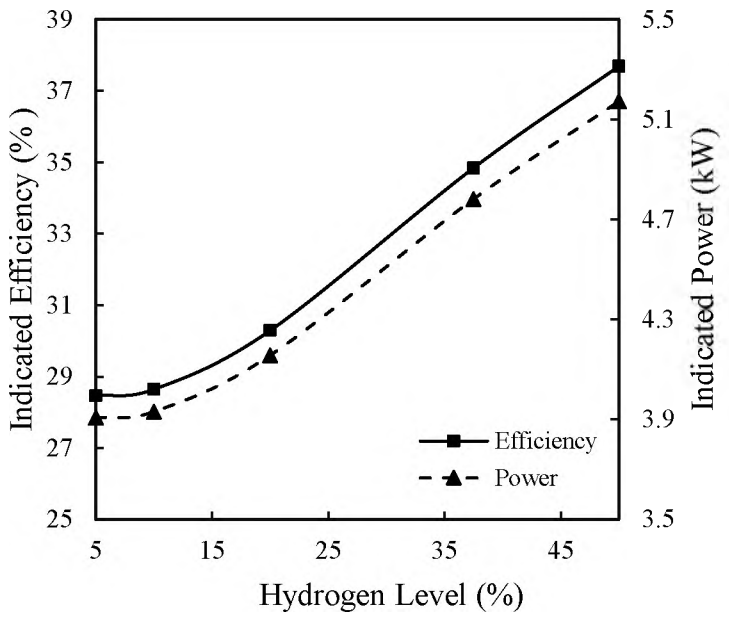

Figure 7. Effect of hydrogen level on engine power and efficiency at 0% EGR and 10 CABTDC injection timing.

5.1.1. Effect of Hydrogen Variation on the Ignition Delay. Ignition delay is the period of time between when fuel injects into the cylinder and the start of combustion [4]. The ignition delay period consists of physical and chemical delays taking place simultaneously. The fuel's properties and composition are responsible for the physical time delay. While the fuel reactions in the combustion chamber are the reason for the chemical delay period, the chemical reactions depend on cylinder temperature, cylinder pressure, and fuel properties [39]. The chemical delay period is the interval between the start of compression and the H2O2 molecule breakdown associated with the increased

active radical OH concentration that leads to pressure rise [40]. Figure 8a illustrates that when the H2O2 species starts to dissociate, the active radical OH forms, causing a pressure rise inside the cylinder.

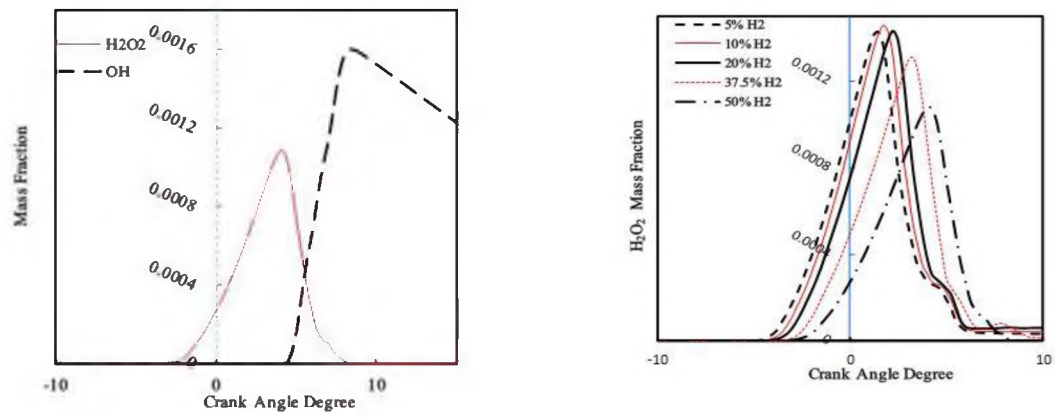

A B

Figure 8. Variation of species mass fraction with crank angle.

Variation of H_2O_2 mass fraction with different hydrogen ratios is shown in Figure 8b. By increasing the hydrogen level in the diesel engine, formation, as well as decomposition, of H_2O_2 was delayed, as depicted in Figure 8b. This led to a delay in forming the active radical OH, thereby delaying ignition timing.

5.2. EFFECT OF EXHAUST GAS RECIRCULATION ON ENGINE OUTPUTS

In this section, the effect of EGR on both NO_X and soot emissions, as well as the engine efficiency, is presented. Figure 9 demonstrates the effect of EGR variations on the engine emissions. The hydrogen level and diesel injection timing (IT) was fixed at 50% and 10 CA BTDC, respectively. The figure illustrates that EGR is indeed valuable in

terms of decreasing NO_x emissions: NO_x was observed to decrease by approximately 44%, 74%, 88% at 5%, 10%, 15% of EGR utilization, respectively, compared to no EGR. Decreasing the combustion temperature as one of the most important routes of NO_x formation is the main reason for the reduction in NO_x emission. It was also found that, as EGR increased, the air/fuel volume inside the engine cylinder decreased; therefore, the soot oxidation rate was decreased, leading to increased soot formation. However, the efficiency was found slightly decreased by increased EGR level, as shown in Figure 10. Because of a reduction in air/fuel volume and hydrogen flame speed inside the engine with increased EGR level, the engine power, along with efficiency, decreased.

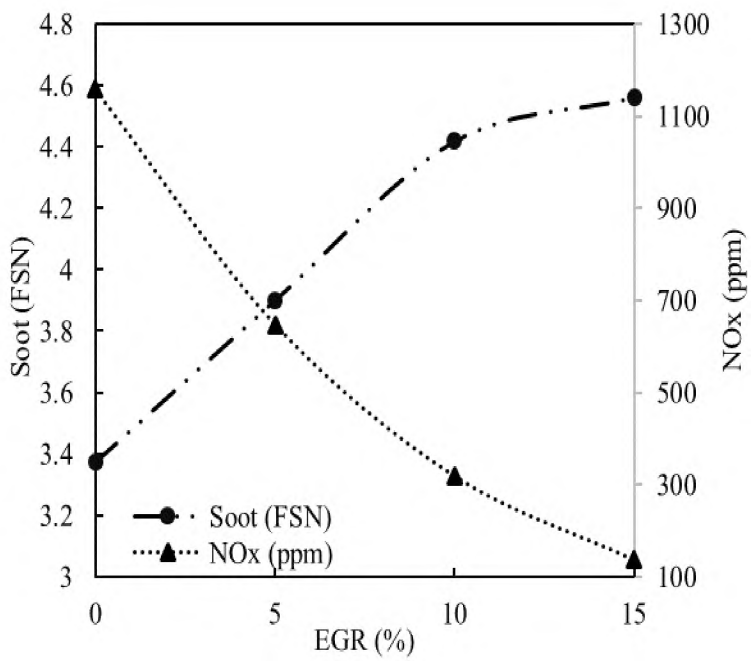

Figure 9. Variation of soot and NO_x emissions with EGR level at 50% hydrogen and 10 CA BTDC injection timing.

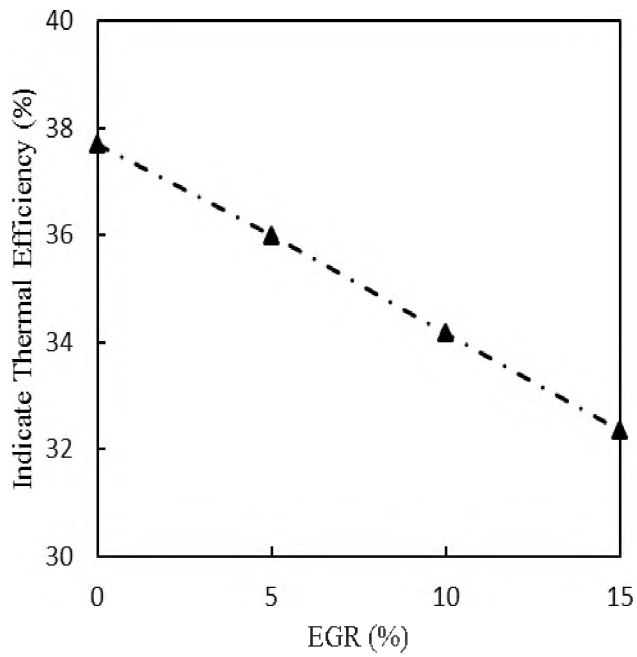

Figure 10. Effect of EGR on the engine efficiency at 50% hydrogen and 10 CA BTDC injection timing.

5.3. EFFECT OF DIESEL INJECTION TIMING ON NO_X, SOOT, AND EFFICIENCY

The parameter of diesel injection timing has an important effect on hydrogen/diesel engine performance and output pollutants, as shown in Figures 11 and 12. For these computations, the hydrogen level was 50% and the EGR level was 0%. From Figure 11, the engine efficiency was observed to significantly increase with advanced diesel injection timing. NO_X emissions in Figure 12 increased, as well. Since the combustion takes place earlier as the diesel injects inside the cylinder early, enough time is provided to complete the combustion. Therefore, the in-cylinder pressure and temperature increase, which leads to an improvement of the output power and efficiency. However, NO_X emissions also increase. The soot emissions shown in Figure 12 decreased

with advanced injection timing because, with enough time, most of the soot formed at the first stage of combustion is depleted due to an oxidation.

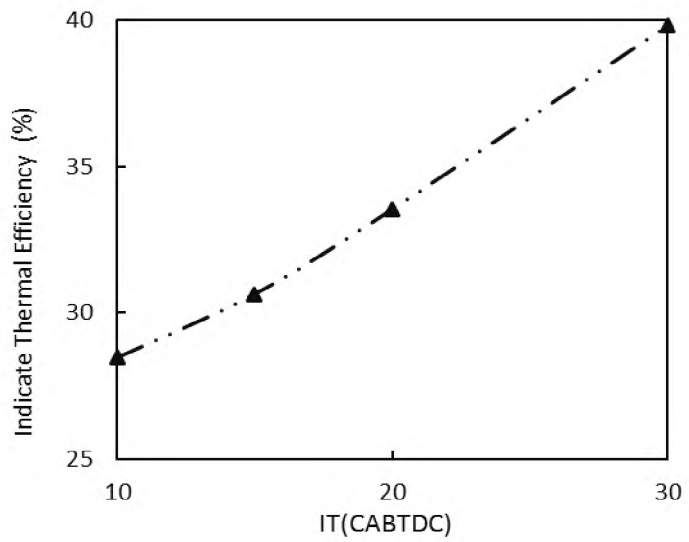

Figure 11. Effect of injection timing on the engine efficiency at 50% hydrogen and 0% EGR.

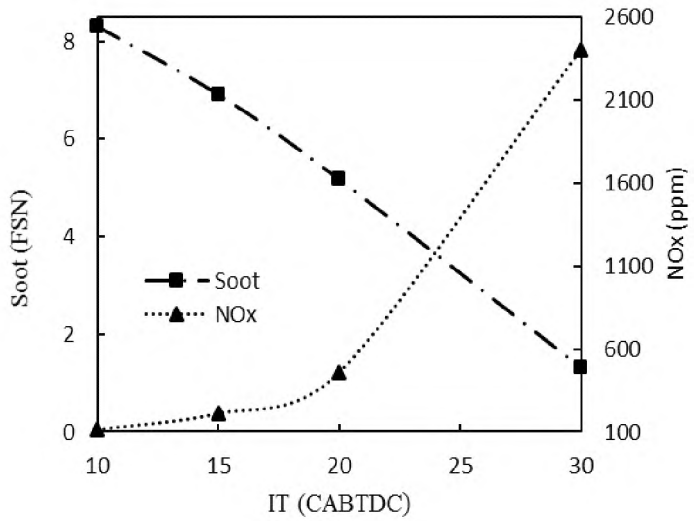

Figure 12. Effect of injection timing on NO_X, and soot emissions at 50% hydrogen and 0% EGR.

6. SUMMARY AND CONCLUSIONS

The present study considered the effect of operation conditions on the engine performance and emissions for a CI dual-fuel engine fueled by hydrogen/diesel mixtures. The relationships between the efficiency, soot, and NO_X emissions, and the operating parameters (hydrogen variations, EGR, and injection timing), were studied in a systematic way. An advanced CFD software was used in this study and the results were validated against experimental data with good agreement. Effects of the considered operating conditions on the engine performance and emissions are summarized as follows:

- Injecting more hydrogen inside the cylinder led to a reduction in soot emission by ~ 60% due to replacing hydrocarbon diesel fuel by the carbon-free hydrogen fuel. NO_X emissions and efficiency were observed to increase with hydrogen by 33% and 25%, respectively, due to high combustion temperature and in-cylinder pressure rise.
- Ignition timing, as one of the most important parameters in diesel engines, was considered at different hydrogen levels. It was found that, as hydrogen level increased, the ignition timing occurred late due to the late formation of active radical OH.
- NO_X emissions were reduced by 88% with increasing the EGR level to 15%, compared to no EGR case, due to the reduction of in-cylinder temperature. However, soot emission increased with the EGR level.
- With advanced injection timing, soot emission was reduced because, with enough

time, most of the soot formed at the first stage of combustion was depleted due to oxidation.

- NO_X emission increased with increasing diesel injection timing because, as the injection timing was advanced, reactions took place earlier, leading to an increase in the in-cylinder temperature.

Multi-objective optimization techniques can be considered for future work to find the best operating conditions for the highest engine performance and lowest pollutant emissions.

ACKNOWLEDGMENTS

The authors would like to thank the Department of Mechanical and Aerospace Engineering at Missouri S&T for the computational facilities and the Libyan Government for the financial support of Abdulhakim I. Jabbr. Also, the authors would like to give their sincere thanks to Dr. Hassan A. Khairallah from Tobruk University, Libya, for his help.

REFERENCES

[1] Shivaprasad K, Kumar G, Guruprasad K. Performance, emission and fuel induction system of hydrogen fuel operated spark ignition engine-A review. International Journal of Modern Engineering Research (IJMER). 2012;2:565-71.

[2] Saravanan N, Nagarajan G. An experimental investigation of hydrogen-enriched air induction in a diesel engine system. International Journal of Hydrogen Energy. 2008;33:1769-75.

[3] Ghazal OH. Performance and combustion characteristic of CI engine fueled with hydrogen enriched diesel. International Journal of Hydrogen Energy. 2013;38:15469-76.

[4] Heywood JB. Internal combustion engine fundamentals. 1988.

[5] Ma F, Wang J, Wang Y, Wang Y, Zhong Z, Ding S, et al. An investigation of optimum control of a spark ignition engine fueled by NG and hydrogen mixtures. International Journal of Hydrogen Energy. 2008;33:7592-606.

[6] Khairallah HA, Vaz WS, Koylu UO. Influence of ignition timing and EGR on the NO_x emission and the performance of an SI engine fueled with hydrogen. ASME 2015 International Mechanical Engineering Congress and Exposition: American Society of Mechanical Engineers; 2015. p. V06AT7A060-V06AT07A.

[7] Subramanian V, Mallikarjuna J, Ramesh A. Performance, emission and combustion characteristics of a hydrogen fueled SI engine-an experimental study. SAE Technical Paper; 2005;No. 2005-26-349.

[8] Bose PK, Maji D. An experimental investigation on engine performance and emissions of a single cylinder diesel engine using hydrogen as inducted fuel and diesel as injected fuel with exhaust gas recirculation. International Journal of Hydrogen Energy. 2009;34:4847-54.

[9] Loganathan M, Velmurugan A, Gunasekaran EJ, Tamilarasan P. Combustion analysis of a hydrogen-diesel fuel operated DI diesel engine with exhaust gas recirculation. Frontiers in Energy. 2017:1-7.

[10] Aydin K, Kenanoğlu R. Effects of hydrogenation of fossil fuels with hydrogen and hydroxy gas on performance and emissions of internal combustion engines. International Journal of Hydrogen Energy. 2018;43(30):14047-58.

[11] An H, Yang W, Maghbouli A, Li J, Chou S, Chua K. A numerical study on a hydrogen assisted diesel engine. International Journal of Hydrogen Energy. 2013;38:2919-28.

[12] Sandalcı T, Karagöz Y. Experimental investigation of the combustion characteristics, emissions and performance of hydrogen port fuel injection in a diesel engine. International Journal of Hydrogen Energy. 2014;39:18480-9.

[13] Hosseini SM, Ahmadi R. Performance and emissions characteristics in the combustion of co-fuel diesel-hydrogen in a heavy duty engine. Applied Energy. 2017;205:911-25.

[14] Zhou J, Cheung C, Leung C. Combustion, performance, regulated and unregulated emissions of a diesel engine with hydrogen addition. Applied Energy. 2014;126:1-12.

[15] Lata D, Misra A. Theoretical and experimental investigations on the performance of dual fuel diesel engine with hydrogen and LPG as secondary fuels. International Journal of Hydrogen Energy. 2010;35:11918-31.

[16] Lata D, Misra A, Medhekar S. Effect of hydrogen and LPG addition on the efficiency and emissions of a dual fuel diesel engine. International Journal of Hydrogen Energy. 2012;37:6084-96.

[17] SinghYadav V, Soni S, Sharma D. Performance and emission studies of direct injection CI engine in duel fuel mode (hydrogen-diesel) with EGR. International Journal of Hydrogen Energy. 2012;37:3807-17.

[18] Khairallah HA. Combustion and pollutant characteristics of IC engines fueled with hydrogen and diesel/hydrogen mixtures using 3D computations with detailed chemical kinetics PhD Thesis, Missouri University of Science and Technology, USA, 2015.

[19] Miyamoto T, Hasegawa H, Mikami M, Kojima N, Kabashima H, Urata Y. Effect of hydrogen addition to intake gas on combustion and exhaust emission characteristics of a diesel engine. International Journal of Hydrogen Energy. 2011;36:13138-49.

[20] Saravanan N, Nagarajan G, Kalaiselvan K, Dhanasekaran C. An experimental investigation on hydrogen as a dual fuel for diesel engine system with exhaust gas recirculation technique. Renewable Energy. 2008;33:422-7.

[21] Verhelst S, Vancoillie J, Naganuma K, De Paepe M, Dierickx J, Huyghebaert Y, et al. Setting a best practice for determining the EGR rate in hydrogen internal combustion engines. International Journal of Hydrogen Energy. 2013;38:2490-503.

[22] Khairallah HA, Koylu UO. Combustion Simulation of a Direct Injection Diesel Engine with Hydrogen Fuel Using a 3D Model with Multi-Fuel Chemical Kinetics. SAE Technical Paper; 2014;No. 2014-01-1317.

[23] Hu E, Huang Z. Optimization on Ignition Timing and EGR Ratio of a Spark-Ignition Engine Fuelled with Natural Gas-Hydrogen Blends. SAE Technical Paper; 2011;No. 2011-01-0918.

[24] Shin B, Cho Y, Han D, Song S, Chun KM. Hydrogen effects on NO_x emissions and brake thermal efficiency in a diesel engine under low-temperature and heavy-EGR conditions. International Journal of Hydrogen Energy. 2011;36:6281-91.

[25] Hountalas D, Mavropoulos G, Binder K. Effect of exhaust gas recirculation (EGR) temperature for various EGR rates on heavy duty DI diesel engine performance and emissions. Energy. 2008;33:272-83.

[26] Pariotis EG, Hountalas DT, Rakopoulos C. Modeling the effects of EGR on a heavy duty DI diesel engine using a new quasi-dimensional combustion model. SAE Technical Paper; 2005;No. 2005-01-1125.

[27] Komninos N, Rakopoulos C. Modeling HCCI combustion of biofuels: A review. Renewable and Sustainable Energy Reviews. 2012;16:1588-610.

[28] Shi L, Cui Y, Deng K, Peng H, Chen Y. Study of low emission homogeneous charge compression ignition (HCCI) engine using combined internal and external exhaust gas recirculation (EGR). Energy. 2006;31:2665-76.

[29] Swain M, Swain M, Leisz A, Adt R. Hydrogen peroxide emissions from a hydrogen fueled engine. International Journal of Hydrogen Energy. 1990;15:263-6.

[30] Sinclair L, Wallace J. Lean limit emissions of hydrogen-fueled engines. International Journal of Hydrogen Energy. 1984;9:123-8.

[31] Korakianitis T, Namasivayam A, Crookes R. Natural-gas fueled spark-ignition (SI) and compression-ignition (CI) engine performance and emissions. Progress in Energy and Combustion Science. 2011;37:89-112.

[32] Zareei J, Kakaee A. Study and the effects of ignition timing on gasoline engine performance and emissions. European Transport Research Review. 2013;5:109-16.

[33] Lawankar S, Dhamande DL, Khandare DS. Experimental study of effect of ignition timing and compression ratio on NO_x emission of LPG fuelled engine. International Journal of Scientific & Engineering Research. 2012;3.

[34] Saravanan N, Nagarajan G, Narayanasamy S. An experimental investigation on DI diesel engine with hydrogen fuel. Renewable Energy. 2008;33:415-21.

[35] Saravanan N, Nagarajan G. Performance and emission studies on port injection of hydrogen with varied flow rates with Diesel as an ignition source. Applied Energy. 2010;87:2218-29.

[36] Wang H, Yao M, Reitz RD. Development of a reduced primary reference fuel mechanism for internal combustion engine combustion simulations. Energy & Fuels. 2013;27:7843-53.

[37] Nagle J, Strickland- Constable, R.F. Oxidation of Carbon between 1000 - 2000°C. Proceedings of the Fifth Conference on Carbon. New York: Pergamon (1962).

[38] Saravanan N, Nagarajan G, Sanjay G, Dhanasekaran C, Kalaiselvan K. Combustion analysis on a DI diesel engine with hydrogen in dual fuel mode. Fuel. 2008;87:3591-9.

[39] Aldhaidhawi M, Chiriac R, Badescu V. Ignition delay, combustion and emission characteristics of Diesel engine fueled with rapeseed biodiesel–A literature review. Renewable and Sustainable Energy Reviews. 2017;73:178-86.

[40] Maroteaux F, Vaglieco BM, Mancaruso E. N-heptane ignition delay time with temperature criterion for HCCI combustion. Fuel. 2018;225:483-9.

III. MULTI-OBJECTIVE OPTIMIZATION OF OPERATING PARAMETERS FOR A H2/DIESEL DUAL-FUEL COMPRESSION-IGNITION ENGINE

ABSTRACT

This numerical study covers the engine performance and emissions of a dual-fuel compression-ignition engine fueled by hydrogen/diesel mixtures. Advanced simulations of the combustion process were performed by focusing on simulating the engine performance and emissions at different hydrogen quantities. Different factors that have significant effects on engine performance and emissions, such as exhaust gas recirculation and modifying diesel injection timing, were also considered in this study. The relationship between the performance, emissions, and the operating parameters considered in this work are investigated and explained. A significant reduction of soot emissions by approximately 32.5% has been achieved by increasing hydrogen levels up to 37.5%; however, this has led to an increase in nitrogen oxides (NOx) emissions by ~22%. To overcome this problem, the optimum operating parameters that will lead to minimum emissions and maximum efficiency were also sought. Hydrogen rates, exhaust gas recirculation (EGR) rates, and diesel injection timing were the main operating conditions while the engine performance and NOx/soot emissions were the objectives. The best operating conditions for hydrogen/diesel engines were obtained by solving the multi-objective problem of maximizing the efficiency while minimizing the NOx and soot emissions. This multi-objective optimization problem (MOOP) with conflicting objectives was solved by using different optimization techniques, including regression analysis, artificial neural networks, and genetic algorithms. By solving MOOP, the first

preferred operating condition at ~ 13% hydrogen, 4% EGR, and 30 BTDC of diesel injection timing was obtained.

1. INTRODUCTION

Combustion emissions and fuel economy are the primary areas of focus in the study of internal combustion (IC) engines. With more strict emission legislations and greater environmental impact, compression-ignition (CI) engines are considered to be the main source of pollutants that have adversely effected the environment [1, 2]. Nitrogen oxides (NOx) and particulate matter (PM) are generally the main components of emissions formed during the combustion of diesel fuel in CI engines. The exact compositions of diesel exhaust emissions depend on the fuel composition and its physical properties along with the engine type [3]. Alternative fuels such as hydrogen and biofuel have attracted considerable attention as possible fuels to be utilized in IC engines. It is possible to add renewable, clean, and alternative fuels to fossil fuels in order to minimize harmful emissions while using existing traditional engine without design modifications [4].

The free-carbon fuel nature of hydrogen can make it the first option for use with hydrocarbon fuels in the engine cylinder. Hydrogen can be supplemented directly into spark-ignition (SI) engines since the ignition source (spark plug) is introduced. On the other hand, it can only be used as a secondary fuel in compression=ignition engines due to its higher auto-ignition temperature (858 K) compared to diesel fuel (525 K) [5]. Thus, a source of ignition such as diesel fuel is required to ignite the mixture. However, the

dual-fuel (hydrogen/diesel) CI engine is an option for reducing the amount of diesel exhaust and improving engine performance [6, 7]. Even though hydrogen has exceptional combustion properties, such as high burning velocity, wide flammability range, and low ignition energy, NOx emissions are still undesirable exhaust emissions from hydrogen combustion [8]. Applying the exhaust gas recirculation (EGR) technique can overcome that problem and help to reduce NOx emissions; however, that can lead to increased soot emission, which can be reduced by modifying the start of the diesel injection timing (IT). The reduction in the in-cylinder temperature has been achieved by using EGR, which minimized NOx formation. However, a significant reduction in the power occurs due to EGR utilization [9-11]. The study in [12] was performed in a dual-fuel diesel-hydrogen CI engine operating at low loads. Diesel injection and EGR techniques were presented in that experimental work. Running the engine at higher EGR with advanced diesel injection caused the thermal efficiency to increase and decreased NOx and CO emissions; however, a higher soot formation rate was observed at higher EGR rates. Maximizing the power and minimizing both NOx and soot emissions are the main goals of engine designers. However, the commonly adopted measures to reduce NOx and soot emissions also caused the efficiency to decrease. Therefore, that problem becomes a multi-objective optimization problem with conflicting objectives. Another hydrogen diesel dual fuel combustion study in [13] was performed for a combined heat and power (CHP) system. The operating conditions of hydrogen levels, engine speeds, and engine loads were considered. The results show that the hydrogen operation could achieve higher thermal efficiency than a conventional diesel operation at relatively high engine load conditions. CO2 and soot emissions were significantly reduced by replacing conventional fossil fuel

with hydrogen, while NOx was increased with an increase in hydrogen fraction. However, methods such as EGR and modifying diesel injection timing were not considered.

Several studies were carried out in the field of optimization, especially in IC engines. Optimization studies can be divided in two broad categories; geometry optimization and operating conditions optimization. Optimization of geometry typically involves finding the best cylinder geometry that minimizes certain fitness functions by using an optimization algorithm. The study in [14] determined the cylinder geometry for a direct-injection diesel engine. To optimize three fitness functions (HC, NOx, and soot) for different operating conditions (load and speed), eight different parameters were considered. That was related to a previous work that included nine parameters, with three of them related to the engine geometry [15]. Genetic algorithm (GA) approaches were used to decrease the emissions as well as the fuel consumption. The study in [16] was performed on a dimethyl ether fueled CI engine. Eleven decision variables were used, including some relevant to operating conditions, with the targets being the same as in [15]. The study in [17] focuses on stoichiometric combustion of diesel engines, attempting to reduce the fuel consumption. Due to the claim that emissions were manageable with after-treatment devices, the emissions were not considered as an optimization objective. The Artificial Neural Network (ANN) approach was introduced in the study [18] to reduce the computational time needed by GAs. ANNs were used to estimate the efficiency and NOx for a spark-ignition engine. Numerous engine parameters were used as inputs while the geometry was fixed. The study in [19]

considered three different piston bowl geometries to optimize the NOx, soot, and gross indicated mean effective pressure by using GA-ANN methods.

The problem with geometry optimization is that implementation of the results could be very difficult given that new geometries are usually proposed. In the short term, it is more practical to consider finding the optimum (in the context of multiple conflicting objectives) operating conditions for existing engine geometries. It is necessary to adopt a multi-objective approach in order to find multiple suitable points from a Pareto-optimal front in order to give the designer a wide range of suitable operating points. That would allow the designer to account for real-world conditions where the engine is likely to face different loads and speeds.

The study in [20] focused on the trade-off between NOx, soot, and specific fuel consumption using a phenomenological model of a diesel engine. The only decision variable used was the shape of the injection rate. The same group later considered more operating conditions as decision variables (boost pressure, EGR rate, etc.) and obtained Pareto fronts for the three objectives [21]. The study in [22] used a similar approach as [19] to estimate the objective functions, which were NOx, opacity, and brake specific fuel consumption of diesel fuel for a CI engine enriched with hydrogen. Nine decision variables were used. However, no multi-objective optimization to obtain Pareto fronts was considered. Instead, trade-offs between the cases considered were presented. An experimental approach to study the effects of the compression ratio and the equivalence ratio on the emissions (CO, HO, and NOx) of an 80% hydrogen-ethanol SI engine was presented in [23]. Once again, no multi-objective optimization was performed. A study on a hybrid hydrogen-gasoline engine [24] was also conducted. That engine was fueled

by hydrogen at start-up conditions, a blend at idle and low loading conditions, and pure gasoline at high loading conditions. Various operating conditions were tested, all at lean conditions. The researchers did not consider any optimization of trade-offs between the efficiency, emissions, and other performance measures studied. The same group presented results for a spark-ignition pure hydrogen engine for a range of lean operating conditions [25]. The power output was not considered; instead, the emphasis was on emissions reduction. Another similar example for a diesel engine run using biofuels was in [26], in which the aim was to find the best fuel blend and EGR rate. However, only a limited number of blends were tested. The study in [27] was performed for an SI engine with the goal to optimize the spark timing (IT) and the air-fuel ratio. The objectives, which were considered separately, were the brake specific fuel consumption and the torque. No emissions were considered as objectives. The study in [28] followed a classical multi-objective approach for diesel-hydrogen mixtures. However, no emissions were considered in any of the objective functions, and the authors failed to note the precise operating conditions corresponding to the optimal solution. The study in [29] was performed for a hydrogen SI engine with the excess air ratio and IT being used to optimize the brake thermal efficiency and power output. No emissions were considered, and the two objectives were not considered in a multi-objective sense. A similar study was conducted in [30]. Several operational parameters were used to optimize an abnormal combustion objective and a power objective. The decision variables were the excess air coefficient and the IT. The study in [31] was to examine the effect of hydrogen enrichment in a diesel engine. It was noted that the CO and smoke decreased, but the NOx increased. No optimization was done as only a few cases were considered.

The present study systematically investigates the relation between three engine outputs (efficiency, soot, and NOx emissions) and three operating parameters (hydrogen levels, exhaust gas recirculation rate (EGR), and the diesel injection timing (IT)) for a hydrogen-fueled CI engine. Each parameter was varied over an extensive search domain while the other two were held constant in order to properly characterize the input-output relationship and guarantee that the best operating points lay within the search domain considered. There are limited studies that deal with the size of the search domain considered here for hydrogen/diesel mixture, and the operating conditions have not been considered before. Furthermore, there are few studies that solve a multi-objective optimization problem (MOOP) and present a range of alternate solutions. The advantage of the present approach is that multiple conflicting objectives can be considered simultaneously in an equitable manner and the solution produces multiple alternate solutions. Using a GA approach is more likely to find a global optimum, as well. The main contribution of this study is to present detailed explanations of the computational results obtained using a 3D commercial-grade combustion code and solving a MOOP to minimize the NOx and maximize the power and efficiency.

2. COMPUTATIONAL METHODS

Computational Fluid Dynamics (CFD) software was used in this study to investigate the engine performance and the exhaust emissions inside the engine cylinder. In this paper, the simulation of the combustion process was performed using AVL FIRE® 3D CFD code, coupled with detailed chemical reaction kinetics of a

hydrogen/diesel mixture using the CHEMKIN software package. The engine model used in this study was created and validated in a previous work [32] to predict the thermal efficiency and emissions of NOx and soot in a hydrogen/diesel dual-fuel CI engine. Therefore, the computational simulations used in this work were extensively validated against independent experiments [33, 34] for engine performance and exhaust emissions. The reaction mechanism applied in this work has 76 species and 349 elementary reactions for both hydrogen and diesel chemical reactions. Diesel fuel consists of many hydrocarbon components, and it is very difficult to find the specific chemical formula of diesel. Therefore, n-heptane was represented instead of diesel due to its cetane number (56), which is close to diesel cetane number (50). A group of nitric oxide (NO) reactions for hydrocarbon fuel is added to estimate the NOx formation. Hydrogen is injected at the intake port and assumed to be inside the cylinder mixed with air when diesel is directly injected into the combustion chamber. The engine was run at a fixed speed of 1500 rpm and a maximum brake power of 3.74 kW.

2.1. MODEL PARAMETERS

In this numerical study, the target engine model was created using a commercial 3D engine software, AVL Fire. The model was run at different operating conditions according to experimental operating conditions. The simulation model was validated with experimental data [34, 35, 38] that considered the same engine geometry to measure the engine output power, efficiency, and emission characteristics of a hydrogen/diesel dual-fuel engine. The specifications of the simulated single cylinder engine, as well as the operating conditions, are shown in Table 1.

Table 1. Engine specifications.

Item	Specification
Number of cylinders	1
Bore (mm)	80
Stroke (mm)	110
Engine speed (rpm)	1500
Compression ratio (-)	16.5:1
Connecting rod length (mm)	235
Max. brake power (kW)	3.74
Piston type (-)	Flat
Number of injector nozzle holes (-)	4
Hole diameter (mm)	0.169
Spray angle (-)	160°
Fuel amounts (Vol. %)	7.14
Initial temperature (K)	333
Initial pressure (bar)	1
Injection timing (CA)	23° BTDC
Injection duration (-)	30°

2.2. NOx FORMATION

There are three known NO_X formation pathways, which are prompt NO_X, fuel NO_X, and thermal NO_X. The prompt NO_X mechanism is one of the most complex mechanisms. It includes hundreds of species and reactions, and it is generated under faster reaction conditions between N_2, O_2, and hydrocarbons. At low-temperature combustion and in the presence of hydrocarbon fuel at rich conditions, prompt NO_X is considered to be an important mechanism. However, at higher temperatures, it is trivial compared to the thermal NO_X mechanism. Thermal NO_X is produced by the high temperature reaction of N_2 with O_2, and it is known as the Zeldovich mechanism. The last NO_X formation mechanism is fuel NO_X. It is generated by the direct oxidation of organic

nitrogen compounds found in the fuel. Even though fuel NO_X is a trivial mechanism for a high-quality fuel, such as natural gas, that has no organic nitrogen compounds, it could be an important mechanism when fuels such as coal and oil (e.g., residual fuel oil) are used with significant amounts of organically bound nitrogen.

In this study, the adopted NO_X formation mechanism was derived from the Zeldovich model [34]. Hydrocarbon fuel constants [35] were used to predict NO formation accurately. The reactions 1, 2, and 3 below are very important at high combustion temperatures (≥ 1800 K) because species O and OH are produced only at high temperatures. The reaction mechanism can be expressed in terms of the so-called extended Zeldovich mechanism.

$$N_2 + O \leftrightarrow NO + N. \tag{1}$$

$$N + O_2 \leftrightarrow NO + O \tag{2}$$

$$N + OH \leftrightarrow H + N \tag{3}$$

Reaction (1) can be accepted as the rate-limiting step of NO formation compared to the other reactions. Decomposition of the strong N_2 triple-bond requires a very high activation energy (temperature). Therefore, the reaction is dramatically fast at high temperatures. Basically, it can be seen that the thermal nitric oxide formation is mainly determined by only five chemical species (O, H, OH, N, and O_2) and not by the fuel being used. A complex reaction mechanism must be used in order to determine NO concentration. The net rate of NO formation via reactions (1-3) is given by the following:

$$\frac{\partial C_{NO}}{\partial t} = k_{1f}C_O C_{N_2} + k_{2f}C_N C_{O_2} + k_{3f}C_N C_{OH} - k_{1b}C_{NO}C_N - k_{2b}C_{NO}C_O - k_{3b}C_{NO}C_H \quad (4)$$

Forward k_f and backward k_b reaction rates are considered where C is the concentration of species and given in mole/cm^3.

2.3. SOOT FORMATION

The regulations on soot emissions have become more rigid due to the emissions' negative influence on human health and the environment. Understanding soot formation is very important in order to apply the best operating conditions that will result in a reduction in soot emissions. Under high temperature and fuel-rich conditions, as typically found in diesel combustion, hydrocarbon fuels exhibit a strong tendency to form carbonaceous particles (soot), which form in the early stages of combustion. Most of the soot formed in the early stages of the combustion process is depleted due to oxidation. The most important parameters during the soot formation are the local air/fuel ratio (C/H ratio and C/O ratio), temperature, pressure, and residence time. The Hiroyasu-Nagel model [36], which is by default inserted into the AVL software to model the soot emissions, was considered in this work.

The conservation of the soot mass fraction ϕ_S has the form

$$\frac{\partial}{\partial t}\left(\bar{p}\tilde{\phi}_s\right) + \frac{\partial}{\partial x_j}\left(\bar{p}u_j\,\bar{\phi}_s\right) = \frac{\partial}{\partial x_j}\left(\frac{\mu_{eff}}{\sigma_s}\frac{\partial\tilde{\phi}_s}{\partial x_j}\right) + S_{\phi_s}\,. \quad (5)$$

The soot formation is rate defined as the following:

$$S_{\phi_s} = S_n + S_g + S_{O_2}. \tag{6}$$

where S_n represents the crystal nucleus source item, S_g represents the surface source term growth, and S_{O_2} represents the oxidation of the source term, which is a function of the soot concentration, oxygen, and temperature:

$$S_{O_2} = -F(\phi_s, P_{O_2}, T). \tag{7}$$

3. PROBLEM DESCRIPTION

This numerical work was conducted on diesel engines under different operating conditions. Hydrogen variation, EGR, and injection timing of diesel are essentially the operation parameters considered in this paper. The parameters influencing the engine performance and emissions were the main considerations.

Table 2. Operating parameters and objectives.

Parameters	Value	Objective
Injection Time (BTDC)	10, 15, and 20	Min [Soot Emission (FSN)]
H_2 energy ratio (%)	5, 10, 20, and 37.5	Max [Indicated Thermal Efficiency (%)]
EGR Level (%)	0, 5, 10, and 15	Min [NO_x Emission (ppm)]

As shown in Table 2, the objective of this work was to investigate the potential effects of considered operating parameters on performance and emission characteristics

of a diesel engine enriched with hydrogen fuel. Minimum soot and NO_x emissions and maximum indicated thermal efficiency are the desired objectives in this study.

4. COMPUTATIONAL RESULTS

4.1. EMISSIONS

In this section, the influences of different operating conditions in a dual-fuel hydrogen/diesel engine on soot emissions were studied. Figure 1a illustrates the effect of hydrogen rates on soot emissions at different ITs.

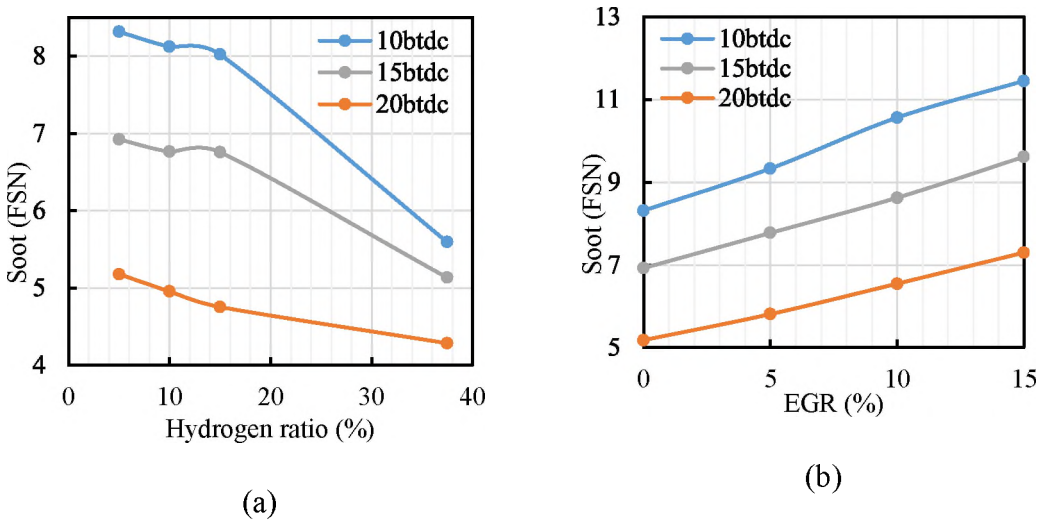

Figure 1. Effect of hydrogen and EGR levels on soot emissions at different diesel injection timings.

Increasing the hydrogen rates inside the cylinder led to a significant reduction in soot concentration of 50% at 37.5% hydrogen. The reason for this was a reduction in hydrocarbon fuel (diesel) volume inside the cylinder and an increase in the free carbon

fuel of hydrogen. Soot emissions were also shown to decrease with advanced IT because most of the soot formed in the first stage of combustion depleted with time due to oxidation. Figure 1b shows how soot emissions are affected by EGR variations. It can be observed from the figure that as EGR levels increased, soot emissions also increased as the air/fuel volume inside the cylinder decreased and was replaced with the recirculated exhaust gas; therefore, the soot oxidation rate decreased, which led to increased soot formation.

In general, an oxide of nitrogen (NO_x) is the summation of nitrogen oxide (NO) and nitrogen dioxide (NO_2) along with a greenhouse gas known as nitrous oxide (N_2O), which can be formed at low combustion temperatures. The main species in NO_x emissions is NO, which forms at high temperatures.

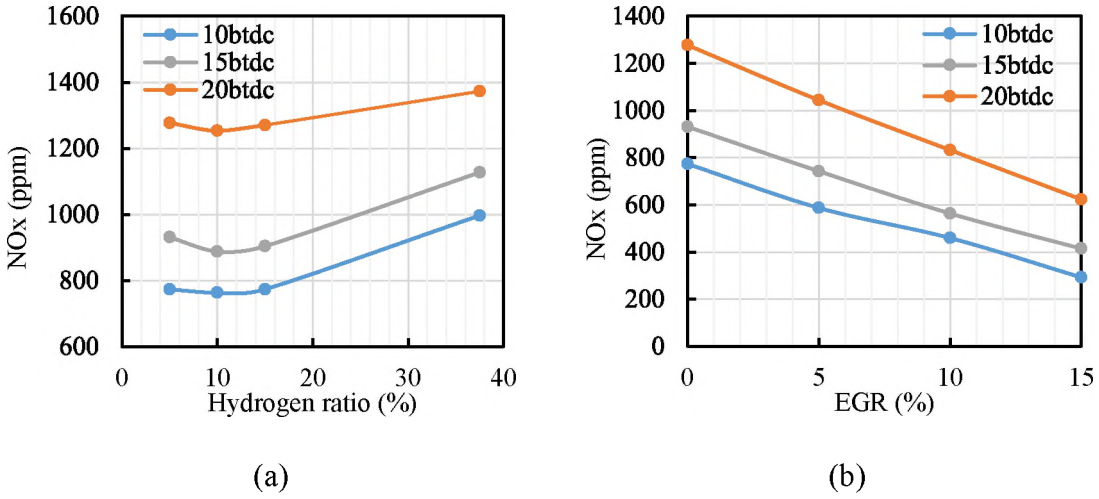

Figure 2. Effect of variations of hydrogen and EGR on NOx emissions at different IT.

Increasing hydrogen rates inside the engine raise the combustion temperature, which is the main rout of NOx formation. Therefore, NOx emissions increase, as shown

in Figure 2a. The NO_X emissions were also observed to increase with advanced injection timing. As diesel fuel is injected early inside the cylinder, the combustion takes place earlier, allowing for enough time to complete the combustion. This causes a rise in the cylinder pressure and temperature, leading to increased NO_X emission. On the other hand, in order to reduce and control NO_X emissions, in-cylinder temperature has to be reduced, which occurs when applying EGR technique, as shown in Figure 2b. NO_X emissions decreased with increased EGR quantity due to a reduction in combustion temperature and dilution caused by recirculated exhaust gas.

4.2. ENGINE PERFORMANCE

Figures 3a and 3b show the influence of both hydrogen and EGR quantities on the engine efficiency at different diesel injection timings.

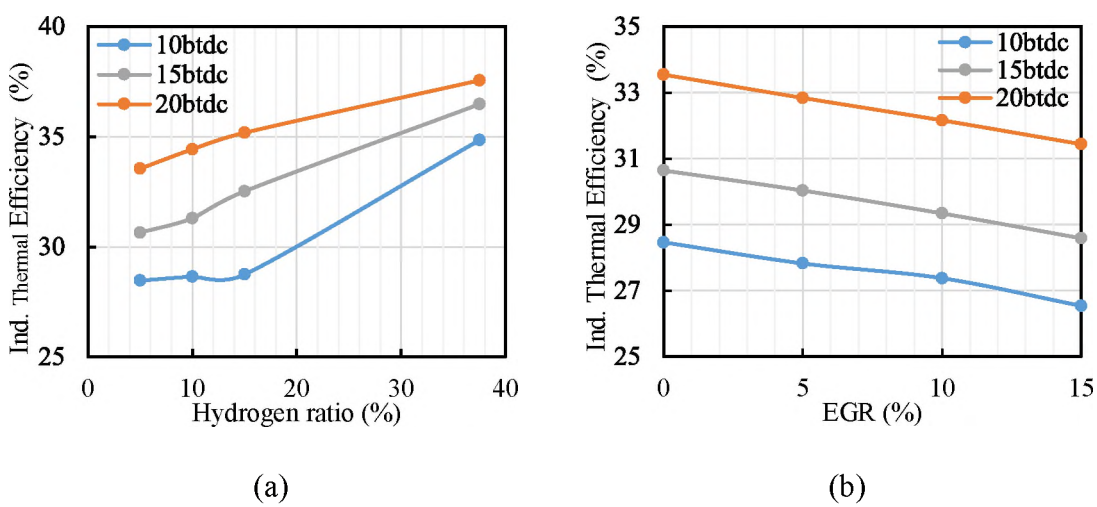

Figure 3. Effect of hydrogen and EGR variations on the engine efficiency at different IT.

As the hydrogen amount was increased, the pressure inside the cylinder significantly increased; thus, the engine efficiency increased. On the other hand, the engine efficiency was found to decrease with increased quantities of recirculated exhaust gas. This is due to a reduction in the air/fuel volume and hydrogen flame speed inside the engine with increased EGR levels. However, the engine efficiency was observed to significantly increase with advanced diesel injection timing. Advanced diesel injection provides sufficient time to complete the combustion, leading to a rise in pressure and temperature inside the cylinder and, therefore, improvement in output power and efficiency.

5.DATA ANALYSIS

5.1. ANALYSIS OF VARIANCE (ANOVA)

Analysis of variance (ANOVA) was used to determine the most significant parameters (based on the simulation results shown in Section 4) among hydrogen level (H_2), exhaust gas recirculation (EGR), and injection timing (IT) that affect the engine efficiency, NO_X, and soot emissions. These factors will be used in the regression model and neural network model. The results of ANOVA are shown in Table 3 for each response variable. When the p-value of a specific term (factor) is less than 0.05, then the term is significant, which means that hypothesis of equal means for a given factor can be rejected. A, B, and C in Table 3 represent hydrogen levels, EGR, and diesel injection timing, respectively. All parameters and their interactions have significant effects on NO_X

emissions, and they will be used in the regression analysis; this means that the selected factors in the ANOVA explained the variance.

Table 3. Results of the analysis of variance.

	Source	DF	Sum of Squares	Mean Square	F Value	Pr > F
NOx	A	1	5107805	5107805	53.974	9.25E-10
	B	1	9210614	9210614	97.328	7.45E-14
	C	1	27207068	27207068	287.495	< 2e-16
	AB	1	2124411	2124411	22.448	1.52E-05
	AC	1	2489914	2489914	26.311	3.76E-06
	BC	1	8442313	8442313	89.209	3.47E-13
	ABC	1	929121	929121	9.818	0.00275
	Residuals	56	5299553	94635		
Efficiency	A	1	114.2	114.2	415.784	< 2e-16
	B	1	70.9	70.9	258.242	< 2e-16
	C	1	1067.4	1067.4	3886.808	< 2e-16
	AB	1	7	7	25.651	4.75E-06
	AC	1	22.4	22.4	81.539	1.61E-12
	BC	1	0.7	0.7	2.684	0.107
	ABC	1	0.7	0.7	2.599	0.113
	Residuals	56	15.4	0.3		
Soot	A	1	32.8	32.8	123.434	8.79E-16
	B	1	33.1	33.1	124.791	7.10E-16
	C	1	561.8	561.8	2114.915	< 2e-16
	AB	1	0.5	0.5	1.901	0.173
	AC	1	8.1	8.1	30.469	9.05E-07
	BC	1	8.6	8.6	32.282	4.98E-07
	ABC	1	0.1	0.1	0.488	0.488
	Residuals	56	14.9	0.3		

For engine efficiency, all terms of the ANOVA are significant except for interaction between EGR and IT and the interaction between H_2, EGR, and IT where the P-value is more than 0.05; therefore, these terms will not be used in the regression

analysis. All terms of the ANOVA are significant for soot emission except for the interaction between EGR and H2 and the interaction between H2, EGR, and IT where the P-value is 0.488>0.05; these terms will not be used in the regression analysis.

5.2. REGRESSION BASED MODELING AND ARTIFICIAL NEURAL NETWORK (ANN)

The regression models were developed with three independent variables: hydrogen level, exhaust gas recirculation, and injection timing, respectively. In the regression analysis, the coefficients represent the values of variable coefficients in the regression model. Interaction effects represent the combined effects of factors on the dependent measure. When an interaction effect is present, it means the impact of one factor depends on the level of the other. The correlation coefficient (R^2) or the coefficient of determination is to define the proportion of the total variation that is explained by the regression model. The R^2 value was equal to 0.971, even though the ideal value of R^2 is 1.0.

An artificial neural network (ANN) is a statistical machine learning tool based on the idea of how neurons in the human brain work. The neural network consists of layers and nodes called neurons, and the number of layers and neurons depends on the difficulty of the problem being modeled. The input and output layers have neurons equal to the number of the inputs and the outputs, respectively. The neurons are connected by synapses, which take a value from an input neuron and multiply it by specific weight and output the results. Neurons have a more complicated purpose: they add together all outputs from all synapses and apply activation functions. Artificial neural networks (ANN) have been successfully used in classification, function approximation,

identification, and pattern recognition in various engineering applications [37-39]. Feed-forward neural networks with a sufficient number of hidden neurons can approximate any finite function arbitrarily well. In this study, a neural network was used to map the complex relation between the operating parameters, hydrogen level, EGR level, and injection timing; and the objectives of NO_X emission, soot emission, and efficiency. The three networks were implemented in MATLAB and trained using 64 data points obtained from AVL simulations with an R^2-value of 0.999.

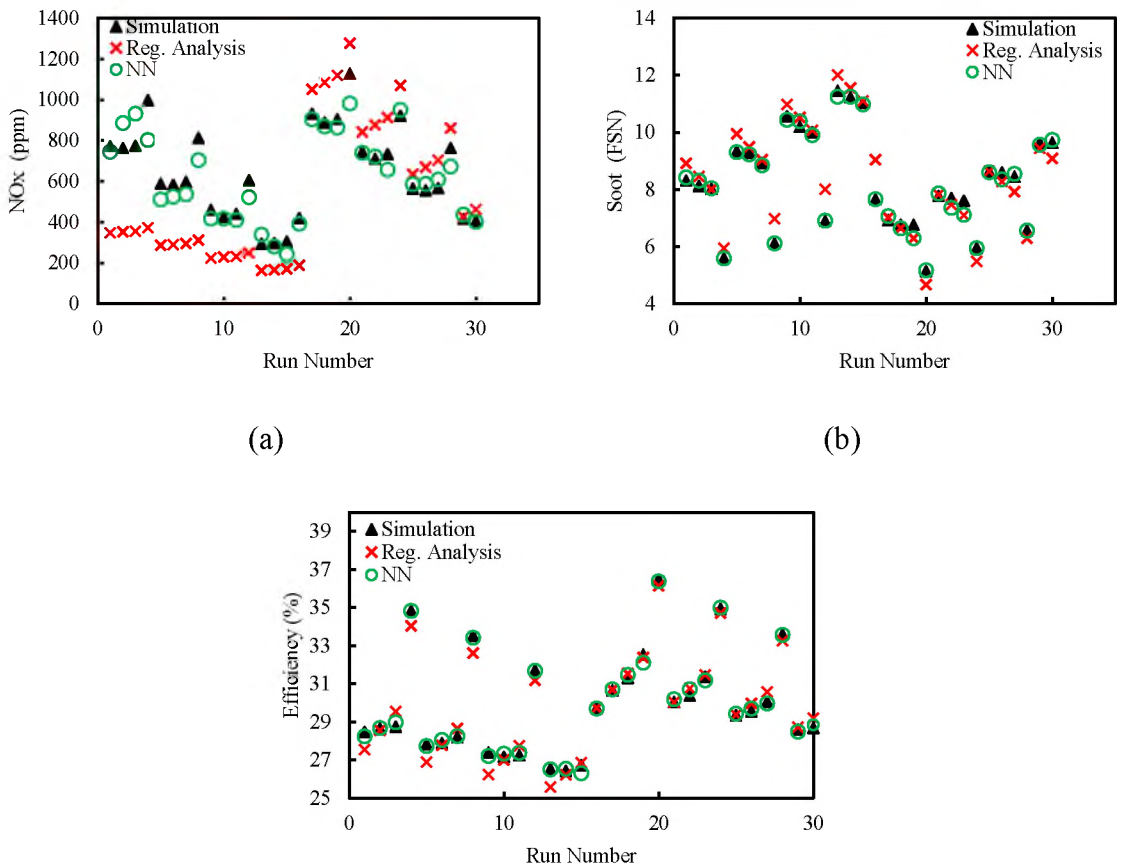

Figure 4. Regression analysis results vs neural network training results for the objectives.

The regression model and the artificial neural network results were tested and validated against the numerical model, as can be seen in Figures 4a, 4b, and 4c, which show NN outputs and regression analysis (RA) model output compared with the AVL computational results. Since every NN point coincides with the associated AVL point, unlike the RA model, it may be concluded that the NN training was successful in learning the input-output relationship and showing better results compared with the RA model. The trained NN was used to approximate the objective values for different solutions (combinations of input parameters) as can be seen in a flowchart process in Figure. 5.

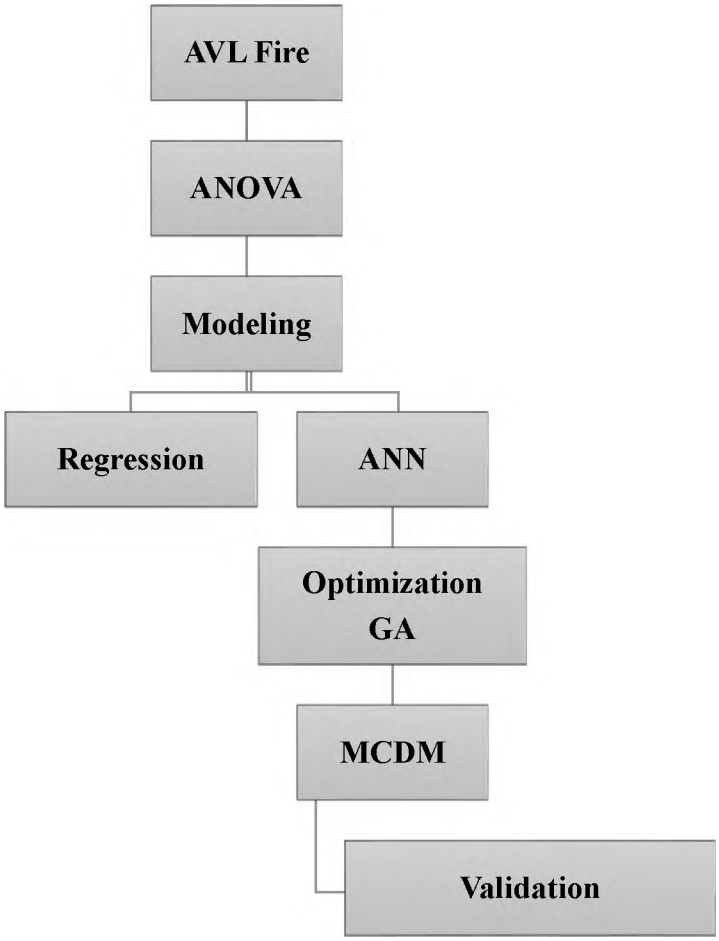

Figure 5. Flowchart of the RA-GA-NN process.

5.3. MULTI-OBJECTIVE GENETIC ALGORITHM OPTIMIZATION

Multi-objective genetic algorithms deal with more than one objective. Unlike single-objective optimization, where the optimal solution is clearly defined, the objectives in the multi-objective optimization are more complex and conflicting. It produces several optimal solutions; these solutions dominate other solutions in the design space, and they form what is known as a Pareto-optimal front curve.

Genetic algorithm is an optimization technique used to solve nonlinear or non-differentiable optimization problems using concepts from evolutionary biology to search for a global minimum. The name genetic algorithm comes from the fact that they mimic evolutionary biology techniques; genetic algorithms work by starting with an initial generation of candidate solutions that are tested against the objective function, then they produce subsequent generations of points from the first generation through selection crossover and mutation. Selection means to retain the best-performing parent from one generation to the next. In crossover, similarities between the different parent variables are selected and kept to create children variables that will be in the next generation. In the mutation step, certain variables in a parent are mutated to take on random values, and a child is created based off of this mutation. Mutation allows genetic algorithms to avoid falling into local minima, and it helps them explore the solution space properly.

6.GA-NN RESULTS

Hydrogen ratios of 5%-37.5%, EGR levels of 0%-15%, and diesel injection timings from 10 to 30 CA BTDC were the operating condition boundaries to be used for

optimization. With hydrogen ratio higher than 37.5%, the combustion at a specific injection timing, such as 10 CA BTDC, will not occur due to a delay in ignition timing, and with higher EGR ratios, soot emission will increase inside the engine cylinder. Tables 4 and 5 show the GA parameters and NN parameters, respectively.

Table 4. GA parameters.

Algorithm	NSGA-II
Population size	20
Number of generations	160
Crossover probability	0.9
Mutation probability	0.33

Table 5. Neural network parameters.

Type	Feed-forward
Number of inputs	3
Number of outputs	1
Number of hidden layers	2
Number of neurons per hidden layer	10
Hidden layer activation function	Log sigmoid
Output layer activation function	Linear
Training function	'train'
Stopping criterion	1000 epochs
R^2-value	0.999

6.1. MULTI-CRITERIA DECISION-MAKING (MCDM)

The result of the multi-objective genetic algorithm optimization is a population of the visible solutions; the Pareto front provides several candidate non-dominated solutions, and these solutions make the boundary of the population of the visible solutions. In order to select or to obtain one optimum from a good set of conditions that

meets all the goals, the desirability function approach was used. The method utilizes an objective function, D(x), called the desirability function, which transforms an estimated response into a scale-free value (d_i) called desirability. The desirable ranges are from zero to one (least to most desirable, respectively). The factor settings with maximum total desirability are the optimal parameter conditions:

$$D(x) = (d_1 \times d_2 \times d_3)^{1/3} = (\prod_{i=1}^{3} d_i)^{1/3}. \quad (8)$$

where 3 is the number of responses in the measure. If any of the responses fall outside the desirability range, the overall function becomes zero. For maximum and minimum responses, the (di) value was assigned as follows:

Maximum:

$d_i = 0$ if response = minimum value

$0 < d_i < 1$ as response varies between the minimum and maximum values

$d_i = 1$ if response = maximum value

Minimum:

$d_i = 1$ if response = minimum value

$0 < d_i < 1$ as response varies between the maximum and minimum values

$d_i = 0$ if response = maximum value

Thirteen different desirable ranges of input parameters and responses, which give a high value of desirability, are shown in Table 6. The table revealed that the highest desirability could be obtained at point 11; these are the optimal conditions to obtain a high value of desirability.

Table 6. The preferred ranges of input parameters and responses.

S.No	H_2 (%)	EGR (%)	IT (BTDC)	NO_x (ppm)	E (%)	Soot (FSN)	Desirability
1	5.144	7.817174	10.245998	393.882	27.888	10.079	0.23529
2	6.603	7.8089378	14.055174	522.155	29.335	8.5296	0.3771
3	6.533	7.7015897	18.736259	765.714	31.910	6.6202	0.53025
4	7.194	6.9712031	15.578704	618.245	30.206	7.7504	0.43415
5	6.948	3.9801071	19.76484	1033.766	33.345	5.5483	0.59499
6	9.401	6.6771079	20.026467	949.665	33.220	5.7220	0.59875
7	6.952	4.4564558	20.772113	1084.233	33.985	5.0868	0.63251
8	6.010	6.5440245	17.323893	731.218	31.166	7.0331	0.49084
9	5.679	7.2822394	11.721041	449.325	28.443	9.4112	0.29908
10	6.763	5.7868803	22.522661	1173.60	34.808	4.2508	0.69259
11	13.22	4.1085619	29.917495	2768.93	40.142	1.2302	0.81648
12	10.11	7.7360473	24.23726	1262.52	35.842	3.2283	0.75003
13	7.193	5.850886	22.778467	1199.92	35.004	4.0731	0.70347

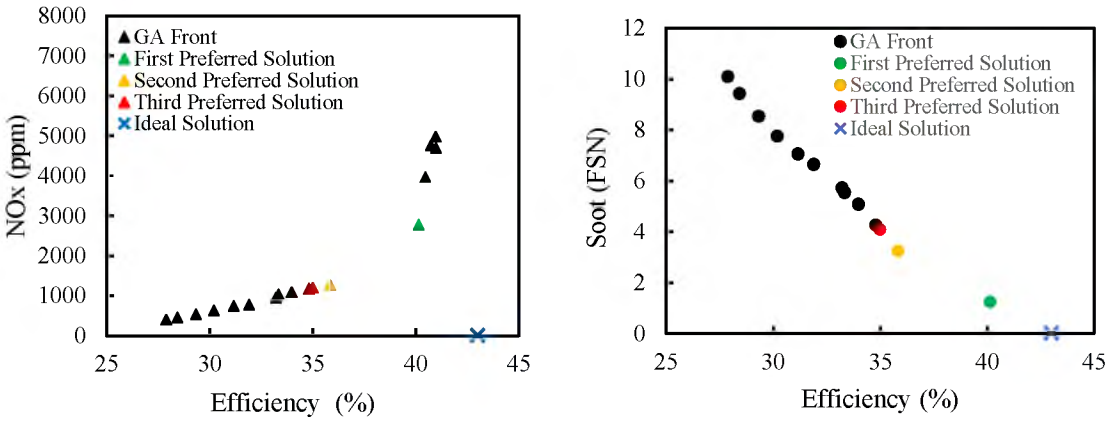

(a) (b)

Figure 6. Combined GA front with top three preferred solutions.

It can be observed from Figures 6a and 6b that the first preferred operating condition is at ~ 13% hydrogen, 4% EGR, and 30 BTDC of diesel injection timing. The figures clearly show that the first preferred solution is in line with the desired objectives

and close to the ideal solution in terms of efficiency and soot emissions. However, NOx emissions are slightly higher compared to the second and third solutions, so the second and the third solutions can be considered instead if interested in reducing NOx emissions. The top three optimum solutions obtained from NN-GA methods were estimated and validated with AVL computational results, as shown in Figure 7 (a, b, c).

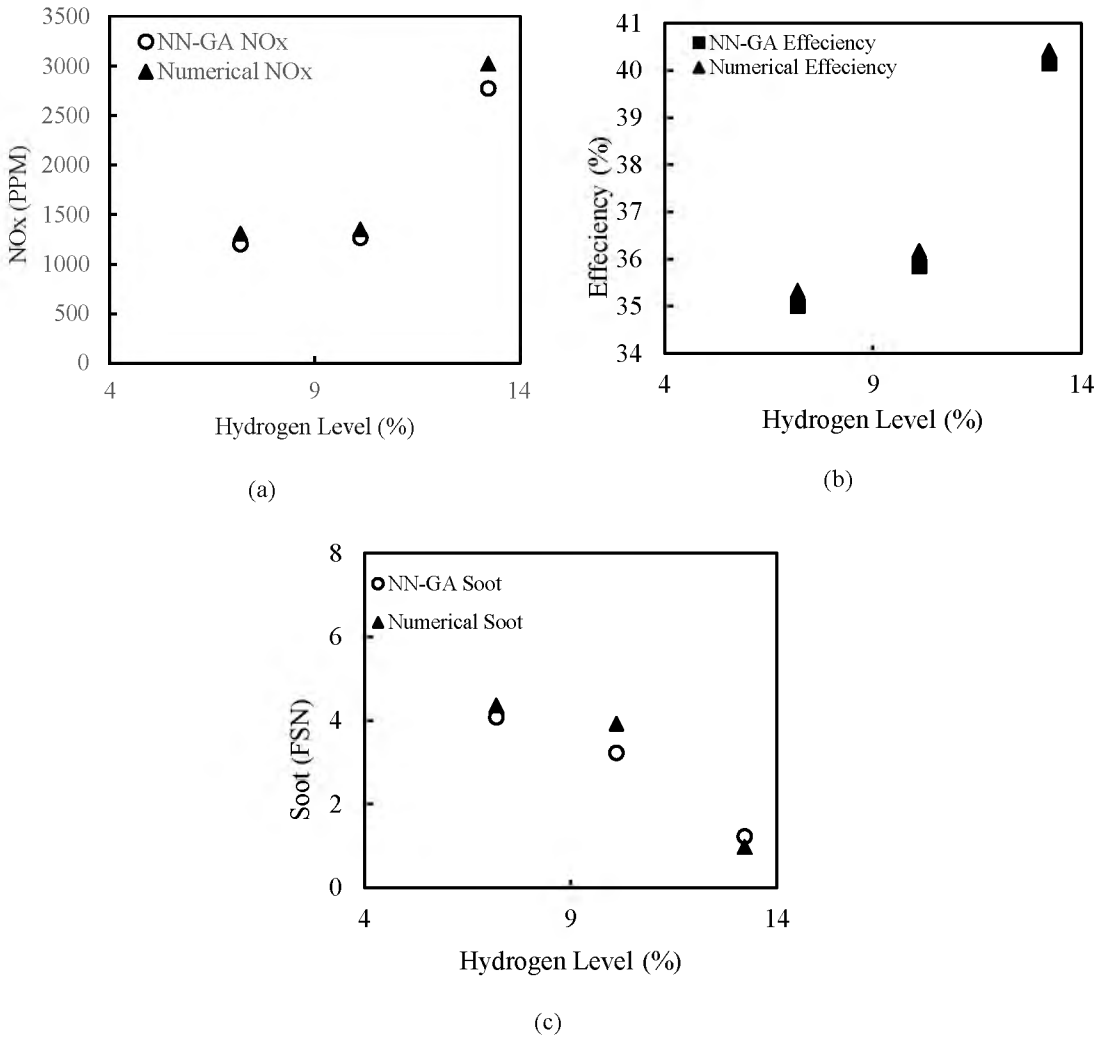

Figure 7. AVL computational results vs NN-GA estimated results for the top three preferred solutions.

7. SUMMARY AND CONCLUSIONS

The present study considers combustion of a dual fuel hydrogen/diesel single cylinder engine. The relationships among the efficiency, soot, and NOx emissions as well as the three operating parameters of hydrogen variation, exhaust gas recirculation ratio, and diesel injection timing advancement, were investigated in a systematic manner. The NOx emissions and the engine efficiency were all highly dependent on in-cylinder temperature, while soot emission was dependent on the level of hydrocarbon fuel inside the engine cylinder. With higher hydrogen quantity inside the engine, the NOx emissions, as well as the efficiency, increased while the soot emissions decreased. Increasing levels of EGR were found to reduce the NOx emissions and the efficiency. On the other hand, increasing the injection timing advancement was found to increase the NOx emissions and the efficiency while reducing soot emissions. ANOVA was used to determine the most significant parameters among the considered operating parameters to use in the regression model and neural network model. The regression model and the artificial neural network results were tested and validated against the numerical model. The NN training was shown better results compared with the RA model, so it was used to approximate the objective values for different solutions. In addition, a GA-NN approach was applied to find the best operating points that maximize efficiency while minimizing NOx and soot emissions. A Pareto-front of non-dominated solutions was obtained, and it was quantified that advanced injection timing (29.9 BTDC) with medium hydrogen and EGR levels (13.2 %-4.1%) gave the best trade-offs between efficiency, NOx emission,

and soot emission (35-40 %, 1200-2700 ppm, and 1-4 FSN) for the engine conditions considered.

ACKNOWLEDGMENTS

The authors would like to thank the Department of Mechanical and Aerospace Engineering at Missouri S&T for the computational facilities and the Libyan Government for the financial support of Abdulhakim I. Jabbr.

REFERENCES

[1] Johnson TV. Diesel emissions in review. SAE International Journal of Engines. 2011;4:143-57.

[2] Rexeis M, Hausberger S. Trend of vehicle emission levels until 2020–prognosis based on current vehicle measurements and future emission legislation. Atmospheric Environment. 2009;43:4689-98.

[3] Greim H. Diesel engine emissions: are they no longer tolerable? Archives of toxicology. 2019:1-8.

[4] Jabbr AI, Vaz WS, Khairallah HA, Koylu UO. Multi-objective optimization of operating parameters for hydrogen-fueled spark-ignition engines. International Journal of Hydrogen Energy. 2016;41:18291-9.

[5] Saravanan N, Nagarajan G, Kalaiselvan K, Dhanasekaran C. An experimental investigation on hydrogen as a dual fuel for diesel engine system with exhaust gas recirculation technique. Renewable Energy. 2008;33:422-7.

[6] Aydin K, Kenanoğlu R. Effects of hydrogenation of fossil fuels with hydrogen and hydroxy gas on performance and emissions of internal combustion engines. International Journal of Hydrogen Energy. 2018.

[7] An H, Yang W, Maghbouli A, Li J, Chou S, Chua K. A numerical study on a hydrogen assisted diesel engine. International Journal of Hydrogen Energy. 2013;38:2919-28.

[8] Ma F, Wang J, Wang Y, Wang Y, Zhong Z, Ding S, et al. An investigation of optimum control of a spark ignition engine fueled by NG and hydrogen mixtures. International Journal of Hydrogen Energy. 2008;33:7592-606.

[9] SinghYadav V, Soni S, Sharma D. Performance and emission studies of direct injection CI engine in duel fuel mode (hydrogen-diesel) with EGR. International Journal of Hydrogen Energy. 2012;37:3807-17.

[10] Khairallah HA. Combustion and pollutant characteristics of IC engines fueled with hydrogen and diesel/hydrogen mixtures using 3D computations with detailed chemical kinetics: Missouri University of Science and Technology; PhD Thesis, 2015.

[11] Lawankar S, Dhamande DL, Khandare DS. Experimental study of effect of ignition timing and compression ratio on NOx emission of LPG fuelled engine. International Journal of Scientific & Engineering Research. 2012;3.

[12] Dimitriou P, Tsujimura T, Suzuki Y. Low-load hydrogen-diesel dual-fuel engine operation–A combustion efficiency improvement approach. International Journal of Hydrogen Energy. 2019;44:17048-60.

[13] Tsujimura T, Suzuki Y. The utilization of hydrogen in hydrogen/diesel dual fuel engine. International Journal of Hydrogen Energy. 2017;42:14019-29.

[14] De Risi A, Donateo T, Laforgia D. Optimization of the combustion chamber of direct injection diesel engines. SAE Technical Paper; 2003.

[15] Wickman DD, Senecal PK, Reitz RD. Diesel engine combustion chamber geometry optimization using genetic algorithms and multi-dimensional spray and combustion modeling. SAE Technical Paper; 2001.

[16] Park S. Optimization of combustion chamber geometry and engine operating conditions for compression ignition engines fueled with dimethyl ether. Fuel. 2012;97:61-71.

[17] Park SW. Optimization of combustion chamber geometry for stoichiometric diesel combustion using a micro genetic algorithm. Fuel Processing Technology. 2010;91:1742-52.

[18] Kesgin U. Genetic algorithm and artificial neural network for engine optimisation of efficiency and NOx emission. Fuel. 2004;83:885-95.

[19] Costa M, Bianchi GM, Forte C, Cazzoli G. A numerical methodology for the multi-objective optimization of the DI diesel engine combustion. Energy Procedia. 2014;45:711-20.

[20] Hiroyasu T, Miki M, Kamiura J, Watanabe S, Hiroyasu H. Multi-objective optimization of diesel engine emissions and fuel economy using genetic algorithms and phenomenological model. SAE Technical Paper; 2002.

[21] Hiroyasu T, Miki M, Kim M, Watanabe S, Hiroyasu H, Miao H. Reduction of heavy duty diesel engine emission and fuel economy with multi-objective genetic algorithm and phenomenological model. SAE Technical Paper; 2004.

[22] Banerjee R, Bose P. Development of a Neuro Genetic Algorithm Based Virtual Sensing Platform for the Simultaneous Prediction of NOx, Opacity and BSFC in a Diesel Engine Operated in Dual Fuel Mode with Hydrogen under Varying EGR Conditions. SAE Technical Paper; 2012.

[23] Yousufuddin S, Venkateswarlu K. Effect of Compression Ratio and Equivalence Ratio on the Emission Characteristics of a Hydrogen-Ethanol Fuelled Spark Ignition Engine. International Journal of Advanced Science and Technology. 2012;40:91-100.

[24] Ji C, Wang S, Zhang B. Performance of a hybrid hydrogen–gasoline engine under various operating conditions. Applied Energy. 2012;97:584-9.

[25] Ji C, Wang S. Combustion and emissions performance of a hydrogen engine at idle and lean conditions. International Journal of Energy Research. 2013;37:468-74.

[26] Jagadish D, Kumar PR, Murhty KM. Performance and emission characteristics of diesel engine run on biofuels based on experimental and semi analytical methods. International Journal of Energy and Environment. 2011;2:899-908.

[27] Kakee A-H, Sharifipour S, Mashadi B, Keshavarz M, Paykani A. Optimization of spark timing and air-fuel ratio of an SI engine with variable valve timing using genetic algorithm and steepest descend method. UPB Sci Bull. 2015;77:61-76.

[28] Deb M, Banerjee R, Majumder A, Sastry G. Multi objective optimization of performance parameters of a single cylinder diesel engine with hydrogen as a dual fuel using pareto-based genetic algorithm. International Journal of Hydrogen Energy. 2014;39:8063-77.

[29] Yang Z, Wang L, Li S. Investigation into the optimization control technique of hydrogen-fueled engines based on genetic algorithms. international journal of hydrogen energy. 2008;33:6780-91.

[30] Zhenzhong Y, Lijun W, Manlou H, Yongdi C. Research on optimal control to resolve the contradictions between restricting abnormal combustion and improving power output in hydrogen fueled engines. International Journal of Hydrogen Energy. 2012;37:774-82.

[31] Sandalcı T, Karagöz Y. Experimental investigation of the combustion characteristics, emissions and performance of hydrogen port fuel injection in a diesel engine. International Journal of Hydrogen Energy. 2014;39:18480-9.

[32] Jabbr AI, Koylu UO. Influence of operating parameters on performance and emissions for a compression-ignition engine fueled by hydrogen/diesel mixtures. International Journal of Hydrogen Energy. 2019;44:13964-73.

[33] Saravanan N, Nagarajan G, Narayanasamy S. An experimental investigation on DI diesel engine with hydrogen fuel. Renewable Energy. 2008;33:415-21.

[34] Saravanan N, Nagarajan G. Performance and emission studies on port injection of hydrogen with varied flow rates with Diesel as an ignition source. Applied Energy. 2010;87:2218-29.

[35] GitHub. chem.inp_15. 2015.

[36] Baukal C. Everything You Need to Know About Nitric Oxides. 2006.

[37] Nishida K, Hiroyasu H. Simplified three-dimensional modeling of mixture formation and combustion in a DI diesel engine. SAE Technical Paper; 1989.

[38] Demuth H, Beale M. Neural network and signal processing toolboxes for use with MATLAB, user guide version 6.1. The MathWorks Inc. 2002.

[39] Abutunis A, Hussein R, Chandrashekhara K. A neural network approach to enhance blade element momentum theory performance for horizontal axis hydrokinetic turbine application. Renewable Energy. 2019;136:1281-93.

[40] Gaja H, Liou F. Defect classification of laser metal deposition using logistic regression and artificial neural networks for pattern recognition. The International Journal of Advanced Manufacturing Technology. 2018;94:315-26.

SECTION

2. SUMMARY AND CONCLUSIONS

The present study considers combustion of hydrogen in IC engines. Numerical studies were conducted on SI engine fueled by hydrogen as a single fuel, and on CI engine fueled by hydrogen/diesel mixture. The studies were carried out for the analysis of performance, combustion, and emission characteristics at various operating parameters. Three-dimensional CFD software, AVL Fire, was utilized to simulate SI and CI engines, and detailed chemical reactions mechanisms were coupled to investigate the emissions formation during the combustion process. The relationships between the operating parameters and the engine outputs, were investigated in a systematic manner. For hydrogen-fueled SI engines (Task I), the power, efficiency, and NO_X emissions were all highly dependent on in-cylinder temperature and pressure. Therefore, the trend was found that for low (0.7) and high equivalence ratios (>1.1), all three parameters were lower than for medium equivalence ratios (0.8-1.0), where the values reached a maximum. Increasing levels of EGR were found to reduce NO_X emissions as well as the power and efficiency. On the other hand, increasing the ignition timing advancement was found to increase all three parameters. In addition, a GA-NN approach was applied to find the best operating points that maximize power while minimizing NO_X. The power and efficiency were found to correlate well, so only the power and NO_X were considered. A Pareto front of non-dominated solutions quantified that fuel-rich conditions with low EGR levels (0-0.47%) and moderately advanced timing (5-10 CA BTDC) gave the best trade-offs

between power and NO_X (8.99-9.06 kW and 343-362 ppm) for the considered engine conditions. The influences of hydrogen variations, EGR rates, and Timing of diesel injection on the efficiency, NO_X, and soot emissions, were investigated (Task II) for CI engine fueled with hydrogen/diesel mixture. The efficiency, and NO_X are the objectives highly dependent on the in-cylinder pressure and temperature. However, soot as the main emission emitted by CI engine, was dependent on the presence of hydrocarbon fuel inside the cylinder. With a higher hydrogen quantity inside the engine, the NO_X emissions and efficiency increased, while the soot emissions decreased. Increasing levels of EGR were found to reduce NO_X emissions and efficiency. On the other hand, increasing the injection -timing advancement was found to increase NO_X emissions and efficiency, while reducing soot emissions. The relationships among the operating parameters of hydrogen variation, exhaust gas recirculation ratio, and diesel injection timing advancement, and the three objectives (outputs) were investigated (Task III) in a large domain of data set A GA-NN approach was applied to find the best operating points that maximize efficiency while minimizing NO_X and soot emissions. It was quantified that advanced injection timing (29.9 BTDC) with medium hydrogen and EGR levels (13.2 %-4.1%) gave the best trade-offs between efficiency, NO_X emission, and soot emission (35-40 %, 1200-2700 ppm, and 1-4 FSN) for the engine conditions considered.

3. RESEARCH RECOMMENDATIONS

Durability research work can be carried out on the hydrogen utilization as a fuel in internal combustion engines. The following is a list of recommended studies that can be considered for future work:

- Water injection (WI) technique can be studied for hydrogen/diesel mixture as it may have a significant effect on NOx emission without affecting the thermal efficiency of the engine.
- The effect of WI associated with EGR and diesel injection timing on the engine performance and emissions needs to be studied.
- Finding the optimum operating parameters among WI, EGR, injection timing, and hydrogen levels needs to be considered.
- To increase the homogeneity of hydrogen/diesel mixture, double diesel injecting timing can be considered for a future study. Double injection timing means injecting a small amount of total mass of diesel at the beginning of cycle to obtain a homogenous mixture and then inject the rest of diesel at the onset of injection timing. This technique may improve the thermal efficiency of the engine.

REFERENCES

[1] Veziroğlu TN, Şahi S. 21st Century's energy: Hydrogen energy system. Energy conversion and management. 2008;49:1820-31.

[2] Rebecca Wright C. There's an unlikely beneficiary of coronavirus: The planetThere's an unlikely beneficiary of coronavirus: The planet. 2020, March 17.

[3] NASA. Airborne Nitrogen Dioxide Plummets Over China. 2020, Febraury 25.

[4] Popovich BPaN. Traffic and Pollution Plummet as U.S. Cities Shut Down for Coronavirus. The New York Times. USA2020, March 22.

APPENDIX A.

REACTION MECHANISM FOR HYDROGEN

```
ELEMENTS
 H   O    N   AR
END
SPECIE
O2          N2
H          H2          O          H2O       OH
HO2        H2O2
N2O        NO          N
AR

THERMO             ! 1995 NASA COMPILATION + CURRAN DATA
CH3O2              L 1/84C   1H   3O   2N   0G   300.000  5000.00
1
 0.66812963E 01 0.80057271E-02-0.27188507E-05 0.40631365E-09-
0.21927725E-13    2
 0.52621851E 03-0.99423847E 01 0.20986490E 01 0.15786357E-01
0.75683261E-07    3
-0.11274587E-07 0.56665133E-11 0.20695879E 04 0.15007068E 02
4
CH4O2              T11/96C   1H   4O   2    0G   200.000  6000.000
1
 6.86907934E+00 1.00840883E-02-3.66515947E-06 5.96302681E-10-
3.58894156E-14    2
-1.98402231E+04-1.24951986E+01 3.72654981E+00 7.51851847E-03
2.35970425E-05    3
-3.52694507E-08 1.42757614E-11-1.83982011E+04 6.52443362E+00-
1.68074366E+04    4
C2H5OH             L 8/88C   2H   6O   1N   0G   200.000  6000.000
1
 0.65624365E+01 0.15204222E-01-0.53896795E-05 0.86225011E-09-
0.51289787E-13    2
-0.31525621E+05-0.94730202E+01 0.48586957E+01-0.37401726E-02
0.69555378E-04    3
-0.88654796E-07 0.35168835E-10-0.29996132E+05 0.48018545E+01-
0.28257829E+05    4
C2H3               T06/93C   2H   3    0    0G   200.000  6000.000
1
 0.47025310E+01 0.72642283E-02-0.25801992E-05 0.41319944E-09-
0.24591492E-13    2
 0.34029675E+05-0.14293714E+01 0.30019602E+01 0.30304354E-02
0.24444315E-04    3
-0.35810242E-07 0.15108700E-10 0.34868173E+05 0.93304495E+01
0.36050230E+05    4
C3H3               BUR 92C   3H   3O   0N   0G   200.000  6000.000
1
 6.64175821E+00 8.08587428E-03-2.84787887E-06 4.53525977E-10-
2.68879815E-14    2
 3.89793699E+04-1.04004255E+01 1.82840766E+00 2.37839036E-02-
2.19228176E-05    3
 1.00067444E-08-1.38984644E-12 4.01863058E+04 1.38447957E+01
4.16139977E+04    4
```

```
C3H4              L12/92C   3H   4O   0N   0G   200.000  6000.000
1
 6.31694869E+00 1.11336262E-02-3.96289018E-06 6.35633775E-10-
3.78749885E-14    2
 2.01174617E+04-1.09718862E+01 2.61307487E+00 1.21223371E-02
1.85405400E-05    3
-3.45258475E-08 1.53353389E-11 2.15415642E+04 1.02503319E+01
2.29622672E+04    4
C3H5              BUR 92C   3H   5O   0N   0G   200.000  6000.000
1
 6.54761132E+00 1.33152246E-02-4.78333100E-06 7.71949814E-10-
4.61930808E-14    2
 1.72714707E+04-9.27486841E+00 3.78794693E+00 9.48414335E-03
2.42343368E-05    3
-3.65604010E-08 1.48592356E-11 1.86261218E+04 7.82822499E+00
2.03259122E+04    4
C3H6              120186C   3H   6          G  0300.00   5000.00
1000.00      1
 0.06732257E+02 0.01490834E+00-0.04949899E-04 0.07212022E-08-
0.03766204E-12    2
-0.09235703E+04-0.01331335E+03 0.01493307E+02 0.02092518E+00
0.04486794E-04    3
-0.01668912E-06 0.07158146E-10 0.01074826E+05 0.01614534E+03
4
C4H2              L 2/93C   4H   2O   0N   0G   200.000  6000.000
1
 8.66704895E+00 6.71505191E-03-2.35355060E-06 3.73635366E-10-
2.21054043E-14    2
 5.10016978E+04-2.18002050E+01-4.07132393E-01 5.20775143E-02-
9.21138340E-05    3
 8.08657403E-08-2.70422080E-11 5.25957367E+04 2.03240223E+01
5.41222513E+04    4
C4H3              L 9/89C   4H   3O   0N   0G   298.150  6000.000
1
 0.84762079E+01 0.88782327E-02-0.30328412E-05 0.47358302E-09-
0.27716627E-13    2
 0.54756540E+05-0.17170551E+02 0.24173247E+01 0.24104782E-01-
0.12813470E-04    3
-0.28606237E-08 0.39194527E-11 0.56506476E+05 0.14471107E+02
0.58181574E+05    4
C4H4              L 9/89C   4H   4O   0N   0G   200.000  6000.000
1
 0.82948104E+01 0.11994381E-01-0.42624075E-05 0.68306978E-09-
0.40680631E-13    2
 0.33550866E+05-0.18426826E+02 0.14049083E+01 0.29531073E-01-
0.15596302E-04    3
-0.32142002E-08 0.45436937E-11 0.35507830E+05 0.17450183E+02
0.37097268E+05    4
CH3OCH3           L12/92C   2H   6O   1N   0G   200.000  6000.000
1
```

```
 5.64844183E+00 1.63381899E-02-5.86802367E-06 9.46836869E-10-
5.66504738E-14    2
-2.51074690E+04-5.96264939E+00 5.30562279E+00-2.14254272E-03
5.30873244E-05    3
-6.23147136E-08 2.30731036E-11-2.39866295E+04 7.13264209E-01-
2.21432171E+04    4
CH3OCH2           T11/82C   2H   5O   1N   0G   300.000  5000.0
1
 0.65567484E+01 0.12180723E-01-0.40628420E-05 0.59495830E-09-
0.31276214E-13    2
-0.40282515E+04-0.81302772E+01 0.35953999E+01 0.13379216E-01
0.53914910E-05    3
-0.10947097E-07 0.38193320E-11-0.27021975E+04 0.92850365E+01
4
CH3OCH2OOH        Jan96 C   2H   6O   3N   0G    300.00  3000.00
1000.       1
 7.66981055E+00 2.35536769E-02-1.15031834E-05 2.84464629E-09-
2.79520304E-13    2
-3.96295537E+04-1.39224857E+01 3.05518950E-02 4.90560834E-02-
4.43030986E-05    3
 2.21548123E-08-4.66587486E-12-3.80282020E+04 2.43189660E+01
4
CH3OCH2OO         Jan96 C   2H   5O   3N   0G    300.00  3000.00
1000.       1
 8.06217488E+00 2.05153644E-02-1.00803231E-05 2.50244952E-09-
2.46544863E-13    2
-2.19951127E+04-1.59505736E+01 4.74967287E-01 4.68199208E-02-
4.55041928E-05    3
 2.44627078E-08-5.51108848E-12-2.04517448E+04 2.17234867E+01
4
CH3OCH2O          Jan96 C   2H   5O   2N   0G    300.00  3000.00
1000.       1
 5.98450336E+00 1.93302785E-02-9.44575204E-06 2.33651645E-09-
2.29626013E-13    2
-2.12266609E+04-7.95685946E+00-1.22386711E-01 3.94270827E-02-
3.47990406E-05    3
 1.69073231E-08-3.44801024E-12-1.99352987E+04 2.26909497E+01
4
CH3OCHO           Jan96 C   2H   4O   2N   0G    300.00  3000.00
1000.       1
 5.46071782E+00 1.70659166E-02-8.38236448E-06 2.08015776E-09-
2.04870146E-13    2
-4.58756417E+04-3.33482124E+00-4.40150386E-01 3.69251939E-02-
3.41468832E-05    3
 1.73800460E-08-3.70831952E-12-4.46516329E+04 2.61277510E+01
4
HCOOCH3                 C   2H   4O   2N   0G   300.000  5000.000
1
 0.83982000E 01 0.11267000E-01-0.41325000E-05 0.72745000E-09-
0.48932000E-13    2
```

```
-0.48328000E 05-0.18820000E 02-0.15323000E 01 0.43051000E-01-
0.45098000E-04    3
 0.26064000E-07-0.63345000E-11-0.45711000E 05 0.31603000E 02
4
HCOOH             L 8/88C   1H   2O   2N   0G   200.000  6000.000
1
 5.69579404E+00 7.72237361E-03-3.18037808E-06 5.57949466E-10-
3.52618226E-14    2
-4.81599723E+04-6.01680080E+00 3.23262453E+00 2.81129582E-03
2.44034975E-05    3
-3.17501066E-08 1.20631660E-11-4.67785606E+04 9.86205647E+00-
4.55312460E+04    4
COOCH3                  C   2H   3O   2    0G   300.000  5000.000
1
 0.76505900E 01 0.99082000E-02-0.37559700E-05 0.67845900E-09-
0.46572100E-13    2
-0.24947700E 05-0.12937300E 02-0.89045900E 00 0.38842600E-01-
0.42829300E-04    3
 0.25682800E-07-0.63729700E-11-0.22835200E 05 0.29911300E 02
4
C7H16             P10/95C   7H  16    0    0G   300.000  5000.000
1391.000    1
 2.22148969e+01 3.47675750e-02-1.18407129e-05 1.83298478e-09-
1.06130266e-13    2
-3.42760081e+04-9.23040196e+01-1.26836187e+00 8.54355820e-02-
5.25346786e-05    3
 1.62945721e-08-2.02394925e-12-2.56586565e+04 3.53732912e+01
C7H15-1    2/10/95      C   7H  15    0    0G   300.000  5000.000
1391.000    1
 2.17940709e+01 3.26280243e-02-1.11138244e-05 1.72067148e-09-
9.96366999e-14    2
-9.20938221e+03-8.64954311e+01-4.99570406e-01 8.08826467e-02-
5.00532754e-05    3
 1.56549308e-08-1.96616227e-12-1.04590223e+03 3.46564011e+01
4
C7H15-2    2/10/95      C   7H  15    0    0G   300.000  5000.000
1391.000    1
 2.16368842e+01 3.23324804e-02-1.09273807e-05 1.68357060e-09-
9.71774091e-14    2
-1.05873616e+04-8.52209653e+01-3.79155767e-02 7.56726570e-02-
4.07473634e-05    3
 9.32678943e-09-4.92360745e-13-2.35605303e+03 3.37321506e+01
4
C7H15O2    7/23/98      C  7.H 15.O  2.   0.G   300.000  5000.000
1
 2.49023689e+01 3.50716920e-02-1.20440306e-05 1.87464822e-09-
1.08947791e-13    2
-2.82976050e+04-9.73923542e+01 2.37499334e+00 8.34651906e-02-
5.13897320e-05    3
 1.64217662e-08-2.19505216e-12-1.99237961e+04 2.53067342e+01
4
```

```
C7H14O2H   7/23/98      C  7.H 15.O  2.   0.G   300.000  5000.000
1
 2.70028807e+01 3.22272216e-02-1.09366516e-05 1.68977918e-09-
9.77321946e-14    2
-2.27229231e+04-1.06332170e+02 2.49875186e+00 8.32443344e-02-
4.85933986e-05    3
 1.28927950e-08-1.09878385e-12-1.36530733e+04 2.73754005e+01
4
C7H14O2HO2   7/23/98    C  7.H 15.O  4.   0.G   300.000  5000.000
1
 3.23937788e+01 3.33911097e-02-1.15672104e-05 1.81146023e-09-
1.05739941e-13    2
-4.36321048e+04-1.32597311e+02 3.84933185e+00 9.45955097e-02-
5.94934121e-05    3
 1.78836457e-08-2.00618696e-12-3.32051631e+04 2.25912030e+01
4
C7KET12    7/23/98      C  7.H 14.O  3.   0.G   300.000  5000.000
1
 2.97472906e+01 3.06622294e-02-1.05563590e-05 1.64627343e-09-
9.58171675e-14    2
-5.66856828e+04-1.22432490e+02 5.82433697e-01 1.01207869e-01-
7.65855996e-05    3
 3.00738606e-08-4.82902792e-12-4.68054419e+04 3.33331449e+01
4
C7KET21    2/10/95      C  7.H 14.O  3.   0.G   300.000  5000.000
1382.000     1
 2.80512936e+01 3.27356029e-02-1.14107044e-05 1.79404506e-09-
1.05002142e-13    2
-5.89640173e+04-1.11392338e+02 4.19023030e+00 8.43118237e-02-
5.44315814e-05    3
 1.85837721e-08-2.72768938e-12-5.00570382e+04 1.85783455e+01
4
C6H12      2/14/95      C  6.H 12.O  0.   0.G   300.000  5000.000
1
 1.78337529e+01 2.67377658e-02-9.10036773e-06 1.40819768e-09-
8.15124244e-14    2
-1.42062860e+04-6.83818851e+01-1.35275205e+00 6.98655426e-02-
4.59408022e-05    3
 1.56967343e-08-2.21296175e-12-7.34368617e+03 3.53120691e+01
4
C5H11CHO   2/29/96      C   6H  12O   1    0G   300.000  5000.000
1
 1.98891043e+01 2.71869340e-02-9.27391515e-06 1.43744158e-09-
8.33090761e-14    2
-3.97523444e+04-7.60741671e+01 1.37517192e+00 6.65669689e-02-
4.04423050e-05    3
 1.23836270e-08-1.52905857e-12-3.28740986e+04 2.48343934e+01
4
C5H11CO    2/29/96      C  6.H 11.O  1.   0.G   300.000  5000.000
1
```

```
 1.94783812e+01 2.50466029e-02-8.54861346e-06 1.32557944e-09-
7.68503296e-14    2
-2.07923937e+04-7.21995578e+01 2.14479069e+00 6.17863563e-02-
3.74134690e-05    3
 1.13283795e-08-1.36917698e-12-1.43451172e+04 2.23128045e+01
4
C5H11             T03/97C  5.H 11.   0.   0.G   298.150  5000.000
1
 1.13324106E+01 3.03659897E-02-1.13934480E-05 1.99539733E-09-
1.32825012E-13    2
-5.95299959E+03-3.13564905E+01 3.57867617E+00 3.04236365E-02
3.27768270E-05    3
-5.86453147E-08 2.39315107E-11-2.60420265E+03 1.42591121E+01
6.68760000E+03    4
C4H9              P10/84C  4.H  9.   0.   0.G   200.000  6000.000
1
 9.43040607E+00 2.34271349E-02-8.53599182E-06 1.39748355E-09-
8.44057456E-14    2
 2.14214862E+03-2.42207994E+01 3.54885235E+00 1.78747638E-02
5.00782825E-05    3
-7.94475071E-08 3.35802354E-11 4.74011588E+03 1.11849382E+01
6.89397210E+03    4
C3H7            N-L 9/84C   3H   7    0    0G   300.000  5000.000
1
 0.77026987E 01 0.16044203E-01-0.52833220E-05 0.76298590E-09-
0.39392284E-13    2
 0.82984336E 04-0.15480180E 02 0.10515518E 01 0.25991980E-01
0.23800540E-05    3
-0.19609569E-07 0.93732470E-11 0.10631863E 05 0.21122559E 02
0.12087447E 05    4
C2H2              L 1/91C  2.H  2.   0.   0.G   200.000  6000.000
1
 4.65878504E+00 4.88396547E-03-1.60828775E-06 2.46974226E-10-
1.38605680E-14    2
 2.57594044E+04-3.99834772E+00 8.08681094E-01 2.33615629E-02-
3.55171815E-05    3
 2.80152437E-08-8.50072974E-12 2.64289807E+04 1.39397051E+01
2.74459950E+04    4
C2H4O             L 8/88C   2H   4O   1    0G   200.000  6000.000
1
 0.54887641E+01 0.12046190E-01-0.43336931E-05 0.70028311E-09-
0.41949088E-13    2
-0.91804251E+04-0.70799605E+01 0.37590532E+01-0.94412180E-02
0.80309721E-04    3
-0.10080788E-06 0.40039921E-10-0.75608143E+04 0.78497475E+01-
0.63304657E+04    4
A1                MF /94C   6H   6    0    0G   300.000  4000.000
1
 0.17246994E+02 0.38420164E-02 0.82776232E-05-0.48961120E-08
0.76064545E-12    2
```

```
 0.26646055E+04-0.71945175E+02-0.48998680E+01 0.59806932E-01-
0.36710087E-04    3
 0.32740399E-08 0.37600886E-11 0.91824570E+04 0.44095642E+02
4
A1-               MF /94C   6H   5    0    0G   300.000  4000.000
1
 0.14493439E+02 0.75712688E-02 0.37894542E-05-0.30769500E-08
0.51347820E-12    2
 0.33189977E+05-0.54288940E+02-0.49076147E+01 0.59790771E-01-
0.45639827E-04    3
 0.14964993E-07-0.91767826E-12 0.38733410E+05 0.46567780E+02
4
CH3CHO            L 8/88C   2H   4O   1     G   200.000  6000.000
1000.000    1
 0.54041108E+01 0.11723059E-01-0.42263137E-05 0.68372451E-09-
0.40984863E-13    2
-0.22593122E+05-0.34807917E+01 0.47294595E+01-0.31932858E-02
0.47534921E-04    3
-0.57458611E-07 0.21931112E-10-0.21572878E+05 0.41030159E+01
4
CH2CHO            SAND86O   1H   3C   2     G   300.000  5000.000
1000.000    1
 0.05975670E+02 0.08130591E-01-0.02743624E-04 0.04070304E-08-
0.02176017E-12    2
 0.04903218E+04-0.05045251E+02 0.03409062E+02 0.10738574E-01
0.01891492E-04    3
-0.07158583E-07 0.02867385E-10 0.15214766E+04 0.09558290E+02
4
END
REACTIONS
 H2    + O2            = OH    + OH           1.700E+13  0.00
47780. !100
 H2    + OH            = H2O   + H            1.170E+09  1.30
3626. !101
 O     + OH            = O2    + H            4.000E+14 -0.50
0. !102
 O     + H2            = OH    + H            5.060E+04  2.67
6290. !103
 H     + HO2           = O     + H2O          3.100E+10  0.00
3590. !104
 O     + OH    + M     = HO2   + M            1.000E+16  0.00
0. !105
 H     + O2    + M     = HO2   + M            2.800E+18  -.86
0.0!106
 H     + O2    + O2    = HO2   + O2           2.080E+19 -1.24
0.0!107
 H     + O2    + H2O   = HO2   + H2O          11.26E+18  -.76
0.0!108
 H     + O2    + N2    = HO2   + N2           2.600E+19 -1.24
0.0!109
```

```
 OH    + HO2           = H2O   + O2           7.500E+12  0.00
0. !110
 H     + HO2           = OH    + OH           1.700E+14  0.0
875. !111
 O     + HO2           = O2    + OH           1.400E+13  0.00
1073. !112
 OH    + OH            = O     + H2O          6.000E+08  1.30
0. !113
 H     + H     + M     = H2    + M            1.000E+18 -1.00
0. !114
 H     + H     + H2    = H2    + H2           9.200E+16 -0.60
0. !115
 H     + H     + H2O   = H2    + H2O          6.000E+19 -1.25
0. !116
 H     + OH    + M     = H2O   + M            1.600E+22 -2.00
0. !118
 H     + O     + M     = OH    + M            6.200E+16 -0.60
0. !119
 O     + O     + M     = O2    + M            1.890E+13  0.00  -
1788. !120
 H     + HO2           = H2    + O2           1.250E+13  0.00
0. !121
 HO2   + HO2           = H2O2  + O2           2.000E+12  0.00
0. !122
 OH    + OH   (+M)     = H2O2 (+M)            7.600E+13  -.37
0. !123
     LOW  /  4.300E+18    -.900  -1700.00/
     TROE/   .7346   94.00  1756.00  5182.00 /
 H2O2  + H             = HO2   + H2           1.600E+12  0.00
3800. !124
 H2O2  + OH            = H2O   + HO2          1.000E+13  0.00
1800. !125
 H2O2  + H             = H2O   + OH           1.000E+13  0.00
3590. !126
 H2O2  + O             = H2O   + O2           8.400E+11  0.00
4260. !127
 H2O2  + O             = OH    + HO2          2.000E+13  0.00
5900. !128
 H2    + HO2           = H2O   + OH           6.500E+11  0.00
18800. !129
!
 N2O   + O             = N2    + O2           1.400E+12  0.00
10810. !131
 N2O   + O             = NO    + NO           2.900E+13  0.00
23150. !132
 N2O   + H             = N2    + OH           4.400E+14  0.00
18880. !133
 N2O   + OH            = N2    + HO2          2.000E+12  0.00
21060. !134
 N2O   + M             = N2    + O     + M    1.300E+11  0.00
59620. !135
```

```
 N     + NO            = N2    + O            2.700E+13  0.00
1500. !136
 N     + O2            = NO    + O            9.00E+09   1.00
27200.  !137
 N     + OH            = NO    + H            3.600E+13  0.00
1600. !138
END
```

APPENDIX B.

REACTION MECHANISM FOR HYDROGEN/DIESEL MIXTURE

```
!Development of a Reduced Primary Reference Fuel (PRF) Mechanism
for IC Engine Combustion Simulations
!Energy & Fuels, 2013; 27:7843-53.
!Authors: Hu Wang, Mingfa Yao and Reitz R.D.
!73 species and 296 reactions, based on detailed CH3OH, CH4, and
H2-O2 mechanism from both LLNL and Princeton.
ELEMENTS
h c o n
END
SPECIES
nc7h16
o2          n2            co2           h2o           co
h2
oh          h2o2          ho2           h             o
ch3o         no            no2           n2o          n
ch2o        hco           ch2           ch3           ch4
c2h2        c2h3          c2h4          c2h5          hcco
ch2co       ch3co         ch3cho        ch2cho        ch3o2
ch3oh
ch2oh       ch3o2h        c2h6          c3h3          c3h4
ic8h18
c3h5        c3h6          nc3h7
ic3h7       ic4h7         c4h8          ic4h8         pc4h9
ic4h9
tc4h9       c5h10         ic3h5cho      ch3coch2      c3ket21
nc3h7cho    nc3h7co       ic3h7cho      tc3h6cho      tc3h6o2cho
tc3h6o2hco  ic3h5co       ic3h7co       ch3coch3      ch2cch2oh
ch3coch2o2
ic4h7o      ic4h6oh       c7h15-2       c7h15o2-2     c7h14ooh2-4
c7h14ooh2-4o2
nc7ket24    ac8h17        ac8h17o2      ac8h16ooh-b   ic8eterab
ac8h16ooh-bo2
ic8ketab
END

REACTIONS MOLES CAL/MOLE
nc7h16<=>h+c7h15-2 1.300e+88 -21.01 1.395e+05
rev/ 2.263e+83 -20.31 4.083e+04 /
nc7h16+h<=>c7h15-2+h2 2.600e+06 2.40 4.471e+03
rev/ 1.807e+01 3.38 9.318e+03 /
nc7h16+o<=>c7h15-2+oh 9.540e+04 2.71 2.106e+03
rev/ 3.481e-01 3.67 5.541e+03 /
nc7h16+oh<=>c7h15-2+h2o 1.900e+06 2.00 -5.960e+02
rev/ 3.624e+02 2.87 1.914e+04 /
nc7h16+ho2<=>c7h15-2+h2o2 4.0e+03   3.37  1.372e+04
rev/ 4.982e-01   3.66  2.562e+03 /
nc7h16+o2<=>c7h15-2+ho2 2.800e+13   0.00  5.015e+04
rev/ 1.000e+09   0.63  3.090e+02 /
c7h15-2<=>pc4h9+c3h6 3.15e+19  -1.79  3.136e+04 !9.764e18
rev/ 1.000e+11 0.00 8.200e+03 /
c7h15o2-2<=>c7h15-2+o2 1.357e+23 -2.36 3.767e+04
```

```
rev/ 2.340e+12 0.00 0.000e+00 /
c7h15o2-2<=>c7h14ooh2-4 2.50e+10 0.00 2.045e+04
c7h14ooh2-4o2<=>c7h14ooh2-4+o2 1.389e+23 -2.38 3.760e+04
rev/ 7.540e+12 0.00 0.000e+00 /
c7h14ooh2-4o2<=>nc7ket24+oh 1.250e+10 0.00 1.745e+04
nc7ket24<=>nc3h7cho+ch3coch2+oh 5.000e+16 0.00 3.900e+04
rev/ 0.000e+00 0.00 0.000e+00 /
c7h14ooh2-4<=>oh+ch3cho+c5h10 1.548e+12   0.59  3.009e+04
rev/ 0.000e+00 0.00 0.000e+00 /
!*****************************************
ic8h18<=>tc4h9+ic4h9 7.828e+29 -3.925 8.415e+04
rev/ 3.590e+14 -0.750 0.000e+00 /
ic8h18+h<=>ac8h17+h2 7.341e+05 2.768 8.147e+03
rev/ 5.100e+01 3.404 1.048e+04 /
ic8h18+oh<=>ac8h17+h2o 0.750e+07 1.800 1.431e+03
ic8h18+ho2<=>ac8h17+h2o2  2.00E3   3.59   1.716e+4
ic8h18+o2<=>ac8h17+ho2 6.300e+13 0.000 5.076e+04
rev/ 2.296e+10 0.288 -1.592e+03 /
ic8h18+o<=>ac8h17+oh 8.550e+03 3.050 3.123e+03
rev/ 3.118e-01 3.666 4.048e+03 /
ic8h18<=>ac8h17+h 5.748e+17 -0.360 1.012e+05
rev/ 1.000e+14 0.000 0.000e+00 /
ic4h8+ic4h9<=>ac8h17   6.090e+02   2.48  8.520e+03
rev/ 1.0e+14  -0.14  2.678e+04 /
ac8h17o2<=>ac8h17+o2 3.465e+20 -1.653 3.572e+04
rev/ 4.520e+12 0.000 0.000e+00 /
ac8h17o2<=>ac8h16ooh-b 2.500e+10 0.000 2.045e+04
ac8h16ooh-b<=>ic8eterab+oh 3.000e+11 0.000 1.425e+04
rev/ 0.000e+00 0.000 0.000e+00 /
ac8h16ooh-bo2<=>ac8h16ooh-b+o2 1.361e+23 -2.357 3.728e+04
rev/ 7.540e+12 0.000 0.000e+00 /
ac8h16ooh-bo2<=>ic8ketab+oh 2.500e+10 0.000 2.100e+04
ic8eterab+oh<=>ic4h8+ic3h7co+h2o 1.250e+12 0.000 0.000e+00
rev/ 0.000e+00 0.000 0.000e+00 /
ic8eterab+ho2<=>ic4h8+ic3h7co+h2o2 2.500e+12 0.000 1.770e+04
rev/ 0.000e+00 0.000 0.000e+00 /
ic8ketab<=>ic3h7cho+tc3h6cho+oh 1.000e+16 0.000 3.900e+04
rev/ 0.000e+00 0.000 0.000e+00 /
!-----------------------------------------
ic8h18+c7h15-2=nc7h16+ac8h17    1.5E11 0.0 1.45E4
!=========================================
c5h10=c2h5+c3h5    9.173E20 -1.63 7.399E4
    REV/4.0E12 0.0E0 -5.96E2/
c5h10+o=pc4h9+hco    1.0E11 0.0 0.0E0
c5h10+oh=pc4h9+ch2o    1.0E12 0.0 0.0E0
pc4h9+o2=c4h8+ho2    1.6E24 -3.9 7.6E3
pc4h9=c2h5+c2h4    7.497E17 -1.41 2.958E4
    REV/3.3E11 0.0E0 7.2E3/
pc4h9=c4h8+h    1.159E17 -1.17 3.816E4
    REV/1.0E13 0.0E0 2.9E3/
c4h8+h=c2h4+c2h5    1.6E22 -2.39 1.118E4
```

```
c4h8+h=c3h6+ch3    3.2E22 -2.39 1.118E4
c4h8=c3h5+ch3    5.0E15 0.0 7.1E4
    REV/5.0E12 0.0E0 0.0E0/
c4h8=c2h3+c2h5    1.0E19 -1.0 9.677E4
    REV/9.0E12 0.0E0 0.0E0/
c4h8+oh=nc3h7+ch2o    1.0E12 0.0 0.0E0
    REV/1.62E12 0.0E0 1.323E4/
c4h8+o=c3h6+ch2o    7.23E5 2.34 -1.05E3
    REV/2.0E5 2.34E0 8.028E4/
nc3h7cho+o2=nc3h7co+ho2    2.0E13 0.5 4.22E4
    REV/1.0E7 5.0E-1 4.0E3/
nc3h7cho+oh=nc3h7co+h2o    2.69E10 0.76 -3.4E2
    REV/1.852E10 7.5E-1 3.122E4/
nc3h7cho+ho2=nc3h7co+h2o2    2.8E12 0.0 1.36E4
    REV/1.0E12 0.0E0 1.0E4/
nc3h7co=nc3h7+co    5.325E15 -0.86 1.34E4
    REV/1.5E11 0.0E0 4.8E3/
!-------------------------------------------------
tc4h9=h+ic4h8    4.65E46 -9.83 5.508E4
    REV/5.889E44 -9.42E0 1.698E4/
tc4h9+o2=ic4h8+ho2    7.0E24 -3.9 6.6E3
!---------------------------------------
ic4h9+o2=ic4h8+ho2    1.6E24 -3.9 7.6E3
ic4h9=c3h6+ch3    1.64E37 -7.4 3.867E4
    REV/1.592E34 -7.11E0 1.803E4/
ic4h9=ic4h8+h    4.98E32 -6.23 4.007E4
    REV/1.606E29 -5.24E0 6.265E3/
ic4h8+oh=ic4h7+h2o    5.2E6 2.0 -2.98E2
    REV/4.563E8 1.39E0 3.247E4/
ic4h8+ho2=ic4h7+h2o2    1.928E4 2.6 1.391E4
    REV/1.004E7 1.66E0 1.521E4/
ic4h8=ic4h7+h    3.07E55 -11.49 1.143E5
    REV/3.3E52 -1.11E1 2.446E4/
ic4h8+o2=ic4h7+ho2    6.0E12 0.0 3.99E4
    REV/2.209E12 -2.8E-1 3.0E1/
!----------------------------------------
tc3h6o2cho=tc3h6cho+o2    2.787E25 -4.07 2.845E4
    REV/1.99E17 -2.1E0 0.0E0/
tc3h6cho+ho2=ic3h7cho+o2    3.675E12 0.0 1.31E3
    REV/1.236E14 -2.4E-1 4.335E4/
tc3h6o2cho=tc3h6o2hco    1.0E11 0.0 2.575E4
    REV/8.258E11 -5.2E-1 2.28E4/
tc3h6o2hco=ch3coch3+co+oh    4.244E18 -1.43 4.8E3
tc3h6cho=ic3h5cho+h    2.879E16 -0.63 4.128E4
    REV/1.3E13 0.0E0 1.2E3/
!---------------------------------------------
ic3h7cho+oh=ic3h7co+h2o    2.69E10 0.76 -3.4E2
    REV/1.164E10 7.5E-1 3.12E4/
ic3h7cho+oh=tc3h6cho+h2o    1.684E12 0.0 -7.81E2
    REV/1.194E13 -9.0E-2 2.981E4/
ic3h7co=ic3h7+co    1.426E13 -0.04 1.095E4
```

```
    REV/1.5E11 0.0E0 4.81E3/
ic3h7cho+ho2=ic3h7co+h2o2    3.0E12 0.0 1.192E4
    REV/7.707E12 -3.3E-1 1.199E4/
!-----------------------------------------
ic4h7+ho2=ic4h7o+oh    7.0E12 0.0 -1.0E3
    REV/2.182E13 -1.7E-1 1.205E4/
ch3o2+ic4h7=ch3o+ic4h7o    7.0E12 0.0 -1.0E3
    REV/2.131E15 -7.5E-1 1.681E4/
ic4h7+o2=c3h4+ch2o+oh    7.29E29 -5.71 2.145E4
ic4h7=c3h4+ch3    1.23E47 -9.74 7.426E4
    REV/3.017E41 -8.7E0 2.662E4/
ic4h7+o2=ic3h5cho+oh    2.47E13 -0.45 2.302E4
    REV/1.62E14 -7.6E-1 7.339E4/
ic4h7+o2=ch3coch2+ch2o    7.14E15 -1.21 2.105E4
    REV/1.226E15 -1.2E0 9.019E4/
ic4h7o=ic4h6oh    1.391E11 0.0 1.56E4
    REV/4.233E11 -1.6E-1 3.167E4/
ic4h7o+o2=ic3h5cho+ho2    3.0E10 0.0 1.649E3
    REV/6.312E10 -1.4E-1 3.898E4/
ic4h7o=ic3h5cho+h    5.0E13 0.0 2.91E4
    REV/3.071E11 5.3E-1 1.647E4/
ic4h6oh+ho2=ch2cch2oh+ch2o+oh    1.446E13 0.0 0.0E0
ch2cch2oh+o2=ch2oh+co+ch2o    4.335E12 0.0 0.0E0
!----------------------------------------------
ic3h5cho+oh=ic3h5co+h2o    2.69E10 0.76 -3.4E2
    REV/4.4E10 7.8E-1 3.608E4/
ic3h5cho+ho2=ic3h5co+h2o2    1.0E12 0.0 1.192E4
    REV/9.709E12 -3.1E-1 1.688E4/
ic3h5co=c3h5+co    1.278E20 -1.89 3.446E4
    REV/1.51E11 0.0E0 4.809E3/
!=====================================
nc3h7+h=c2h5+ch3    3.7E24 -2.92 1.25E4
nc3h7+oh=c3h6+h2o    2.4E13 0.0 0.0E0
nc3h7+o2=c3h6+ho2    1.71E42 -9.211 1.979E4
nc3h7=ch3+c2h4    2.284E14 -0.55 2.84E4
    REV/4.1E11 0.0E0 7.204E3/
nc3h7=h+c3h6    2.667E15 -0.64 3.682E4
    REV/1.0E13 0.0E0 2.5E3/
!-------------------------------------------
ic3h7+o2=c3h6+ho2    3.9E48 -11.002 2.125E4
ic3h7=h+c3h6    8.569E18 -1.57 4.034E4
    REV/1.3E13 0.0E0 1.56E3/
ic3h7+h=c2h5+ch3    2.0E13 0.0 0.0E0
    REV/4.822E9 6.9E-1 1.209E4/
ic3h7+oh=c3h6+h2o    2.41E13 0.0 0.0E0
    REV/2.985E12 5.7E-1 8.382E4/
ic3h7+o=ch3coch3+h    4.818E13 0.0 0.0E0
    REV/1.293E16 -1.9E-1 7.938E4/
ic3h7+h=c3h6+h2    3.2E12 0.0 0.0E0
!---------------------------------------------
ch3coch3=ch3co+ch3    1.219E23 -1.99 8.395E4
```

```
    REV/1.0E13 0.0E0 0.0E0/
ch3coch3+oh=ch3coch2+h2o    1.054E10 0.97 1.586E3
    REV/6.931E9 9.7E-1 2.325E4/
ch3coch3+o2=ch3coch2+ho2    1.2E14 0.0 4.6E4
    REV/2.0E12 0.0E0 2.0E3/
ch3coch3+ho2=ch3coch2+h2o2    1.7E13 0.0 2.046E4
    REV/1.0E11 0.0E0 8.0E3/
ch3coch2=ch2co+ch3    1.0E14 0.0 3.1E4
    REV/1.0E11 0.0E0 6.0E3/
ch3coch2o2=ch3coch2+o2    8.093E15 -1.11 2.745E4
    REV/1.2E11 0.0E0 -1.1E3/
ch2o+ch3coch2o2=hco+c3ket21    1.288E11 0.0 9.0E3
    REV/2.512E10 0.0E0 1.01E4/
ho2+ch3coch2o2=c3ket21+o2    1.0E12 0.0 0.0E0
c3ket21=ch2o+ch3co+oh    1.5E16 0.0 4.2E4
!****************C3H6***************from UCSD_C4 mechanism
c3h6+o<=>c2h5+hco                        3.500e+07    1.650   -
972.75
c3h6+oh<=>c3h5+h2o                       3.100e+06    2.000   -
298.28
c3h6+o<=>ch2co+ch3+h                     1.200e+08    1.650
327.44
c3h6+h<=>c3h5+h2                         1.700e+05    2.500
2492.83
c3h6+h<=>c2h4+ch3                        1.600e+22   -2.390
11185.47
!****************C3H5************************
c3h5+h<=>c3h4+h2                         1.800e+13    0.000
0.00
c3h5+o2<=>c3h4+ho2                       4.990e+15   -1.400
22428.06
c3h5+ch3<=>c3h4+ch4                      3.000e+12   -0.320   -
130.98
c2h2+ch3(+m)<=>c3h5(+m)                  6.000e+08    0.000
0.00
     low  /  2.000e+09    1.000      0.00 /
     troe/     0.5    1e+30         0        /
c3h5+oh<=>c3h4+h2o                       6.000e+12    0.000
0.00
c3h5+h(+m)<=>c3h6(+m)                    2.000e+14    0.000
0.00
h2/2.00/ h2o/6.00/ co/1.50/ co2/2.00/ ch4/2.00/ c2h6/3.00/
     low  /  1.330e+60  -12.000   5967.97 /
     troe/    0.02     1097      1097      6860 /
c3h5+ho2<=>c3h6+o2                       2.660e+12    0.000
0.00
c3h5+ho2<=>oh+c2h3+ch2o                  3.000e+12    0.000
0.00
ch3+c2h3<=>c3h5+h                        1.500e+24   -2.830
18618.55
!*****************C3H4***************************
```

```
c3h4+o<=>c2h4+co                          2.000e+07    1.800
1000.00
ch3+c2h2<=>c3h4+h                         2.560e+09    1.100
13643.88
c3h4+o<=>hcco+ch3                         7.300e+12    0.000
2250.00
c3h4+oh<=>c3h3+h2o                        5.300e+06    2.000
2000.00
c3h4+h(+m)<=>c3h5(+m)                     4.000e+13    0.000
0.00
     low  /  3.000e+24   -2.000      0.00 /
     troe/     0.8    1e+30         0        /
c3h4+o2<=>ch3+hco+co                      4.000e+14    0.000
41826.00
!*********************C3H3************************
c3h3+h(+m)<=>c3h4(+m)                     3.000e+13    0.000
0.00
     low  /  9.000e+15    1.000      0.00 /
     troe/     0.5    1e+30         0        /
c3h3+ho2<=>c3h4+o2                        2.500e+12    0.000
0.00
c3h3+o2<=>ch2co+hco                       3.000e+10    0.000
2868.07
c3h3+hco<=>c3h4+co                        2.500e+13    0.000
0.00
c3h3+ho2<=>oh+co+c2h3                     8.000e+11    0.000
0.00
!********************C2H6 from LLNL gasoline
surrogate*************
2ch3(+M)=c2h6(+M)    9.214E16 -1.17 6.358E2
    h2/2.0/
    h2o/6.0/
    co/1.5/
    co2/2.0/
    ch4/2.0/
    c2h6/3.0/
    LOW/1.135E36 -5.246E0 1.705E3/
    TROE/4.05E-1 1.12E3 6.96E1 1.0E10/
c2h5+h(+M)=c2h6(+M)    5.21E17 -0.99 1.58E3
    h2/2.0/
    h2o/6.0/
    co/1.5/
    co2/2.0/
    ch4/2.0/
    c2h6/3.0/
    LOW/1.99E41 -7.08E0 6.685E3/
    TROE/8.42E-1 1.25E2 2.219E3 6.882E3/
c2h6+h=c2h5+h2    1.15E8 1.9 7.53E3
    REV/1.062E4 2.582E0 9.76E3/
c2h6+o=c2h5+oh    3.55E6 2.4 5.83E3
    REV/1.702E2 3.063E0 6.648E3/
```

```
c2h6+oh=c2h5+h2o    1.48E7 1.9 9.5E2
    REV/1.45E4 2.476E0 1.807E4/
c2h6+o2=c2h5+ho2    6.03E13 0.0 5.187E4
    REV/2.921E10 3.34E-1 -5.93E2/
c2h6+ch3=c2h5+ch4    1.51E-7 6.0 6.047E3
    REV/1.273E-8 6.236E0 9.817E3/
c2h6+ho2=c2h5+h2o2    3.46E1 3.61 1.692E4
    REV/1.849E0 3.597E0 3.151E3/
c2h6+ch3o2=c2h5+ch3o2h    1.94E1 3.64 1.71E4
    REV/2.017E1 3.182E0 1.734E3/
c2h6+ch3o=c2h5+ch3oh    2.41E11 0.0 7.09E3
    REV/4.779E8 4.69E-1 9.547E3/
!*****************C2H5****************
c2h4+h(+M)=c2h5(+M)    1.081E12 0.454 1.822E3
    h2/2.0/
    h2o/6.0/
    co/1.5/
    co2/2.0/
    ch4/2.0/
    c2h6/3.0/
    LOW/1.2E42 -7.62E0 6.97E3/
    TROE/9.75E-1 2.1E2 9.84E2 4.374E3/
c2h5+c2h3=2c2h4    6.859E11 0.11 -4.3E3
    REV/4.82E14 0.0E0 7.153E4/
ch3+c2h5=ch4+c2h4    1.18E4 2.45 -2.921E3
    REV/2.39E6 2.4E0 6.669E4/
c2h5+h=2ch3    9.69E13 0.0 2.2E2
    REV/2.029E9 1.028E0 1.051E4/
c2h5+h=c2h4+h2    2.0E12 0.0 0.0E0
    REV/4.44E11 3.96E-1 6.807E4/
c2h5+o=ch3cho+h    1.1E14 0.0 0.0E0
    REV/1.033E17 -5.0E-1 7.742E4/
c2h5+o2=c2h4+ho2    7.561E14 -1.01 4.749E3
    REV/8.802E14 -9.62E-1 1.813E4/
    DUP
c2h5+o2=c2h4+ho2    4.0E-1 3.88 1.362E4
    REV/4.656E-1 3.928E0 2.7E4/
    DUP
c2h5+o2=ch3cho+oh    8.265E2 2.41 5.285E3
    REV/2.247E3 2.301E0 6.597E4/
!**************C2H4*******************
c2h3+h(+M)=c2h4(+M)    1.36E14 0.173 6.6E2
    h2/2.0/
    h2o/6.0/
    co/1.5/
    co2/2.0/
    ch4/2.0/
    c2h6/3.0/
    LOW/1.4E30 -3.86E0 3.32E3/
    TROE/7.82E-1 2.075E2 2.663E3 6.095E3/
c2h4(+M)=c2h2+h2(+M)    8.0E12 0.44 8.877E4
```

```
    h2/2.0/
    h2o/6.0/
    co/1.5/
    co2/2.0/
    ch4/2.0/
    c2h6/3.0/
    LOW/1.58E51 -9.3E0 9.78E4/
    TROE/7.35E-1 1.8E2 1.035E3 5.417E3/
c2h4+h=c2h3+h2    5.07E7 1.93 1.295E4
    REV/1.602E4 2.436E0 5.19E3/
c2h4+o=ch3+hco    8.564E6 1.88 1.83E2
    REV/3.297E2 2.602E0 2.614E4/
c2h4+o=ch2cho+h    4.986E6 1.88 1.83E2
    REV/1.541E9 1.201E0 1.878E4/
c2h4+oh=c2h3+h2o    1.8E6 2.0 2.5E3
    REV/6.029E3 2.4E0 9.632E3/
c2h4+ch3=c2h3+ch4    6.62E0 3.7 9.5E3
    REV/1.908E0 3.76E0 3.28E3/
c2h4+o2=c2h3+ho2    4.0E13 0.0 5.82E4
    REV/2.0E10 1.58E-1 -4.249E3/
c2h4+ch3o=c2h3+ch3oh    1.2E11 0.0 6.75E3
!****************C2H3********************
c2h2+h(+M)=c2h3(+M)    5.6E12 0.0 2.4E3
    h2/2.0/
    h2o/6.0/
    co/1.5/
    co2/2.0/
    ch4/2.0/
    c2h6/3.0/
    LOW/3.8E40 -7.27E0 7.22E3/
    TROE/7.51E-1 9.85E1 1.302E3 4.167E3/
c2h3+o2=c2h2+ho2    2.12E-6 6.0 9.484E3
    REV/1.087E-5 5.905E0 2.403E4/
c2h3+o2=ch2o+hco    8.5E28 -5.312 6.5E3
    REV/3.994E27 -4.883E0 9.345E4/
c2h3+o2=ch2cho+o    5.5E14 -0.611 5.26E3
    REV/3.0E18 -1.386E0 1.63E4/
ch3+c2h3=ch4+c2h2    3.92E11 0.0 0.0E0
    REV/3.497E14 -1.93E-1 7.078E4/
c2h3+h=c2h2+h2    9.64E13 0.0 0.0E0
    REV/9.427E13 2.53E-1 6.924E4/
c2h3+oh=c2h2+h2o    5.0E12 0.0 0.0E0
    REV/5.184E13 1.47E-1 8.413E4/
!***************C2H2******************
c2h2+o2=hcco+oh    2.0E8 1.5 3.01E4
    REV/2.039E6 1.541E0 3.227E4/
c2h2+o=ch2+co    6.94E6 2.0 1.9E3
    REV/4.05E1 3.198E0 4.836E4/
c2h2+o=hcco+h    1.35E7 2.0 1.9E3
    REV/4.755E7 1.65E0 2.08E4/
c2h2+oh=ch2co+h    3.236E13 0.0 1.2E4
```

```
    REV/3.061E17 -8.02E-1 3.579E4/
c2h2+oh=ch3+co    4.83E-4 4.0 -2.0E3
    REV/3.495E-6 4.638E0 5.212E4/
!****************CH3CHO**************
ch3cho=ch3+hco    7.687E20 -1.342 8.695E4
    REV/1.75E13 0.0E0 0.0E0/
ch3cho+h=ch3co+h2    2.37E13 0.0 3.642E3
    REV/1.639E10 6.33E-1 1.76E4/
ch3cho+o=ch3co+oh    5.94E12 0.0 1.868E3
    REV/2.133E9 6.14E-1 1.441E4/
ch3cho+oh=ch3co+h2o    3.37E12 0.0 -6.19E2
    REV/2.472E10 5.27E-1 2.823E4/
ch3cho+o2=ch3co+ho2    3.01E13 0.0 3.915E4
    REV/1.092E11 2.85E-1 -1.588E3/
ch3cho+ch3=ch3co+ch4    7.08E-4 4.58 1.966E3
    REV/4.468E-4 4.767E0 1.746E4/
ch3cho+ho2=ch3co+h2o2    3.01E12 0.0 1.192E4
    REV/1.205E12 -6.2E-2 9.877E3/
ch3cho+oh=ch2cho+h2o    1.72E5 2.4 8.15E2
    REV/1.332E5 2.511E0 2.495E4/
!****************CH2CHO*******************
ch2cho=ch2co+h    4.071E15 -0.342 5.06E4
    REV/5.0E13 0.0E0 1.23E4/
ch2cho+o2=>ch2o+co+oh    8.95E13 -0.6 1.012E4
!****************CH3CO*******************
ch3co(+M)=ch3+co(+M)    3.0E12 0.0 1.672E4
    LOW/1.2E15 0.0E0 1.2518E4/
ch3co+h=ch2co+h2    2.0E13 0.0 0.0E0
    REV/1.037E13 2.01E-1 6.056E4/
ch3co+o=ch2co+oh    2.0E13 0.0 0.0E0
    REV/5.381E12 1.82E-1 5.914E4/
ch3co+ch3=ch2co+ch4    5.0E13 0.0 0.0E0
    REV/2.364E16 -2.45E-1 6.21E4/
!*****************CH2CO***************
ch2+co(+M)=ch2co(+M)    8.1E11 0.0 0.0E0
    h2/2.0/
    h2o/6.0/
    co/1.5/
    co2/2.0/
    ch4/2.0/
    c2h6/3.0/
    LOW/2.69E33 -5.11E0 7.095E3/
    TROE/5.907E-1 2.75E2 1.226E3 5.185E3/
ch2co+h=ch3+co    1.1E13 0.0 3.4E3
    REV/2.4E12 0.0E0 4.02E4/
ch2co+h=hcco+h2    2.0E14 0.0 8.0E3
    REV/1.434E11 4.7E-1 4.52E3/
ch2co+o=ch2+co2    1.75E12 0.0 1.35E3
    REV/2.854E9 8.09E-1 4.944E4/
ch2co+o=hcco+oh    1.0E13 0.0 8.0E3
    REV/3.723E9 4.52E-1 3.108E3/
```

```
ch2co+oh=hcco+h2o    1.0E13 0.0 2.0E3
    REV/7.604E10 3.65E-1 1.341E4/
ch2co+oh=ch2oh+co    2.0E12 0.0 -1.01E3
    REV/8.17E9 4.94E-1 2.453E4/
!*****************HCCO*****************
hcco+oh=>h2+2co    1.0E14 0.0 0.0E0
hcco+o=>h+2co    8.0E13 0.0 0.0E0
hcco+o2=>oh+2co    4.2E10 0.0 8.5E2
!*********CH3OH from Princeton C1-H2 mech****
oh+ch3(+M)=ch3oh(+M)    2.79E18 -1.43 1.33E3
    h2/2.0/
    h2o/6.0/
    ch4/2.0/
    co/1.5/
    co2/2.0/
    LOW/4.0E36 -5.92E0 3.14E3/
    TROE/4.12E-1 1.95E2 5.9E3 6.394E3/
h+ch2oh(+M)=ch3oh(+M)    1.055E12 0.5 8.6E1
    h2/2.0/
    h2o/6.0/
    ch4/2.0/
    co/1.5/
    co2/2.0/
    LOW/4.36E31 -4.65E0 5.08E3/
    TROE/6.0E-1 1.0E2 9.0E4 1.0E4/
h+ch3o(+M)=ch3oh(+M)    2.43E12 0.515 5.0E1
    h2/2.0/
    h2o/6.0/
    ch4/2.0/
    co/1.5/
    co2/2.0/
    LOW/4.66E41 -7.44E0 1.408E4/
    TROE/7.0E-1 1.0E2 9.0E4 1.0E4/
ch3oh+h=ch2oh+h2    3.2E13 0.0 6.095E3
ch3oh+h=ch3o+h2    8.0E12 0.0 6.095E3
ch3oh+o=ch2oh+oh    3.88E5 2.5 3.08E3
ch3oh+oh=ch3o+h2o    1.0E6 2.1 4.967E2
ch3oh+oh=ch2oh+h2o    7.1E6 1.8 -5.96E2
ch3oh+o2=ch2oh+ho2    2.05E13 0.0 4.49E4
ch3oh+hco=ch2oh+ch2o    9.635E3 2.9 1.311E4
ch3oh+ho2=ch2oh+h2o2    3.98E13 0.0 1.94E4
ch3oh+ch3=ch2oh+ch4    3.19E1 3.17 7.172E3
ch3o+ch3oh=ch3oh+ch2oh    3.0E11 0.0 4.06E3
!-----------------------------------------
ch2oh+M=ch2o+h+M    1.0E14 0.0 2.51E4
ch2oh+h=ch2o+h2    6.0E12 0.0 0.0E0
ch2oh+h=ch3+oh    9.635E13 0.0 0.0E0
ch2oh+o=ch2o+oh    4.2E13 0.0 0.0E0
ch2oh+oh=ch2o+h2o    2.4E13 0.0 0.0E0
ch2oh+o2=ch2o+ho2    2.41E14 0.0 5.017E3
    DUP
```

```
ch2oh+o2=ch2o+ho2    1.51E15 -1.0 0.0E0
    DUP
ch2oh+ho2=ch2o+h2o2    1.2E13 0.0 0.0E0
ch2oh+hco=ch3oh+co    1.0E13 0.0 0.0E0
ch2oh+hco=2ch2o    1.5E13 0.0 0.0E0
2ch2oh=ch3oh+ch2o    3.0E12 0.0 0.0E0
ch2oh+ch3o=ch3oh+ch2o    2.4E13 0.0 0.0E0
!*****************CH3O*********************
ch3o+h=ch3+oh    3.2E13 0.0 0.0E0
ch3o+o=ch2o+oh    6.0E12 0.0 0.0E0
ch3o+oh=ch2o+h2o    1.8E13 0.0 0.0E0
ch3o+o2=ch2o+ho2    9.033E13 0.0 1.198E4
    DUP
ch3o+o2=ch2o+ho2    2.2E10 0.0 1.748E3
    DUP
ch3o+ho2=ch2o+h2o2    3.0E11 0.0 0.0E0
ch3o+co=ch3+co2    1.6E13 0.0 1.18E4
ch3o+hco=ch3oh+co    9.0E13 0.0 0.0E0
2ch3o=ch3oh+ch2o    6.0E13 0.0 0.0E0
ch3o+M=ch2o+h+M    8.3E17 -1.2 1.55E4
!**************CH4************************
ch3+ho2=ch4+o2    3.61E12 0.0 0.0E0
    REV/6.281E14 -1.0E-1 5.623E4/
ch3+h(+M)=ch4(+M)    2.138E15 -0.4 0.0E0
    co/2.0/
    co2/3.0/
    h2o/5.0/
    h2/2.0/
    LOW/3.31E30 -4.0E0 2.108E3/
    TROE/0.0E0 1.0E-15 1.0E-15 4.0E1/
ch4+h=ch3+h2    1.727E4 3.0 8.224E3
    REV/6.61E2 3.0E0 7.744E3/
ch4+oh=ch3+h2o    1.93E5 2.4 2.106E3
    REV/4.82E2 2.9E0 1.486E4/
ch4+o=ch3+oh    2.13E6 2.21 6.48E3
    REV/3.557E4 2.21E0 3.92E3/
ch4+ch2=2ch3    2.46E6 2.0 8.27E3
ch4+ho2=ch3+h2o2    3.42E11 0.0 1.929E4
    REV/3.365E11 -3.3E-1 2.502E3/
ch4+ch3o=ch3+ch3oh    1.57E11 0.0 8.842E3
    REV/1.046E9 0.0E0 5.0E4/
ch3+o2=ch2o+oh    5.87E11 0.0 1.424E4
    REV/1.175E11 1.9E-1 6.606E4/
ch3+ho2=ch3o+oh    1.5E13 0.0 0.0E0
    REV/9.284E13 -1.2E-1 2.524E4/
ch3+o2=ch3o+o    1.375E13 0.0 3.052E4
    REV/8.506E14 -4.5E-1 2.479E3/
ch3+oh=ch2o+h2    2.25E13 0.0 4.3E3
    REV/6.756E14 0.0E0 7.603E4/
ch3+o=ch2o+h    8.0E13 0.0 0.0E0
    REV/1.055E15 0.0E0 6.963E4/
```

```
ch3+M=ch2+h+M    1.968E16 0.0 9.252E4
    REV/2.107E11 1.0E0 -1.962E4/
ch3+h=ch2+h2    9.0E13 0.0 1.51E4
    REV/1.818E13 0.0E0 1.04E4/
ch3+oh=ch2+h2o    3.0E6 2.0 2.5E3
    REV/2.623E6 2.0E0 1.296E4/
!***************CH3O2 and CH3O2H***************
ch3+o2(+M)=ch3o2(+M)    1.006E8 1.63 0.0E0
    LOW/3.816E31 -4.89E0 3.432E3/
    TROE/4.5E-2 8.801E2 2.5E9 1.786E9/
ch3o2+ch3=2ch3o    9.0E12 0.0 -1.2E3
    REV/3.484E12 1.8E-1 2.828E4/
2ch3o2=o2+2ch3o    1.4E16 -1.61 1.86E3
2ch3o2=ch2o+ch3oh+o2    3.11E14 -1.61 -1.051E3
ch3o2+ho2=ch3o2h+o2    2.5E11 0.0 -1.57E3
ch3o2h=ch3o+oh    6.31E14 0.0 4.23E4
    REV/1.166E11 6.0E-1 -1.771E3/
ch3o2+ch2o=ch3o2h+hco    1.99E12 0.0 1.167E4
    REV/8.504E12 -5.0E-1 7.009E3/
ch3o2+h2o2=ch3o2h+ho2    1.32E4 2.5 9.56E3
!*****************H2-O2******************
h+o2=o+oh    1.97E14 0.0 1.654E4
o+h2=h+oh    5.08E4 2.67 6.292E3
o+h2o=2oh    2.97E6 2.02 1.34E4
oh+h2=h+h2o    2.16E8 1.51 3.43E3
h2o2+oh=h2o+ho2    1.0E12 0.0 0.0E0
    DUP
h+oh+M=h2o+M    4.5E22 -2.0 0.0E0
    h2/0.73/
    h2o/12.0/
    co/1.9/
    co2/3.8/
h+o2(+M)=ho2(+M)    1.48E12 0.6 0.0E0
    h2/1.3/
    h2o/14.0/
    co/1.9/
    co2/3.8/
    LOW/3.5E16 -4.1E-1 -1.116E3/
    TROE/5.0E-1 1.0E-30 1.0E30/
ho2+o=oh+o2    3.25E13 0.0 0.0E0
    REV/7.857E14 -3.3E-1 5.539E4/
ho2+h=2oh    7.08E13 0.0 3.0E2
ho2+h=h2+o2    1.66E13 0.0 8.2E2
2ho2=h2o2+o2    4.2E14 0.0 1.198E4
    DUP
h2o2(+M)=2oh(+M)    2.95E14 0.0 4.84E4
    h2/2.5/
    h2o/12.0/
    co/1.9/
    co2/3.8/
    LOW/1.27E17 0.0E0 4.55E4/
```

```
    TROE/5.0E-1 1.0E-30 1.0E30/
h2o2+h=h2o+oh    2.41E13 0.0 3.97E3
o+h+M=oh+M    4.72E18 -1.0 0.0E0
    h2/2.5/
    h2o/12.0/
    co/1.9/
    co2/3.8/
2o+M=o2+M    6.17E15 -0.5 0.0E0
    h2/2.5/
    h2o/12.0/
    co/1.9/
    co2/3.8/
h2+M=2h+M    4.57E19 -1.4 1.044E5
    h2/2.5/
    h2o/12.0/
    co/1.9/
    co2/3.8/
2ho2=h2o2+o2    1.3E11 0.0 -1.629E3
    DUP
h2o2+oh=h2o+ho2    5.8E14 0.0 9.56E3
    DUP
h2o2+o=oh+ho2    9.55E6 2.0 3.97E3
h2o2+h=h2+ho2    6.03E13 0.0 7.95E3
ho2+oh=h2o+o2    1.93E20 -2.49 2.94E2
    DUP
ho2+oh=h2o+o2    1.21E9 1.24 -6.58E2
    DUP
!ho2+oh=h2o+o2    2.89E13 0.0 -4.97E2
!*************CO*****************
co+o(+M)=co2(+M)    1.8E10 0.0 2.384E3
    h2/2.5/
    h2o/12.0/
    co/1.9/
    co2/3.8/
    LOW/1.35E24 -2.788E0 4.191E3/
co+oh=co2+h    2.23E5 1.9 -1.16E3
co+o2=co2+o    2.53E12 0.0 4.77E4
co+ho2=co2+oh    3.01E13 0.0 2.3E4
!*************HCO-CH2-CH2O***************
hco+M=h+co+M    4.75E11 0.7 1.49E4
    h2/2.5/
    h2o/6.0/
    co/1.9/
    co2/3.8/
hco+o2=co+ho2    7.58E12 0.0 4.1E2
    REV/9.029E11 3.3E-1 3.293E4/
hco+h=co+h2    7.34E13 0.0 0.0E0
    REV/4.813E14 0.0E0 9.0E4/
hco+o=co+oh    3.02E13 0.0 0.0E0
    REV/8.697E13 0.0E0 8.79E4/
hco+oh=co+h2o    3.02E13 0.0 0.0E0
```

```
hco+o=co2+h    3.0E13 0.0 0.0E0
    REV/9.677E15 0.0E0 1.102E5/
hco+ch3=ch4+co    1.21E14 0.0 0.0E0
    REV/2.073E16 0.0E0 9.048E4/
hco+ho2=ch2o+o2    2.97E10 0.33 -3.861E3
ch2+o2=hco+oh    1.29E20 -3.3 2.84E2
    REV/5.31E19 -3.3E0 7.317E4/
ch2+o=hco+h    8.0E13 0.0 0.0E0
ch2+o2=co+h2o    7.28E19 -2.54 1.809E3
    REV/8.508E20 -2.54E0 1.798E5/
ch2+o=co+2h    5.0E13 0.0 0.0E0
ch2+o2=co2+2h    3.29E21 -3.3 2.868E3
ch2+o2=co2+h2    1.01E21 -3.3 1.508E3
    REV/3.054E23 -3.3E0 1.867E5/
ch2o+oh=hco+h2o    3.43E9 1.18 -4.47E2
    REV/1.186E9 1.18E0 2.938E4/
ch2o+ho2=hco+h2o2    5.82E-3 4.53 6.557E3
    REV/1.194E-2 4.2E0 4.921E3/
ch2o+M=hco+h+M    6.283E29 -3.57 9.32E4
    REV/2.66E24 -2.57E0 4.27E2/
ch2o+h=hco+h2    9.334E8 1.5 2.976E3
    REV/7.453E7 1.5E0 1.765E4/
ch2o+o=hco+oh    4.16E11 0.57 2.762E3
    REV/1.459E10 5.7E-1 1.534E4/
ch2o+ch3=hco+ch4    3.636E-6 5.42 9.98E2
    REV/7.584E-6 5.42E0 1.615E4/
ch2+o2=ch2o+o    3.29E21 -3.3 2.868E3
    REV/3.862E22 -3.3E0 6.318E4/
ch2o+M=co+h2+M    1.826E32 -4.42 8.712E4
    REV/5.07E27 -3.42E0 8.435E4/
ch2+oh=ch2o+h    2.0E13 0.0 0.0E0
ch2+ho2=ch2o+oh    2.0E13 0.0 0.0E0
n2o   + o             = n2    + o2           1.400E+12  0.00
10810. !131
 n2o   + o             = no    + no           2.900E+13  0.00
23150. !132
 n2o   + h             = n2    + oh           4.400E+14  0.00
18880. !133
 n2o   + oh            = n2    + ho2          2.000E+12  0.00
21060. !134
 n2o   + M             = n2    + o     + M    1.300E+11  0.00
59620. !135
 n     + no            = n2    + o            3.270E+12  0.30
0. !136
 n     + o2            = no    + o            6.400E+09  1.00
6280. !137
 n     + oh            = no    + h            7.333E+13  0.00
1120. !138

END
```

APPENDIX C.

PUBLICATIONS

1. Jabbr AI, Vaz WS, Khairallah HA, Koylu UO. Multi-objective optimization of operating parameters for hydrogen-fueled spark-ignition engines. International Journal of Hydrogen Energy. 2016;41:18291-9.
2. Jabbr AI, Koylu UO. Influence of operating parameters on performance and emissions for a compression-ignition engine fueled by hydrogen/diesel mixtures. International Journal of Hydrogen Energy. 2019;44:13964-73.
3. Jabbr AI, Gaja H, Koylu UO. Multi-Objective Optimization of Operating Parameters for Dual-Fuel Compression Ignition Engines. International Journal of Hydrogen Energy. 2020 9 (Under review).
4. Jabbr AI, Koylu UO. Effects of Hydrogen and EGR Variation on Performance and Emissions of a Dual-Fuel Compression Ignition Engine, 23rd World Hydrogen Energy Conference. Istanbul, Turkey. 2020 (Accepted)

VITA

Abdulhakim Jabbr was born in Tawergha, Libya. He received the B.E. in Mechanical Engineering in the year 2004 from Sirte University in Libya, and received his M.S. degree in Mechanical Engineering in 2013 from Missouri University of Science and Technology, Rolla, USA where he pursued the Ph.D. degree as a full time student. His area of research interest includeded internal combustion engines, alternate fuels for spark engines and compression ignition engines, and hydrogen energy. In August 2020, he received his Ph.D in Mechanical Engineering from Missouri S&T.